National Library of Canada
Acquisitions and Bibliographic Services Branch
395 Wellington Street
Ottawa, Ontario
K1A 0N4

Bibliothèque nationale du Canada
Direction des acquisitions et des services bibliographiques
395, rue Wellington
Ottawa (Ontario)
K1A 0N4

Your file Votre référence

Our file Notre référence

NOTICE

The quality of this microform is heavily dependent upon the quality of the original thesis submitted for microfilming. Every effort has been made to ensure the highest quality of reproduction possible.

If pages are missing, contact the university which granted the degree.

Some pages may have indistinct print especially if the original pages were typed with a poor typewriter ribbon or if the university sent us an inferior photocopy.

Reproduction in full or in part of this microform is governed by the Canadian Copyright Act, R.S.C. 1970, c. C-30, and subsequent amendments.

AVIS

La qualité de cette microforme dépend grandement de la qualité de la thèse soumise au microfilmage. Nous avons tout fait pour assurer une qualité supérieure de reproduction.

S'il manque des pages, veuillez communiquer avec l'université qui a conféré le grade.

La qualité d'impression de certaines pages peut laisser à désirer, surtout si les pages originales ont été dactylographiées à l'aide d'un ruban usé ou si l'université nous a fait parvenir une photocopie de qualité inférieure.

La reproduction, même partielle, de cette microforme est soumise à la Loi canadienne sur le droit d'auteur, SRC 1970, c. C-30, et ses amendements subséquents.

Canada

FREE VIBRATION ANALYSIS OF RECTANGULAR ORTHOTROPIC CANTILEVER PLATES WITH POINT SUPPORTS

THESIS SUBMITTED
TO THE SCHOOL OF GRADUATE STUDIES
AS PARTIAL FULFILLMENT OF THE REQUIREMENTS FOR THE
DEGREE OF MASTERS OF APPLIED SCIENCE

By
KHANG V. NGUYEN

Department of Mechanical Engineering
UNIVERSITY OF OTTAWA
© OTTAWA, ONTARIO, 1993.

National Library of Canada
Acquisitions and Bibliographic Services Branch
395 Wellington Street
Ottawa, Ontario
K1A 0N4

Bibliothèque nationale du Canada
Direction des acquisitions et des services bibliographiques
395, rue Wellington
Ottawa (Ontario)
K1A 0N4

Your file Votre référence

Our file Notre référence

THE AUTHOR HAS GRANTED AN IRREVOCABLE NON-EXCLUSIVE LICENCE ALLOWING THE NATIONAL LIBRARY OF CANADA TO REPRODUCE, LOAN, DISTRIBUTE OR SELL COPIES OF HIS/HER THESIS BY ANY MEANS AND IN ANY FORM OR FORMAT, MAKING THIS THESIS AVAILABLE TO INTERESTED PERSONS.

L'AUTEUR A ACCORDE UNE LICENCE IRREVOCABLE ET NON EXCLUSIVE PERMETTANT A LA BIBLIOTHEQUE NATIONALE DU CANADA DE REPRODUIRE, PRETER, DISTRIBUER OU VENDRE DES COPIES DE SA THESE DE QUELQUE MANIERE ET SOUS QUELQUE FORME QUE CE SOIT POUR METTRE DES EXEMPLAIRES DE CETTE THESE A LA DISPOSITION DES PERSONNE INTERESSEES.

THE AUTHOR RETAINS OWNERSHIP OF THE COPYRIGHT IN HIS/HER THESIS. NEITHER THE THESIS NOR SUBSTANTIAL EXTRACTS FROM IT MAY BE PRINTED OR OTHERWISE REPRODUCED WITHOUT HIS/HER PERMISSION.

L'AUTEUR CONSERVE LA PROPRIETE DU DROIT D'AUTEUR QUI PROTEGE SA THESE. NI LA THESE NI DES EXTRAITS SUBSTANTIELS DE CELLE-CI NE DOIVENT ETRE IMPRIMES OU AUTREMENT REPRODUITS SANS SON AUTORISATION.

ISBN 0-315-95961-4

Canada

UNIVERSITÉ D'OTTAWA
UNIVERSITY OF OTTAWA

Abstract

The free vibration analysis of rectangular plates has been of interest to many scholars and practitioners over the years due to their wide range of applications. However, most of the studies involve the typical case of isotropy.

A study has been done in the analysis of free vibration of orthotropic cantilever plates with internal point supports. The analysis makes use of the Superposition Method which, by superimposing appropriate building blocks, can provide "exact" analytical solution to this problem of orthotropy. In each case of symmetric and antisymmetric vibration modes under study, three different plate problems whose Lévy-type solutions can be obtained, are superimposed. The constants in each solution, created during their boundary condition formulations, are adjusted in such a way so their combination would provide boundary conditions the same to those required for the cantilever plate. Upon superimposing, an eigenvalue matrix is created which allows the eigenvalues to be determined. Accuracy of the resultant eigenvalues is verified by recognising that the governing differential equation is satisfied exactly and that the required plate boundary conditions are satisfied to certain desired degree of exactitude.

The objective of this thesis is to describe the necessary modifications to adapt the superposition method to orthotropic plate problems, and to show the mathematical procedures employed in the analysis. In addition, the results of some representative frequency and mode shape studies will be presented which include a wide range of plate geometries and various levels of orthotropy.

Acknowledgements

First and foremost I would like to express my sincere gratitude to Professor D.J. Gorman for his continuous guidance, patience, financial support, and supervision during the course of this work.

Sincere thanks to the staff of the Department of Mechanical Engineering and fellow graduate students D. Michelussi, S. Fulford, N. Li for their support and cooperation.

Special thanks to my father and mother for having me. Last but not least I wish to thank all those of the past, present, and future.

CONTENTS

List of Figures

List of Tables

Nomenclature

a, b	plate dimensions in the x and y directions, respectively
D_x, D_y	orthotropic plate flexural rigidities
DHX	H/D_x
DHY	H/D_y
E_x, E_y	Young's moduli of orthotropic material
G_{xy}	shear modulus of orthotropic material
H	effective torsional rigidity of orthotropic plate
k	number of terms in Lévy-type series solution
M_x, M_y	bending moments in plate
M_xa/D_x	dimensionless M_x
M_yb^2/aD_y	dimensionless M_y
P	harmonic concentrated driving force
P^*	$=-2Pb^3/D_ya^2$ dimensionless concentrated driving force
q(x,y)	lateral loading on plate surface
Q_x, Q_y	shear force in plate
V_x, V_y	plate vertical edge reactions
V_xa^2/D_x	dimensionless V_x
V_yb^3/aD_y	dimensionless V_y
W	plate lateral displacement
x,y	plate coordinates
λ^2	$=\omega a^2\sqrt{(\rho/D_x)}$, eigenvalue
ξ, η	=x/a, y/b respectively dimensionless plate coordinates
ρ	mass of plate per unit area
ω	circular frequency of vibration
ø	=b/a, plate aspect ratio
υ_x, υ_y	Poisson ratios of orthotropic material
υ_x^*	$=2H/D_y - \upsilon_x$
υ_y^*	$=2H/D_x - \upsilon_y$
α_1, α_2	plate solution parameters defined in text
β_m, γ_m	plate solution parameters defined in text
z, R, S	plate solution parameters defined in text

Chapter 1
Introduction

Free vibration analyses of rectangular plates have been of special interest to scholars and practitioners over the years due to their wide range of applications. Most of the studies involve the typical case of isotropy. The use of plates has been found most notably in electronic circuit boards, space platforms, and aircraft wings; these products are being used in new and increasingly demanding physical environments, hence exposing them to greater mechanical and thermal stresses. The design/development engineers must then be more concerned with the natural vibration frequencies of the components to ensure that the driving forces do not excite the associated natural modes to the point of failure. Upon facing a greater task, the designers not only need effective mathematical models to minimize the number of prototypes required for trial and error solutions, but also must scope with the use of new high strength materials in the form of orthotropy.

The study of rectangular plates has employed various techniques including the energy method, finite element analysis, experimental, and analytical solutions. It has been noted that the methods described can provide solutions of plate vibration problems adequately but do not satisfy exactly the governing differential equation, the prescribed boundary conditions, or both. It is to D.J. Gorman's credit [1] that an "exact" analytical technique called the superposition method was developed. Gorman solves the vibration problems of plates by means of the series-type Lévy

solution combined with the method of superposition. This technique allows an original plate problem to break into "building blocks", the solutions of these blocks are superimposed and the constants are then adjusted such that the superimposed set of blocks satisfy the boundary conditions of the original plate. This method has been employed with considerable success in treating vibration problems of isotropic plates with various boundary conditions and point supports. Saliba [2], using this technique fully analysed the free vibration of isotropic cantilever plates with symmetrical edge and internal point supports. This thesis carries the analysis further by analysing the orthotropic cantilever plates.

The objective of the thesis is to provide an analytical "exact" solution to the free vibration problem of orthotropic cantilever plate with internal point supports. The underlying theory of plate vibration as applied to orthotropy is discussed in this chapter, followed in the next by the mathematical procedures used upon arriving towards the final solution. In addition, a comprehensive set of results for the frequencies and associated mode shapes is included, which covers certain plate geometries and different levels of orthotropy.

1.1 GOVERNING DIFFERENTIAL EQUATION

The analysis of rectangular plates discussed in this report has the following assumptions applied [3]:

- Plate thickness is small compared to its side dimensions, and lateral displacement is small compared to the plate thickness.
- There is no deformation in the mid-plane of the plate ie. this plane does not stretch during bending. Points of the plate normal to the mid-plane remain normal after bending.
- Normal stresses in the direction transverse to the plate are disregarded.
- The effects of rotary inertia are negligible and the tensile and compressive forces in plates are insignificant.

Even though the differential equation governing the bending of plates can be found in numerous books on the subject of theory of plates, its development is presented here in detail to

illustrate the important details regarding orthotropic material. Inspection of Figure 1.1 (Ref. [3]) shows the moment and forces acting on the middle plane of a cut-out element, the static loading intensity distributed over the upper surface of the plate is denoted by q.

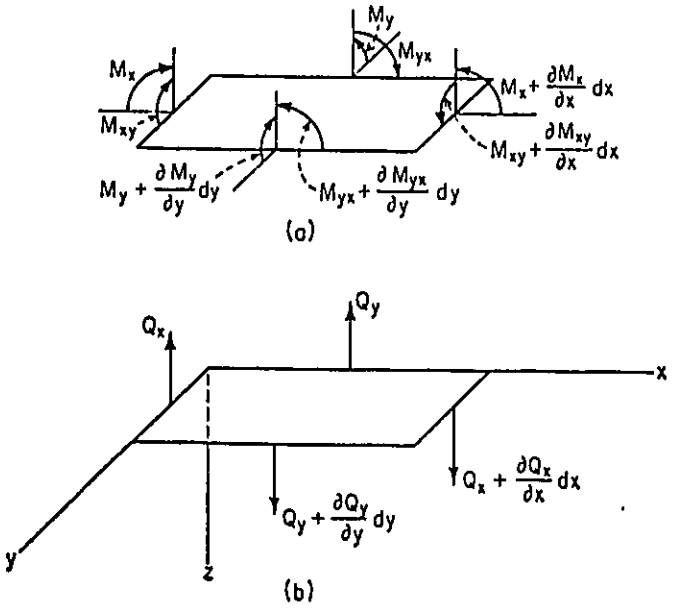

Figure 1.1 Forces and Moments acting on an element

Project all the forces acting on the element in the z axis and divide by the unit area dydx, the following equation of force equilibrium is obtained:

$$\frac{\partial Q_x}{\partial x} + \frac{\partial Q_y}{\partial y} + q = 0$$

Taking moments of all the forces acting on the element with respect to the x axis and divide by dydx, another equation of equilibrium arises:

$$\frac{\partial M_{xy}}{\partial x} - \frac{\partial M_y}{\partial y} + Q_y = 0$$

Similarly, with respect to y-axis

$$\frac{\partial M_{yx}}{\partial x} + \frac{\partial M_x}{\partial x} - Q_x = 0$$

Substitution of Q_y and Q_x into the force equilibrium equation yields

$$\frac{\partial^2 M_x}{\partial x^2} + \frac{\partial^2 M_y}{\partial^2 y} - 2\frac{\partial^2 M_{xy}}{\partial x \partial y} = -q \tag{1.1}$$

For isotropic material, the elastic properties are the same in all directions. For Orthotropic material or sometimes called anisotropic, the homogeneous material has three mutually perpendicular planes of symmetry [4]. All plates studied in this analysis possess what is sometimes called "special orthotropy", ie. the principal directions of orthotropy coincide with the rectangular plate coordinates. Taking these planes as coordinate planes, the relationship between the stress and strain components are represented by the following equations:

$$\begin{aligned}
\sigma_x &= E'_x \varepsilon_x + E'' \varepsilon_y \\
\sigma_y &= E'_y \varepsilon_y + E'' \varepsilon_x \\
\tau_{xy} &= G\gamma_{xy}
\end{aligned}$$

It is recognised that in the case of plane stress, four constants, E_x', E_y',E'', and G are needed to characterize the elastic property of an orthotropic material instead of two (E, υ) for isotropic. With W denoting lateral displacement, the components of strain and stress can be written as

$$\varepsilon_x = -z\frac{\partial^2 W}{\partial x^2} \qquad \varepsilon_y = -z\frac{\partial^2 W}{\partial y^2} \qquad \gamma_{xy} = -2z\frac{\partial^2 W}{\partial x \partial y}$$

$$\begin{aligned}
\sigma_x &= -z\left(E'_x\frac{\partial^2 W}{\partial x^2} + E''\frac{\partial^2 W}{\partial y^2}\right) \\
\sigma_y &= -z\left(E'_y\frac{\partial^2 W}{\partial y^2} + E''\frac{\partial^2 W}{\partial x^2}\right) \\
\tau_{xy} &= -2Gz\frac{\partial^2 W}{\partial x \partial y}
\end{aligned}$$

The normal stresses σ_x, σ_x and shearing stress τ_{xy} produce bending and twisting moments, respectively as

$$M_x = \int_{-h/2}^{h/2} \sigma_x z\,dz = -\left(D_x \frac{\partial^2 W}{\partial x^2} + D_1 \frac{\partial^2 W}{\partial y^2}\right)$$

$$M_y = \int_{-h/2}^{h/2} \sigma_y z\,dz = -\left(D_y \frac{\partial^2 W}{\partial y^2} + D_1 \frac{\partial^2 W}{\partial x^2}\right)$$

$$M_{xy} = \int_{-h/2}^{h/2} \tau_{xy} z\,dz = 2D_{xy} \frac{\partial^2 W}{\partial x \partial y}$$

in which

$$D_x = \frac{E'_x h^3}{12} \qquad D_y = \frac{E'_y h^3}{12} \qquad D_1 = \frac{E'' h^3}{12} \qquad D_{xy} = \frac{G h^3}{12}$$

D_x, D_y are the flexural rigidities of the orthotropic plate and D_1, D_{xy} represent its torsional rigidities. The substitution of the moment expressions into the equilibrium Equation 1.1 yields the governing differential equation for orthotropic plates

$$D_x \frac{\partial^4 W}{\partial x^4} + 2H \frac{\partial^4 W}{\partial x^2 \partial y^2} + D_y \frac{\partial^4 W}{\partial y^4} = q(x,y) \tag{1.2}$$

where $H = D_1 + 2D_{xy}$, is called the *effective* torsional rigidity

For free vibration analysis, the applied static load q(x,y) is replaced by an inertia force, this inertia force opposes acceleration of the plate undergoing oscillatory motion [1]:

$$\rho\, dA \frac{\partial^2 W}{\partial t^2}$$

The form of the free vibration equation, with the introduction of the time variable t is

$$D_x \frac{\partial^4 W(x,y,t)}{\partial x^4} + 2H \frac{\partial^4 W(x,y,t)}{\partial x^2 \partial y^2} + D_y \frac{\partial^4 W(x,y,t)}{\partial y^4} + \rho \frac{\partial^2 W(x,y,t)}{\partial t^2} = 0 \tag{1.3}$$

By separating the displacement function W(x,y,t) into W(x,y)T(t), it can be shown that T(t)=Asin(ωt+α). To further simplify the analysis the dimensionless space variables ξ and η are introduced, where ξ = x/a, η = y/b, a and b are the plate dimensions in the x and y direction respectively. Equation 1.4 then becomes what is known as the governing differential equation (G.D.E.) for free vibration of orthotropic plates

$$\frac{\partial^4 W(\xi,\eta)}{\partial\eta^4} + 2\frac{H}{D_y}\phi^2\frac{\partial^4 W(\xi,\eta)}{\partial\xi^2\partial\eta^2} + \frac{D_x}{D_y}\phi^4\left\{\frac{\partial^4 W(\xi,\eta)}{\partial\xi^4} - \lambda^4 W(\xi,\eta)\right\} = 0 \qquad (1.4)$$

Where

$\phi = b/a$ *plate aspect ratio*

$\lambda^2 = \omega\, a^2\sqrt{\frac{\rho}{D_x}}$ *defined as the eigenvalue*

For a specific orthotropic plate, the objective of the analysis is to solve for Equation 1.4 such that the plate's boundary conditions are satisfied. The solution process involves determining the dimensionless eigenvalue λ^2, from which the natural circular frequency ω is obtained, then the associated displacement W(ξ,η) for the entire plate could be found. Having determined the governing equation, the boundary conditions need to be formulated.

1.2 Formulation of Classical Boundary Conditions

For all plates, boundary conditions are required in solving for the G.D.E. A full description of the classical boundary conditions is presented in this section for reference throughout the thesis work. A more detailed description of the development of the boundary conditions can be found in Ref. [1], [3]. First of all, general expressions for the vertical edge reactions and bending moments of orthotropic plates must be developed.

It has been shown that for rectangular orthotropic plates, there are four material-geometry constants D_x, D_y, υ_x, υ_y. Since the matrix of elastic coefficients must be symmetric, there exists

the further relation called the Betti reciprocal theorem as follows [4],

$$\frac{\upsilon_x}{\upsilon_y} = \frac{D_x}{D_y} \tag{1.5}$$

With the constants D_x, D_y, and H already introduced in section 1.1, the individual Poisson ratios are then available directly from Eq1.5. In terms of the basic coordinates x and y, another form of the bending and torsional moment expressions described in section 1.1 is

$$M_x = -D_x\left(\frac{\partial^2 W(x,y)}{\partial x^2} + \upsilon_y \frac{\partial^2 W(x,y)}{\partial y^2}\right) \tag{1.6}$$

$$M_y = -D_y\left(\frac{\partial^2 W(x,y)}{\partial y^2} + \upsilon_x \frac{\partial^2 W(x,y)}{\partial x^2}\right) \tag{1.7}$$

$$M_{xy} = -2D_t \frac{\partial^2 W(x,y)}{\partial x \partial y} \tag{1.8}$$

Where, as compared to those in 1.1:

$$D_t = D_{xy}, \quad D_x\upsilon_y = D_y\upsilon_x = D_1$$

The Shear Force Q_x is expressed as,

$$Q_x = \frac{\partial M_x}{\partial x} - \frac{\partial M_{xy}}{\partial y} \tag{1.9}$$

Substitution of the moment expressions Eq. 1.6 and 1.8 into the above yields

$$Q_x = -D_x\left\{\frac{\partial^3 W(x,y)}{\partial x^3} + \left[\frac{2D_t}{D_x} + \upsilon_y\right]\frac{\partial^3 W(x,y)}{\partial x \partial y^2}\right\}$$

The vertical edge reaction V_x is

$$V_x = Q_x - \frac{\partial M_{xy}}{\partial y} \tag{1.10}$$

$$\therefore\ V_x = -D_x \left\{ \frac{\partial^3 W(x,y)}{\partial x^3} + \left[\frac{4D_t}{D_x} + \upsilon_y \right] \frac{\partial^3 W(x,y)}{\partial x \partial y^2} \right\}$$

$$but\quad 2H = \upsilon_y D_x + \upsilon_x D_y + 4 D_t \tag{1.11}$$

Therefore, by introducing variable υ_y^* the bracketed term of Equation 1.11 can be expressed as

$$\upsilon_y^* = \frac{4D_t}{D_x} + \upsilon_y = \frac{2H}{D_x} - \upsilon_y \tag{1.12}$$

In a similar manner, introducing υ_x^* as

$$\upsilon_x^* = \frac{2H}{D_y} - \upsilon_x \tag{1.13}$$

The vertical edge reactions and bending moments, in non-dimensionless form are

$$\frac{V_x a^2}{D_x} = -\left\{ \frac{\partial^3 W(\xi,\eta)}{\partial \xi^3} + \frac{\upsilon_y^*}{\phi^2} \frac{\partial^3 W(\xi,\eta)}{\partial \xi \partial \eta^2} \right\} \tag{1.14}$$

$$\frac{V_y b^3}{aD_y} = -\left\{ \frac{\partial^3 W(\xi,\eta)}{\partial \eta^3} + \nu_x^* \phi^2 \frac{\partial^3 W(\xi,\eta)}{\partial \eta \partial \xi^2} \right\} \tag{1.15}$$

$$\frac{M_x a}{D_x} = -\left\{ \frac{\partial^2 W(\xi,\eta)}{\partial \xi^2} + \frac{\upsilon_y}{\phi^2} \frac{\partial^2 W(\xi,\eta)}{\partial \eta^2} \right\} \tag{1.16}$$

$$\frac{M_y b^2}{aD_y} = -\left\{\frac{\partial^2 W(\xi,\eta)}{\partial \eta^2} + \nu_x \phi^2 \frac{\partial^2 W(\xi,\eta)}{\partial \xi^2}\right\} \tag{1.17}$$

1.2.1 Clamped Edge

$$\begin{aligned} W(\xi,\eta)|_{\xi=1} &= 0 \\ \frac{\partial W(\xi,\eta)}{\partial \xi}|_{\xi=1} &= 0 \end{aligned} \tag{1.18}$$

Along the clamped edge ξ=1, Equation 1.18 states that the lateral displacement and the slope normal to the boundary must be equal to zero.

1.2.2 Simply Supported Edge

$$\begin{aligned} W(\xi,\eta)|_{\xi=1} &= 0 \\ \frac{\partial^2 W(\xi,\eta)}{\partial \xi^2}|_{\xi=1} &= 0 \end{aligned} \tag{1.19}$$

Equation 1.19 states that, along the simply supported edge ξ=1, the lateral displacement and bending moment must be zero.

1.2.3 Free Edge

The boundary conditions for a completely free edge are of a more complicated nature than those for the clamped and simply supported edges, especially for the case of rectangular orthotropy. Theoretical development of the free edge conditions are given in details in Ref. [3],[5],[6]. The following two sets of equations state that the bending moment and the vertical edge reaction equal zero.

Along edge ξ = 1

$$\frac{M_x a}{D_x} = -\left[\frac{\partial^2 W(\xi,\eta)}{\partial \xi^2} + \frac{\upsilon_y}{\phi^2} \frac{\partial^2 W(\xi,\eta)}{\partial \eta^2}\right]_{\xi=1} = 0$$

$$\frac{V_x a^2}{D_x} = -\left[\frac{\partial^3 W(\xi,\eta)}{\partial \xi^3} + \frac{\upsilon_y^*}{\phi^2}\frac{\partial^3 W(\xi,\eta)}{\partial \xi \partial \eta^2}\right]_{\xi=1} = 0 \qquad (1.20)$$

Along edge $\eta = 1$

$$\frac{M_y b^2}{aD_y} = -\left[\frac{\partial^2 W(\xi,\eta)}{\partial \eta^2} + \nu_x \phi^2 \frac{\partial^2 W(\xi,\eta)}{\partial \xi^2}\right]_{\eta=1} = 0$$

$$\frac{V_y b^3}{aD_y} = -\left[\frac{\partial^3 W(\xi,\eta)}{\partial \eta^3} + \nu_x^* \phi^2 \frac{\partial^3 W(\xi,\eta)}{\partial \eta \partial \xi^2}\right]_{\eta=1} = 0 \qquad (1.21)$$

1.2.4 Concentrated Force

In the analysis of plates with internal point supports, the solution includes the effects of concentrated forces generated by the point supports. For vibration analysis, this force may be described as Psinωt, where P is the amplitude and ω is the circular frequency. For reasons to be made obvious in the latter chapters, the force is expanded as a Fourier sine series of the Dirac Delta function. This method has been used with considerable success in previous studies [1], [2], [7], [8]. Detailed description of the Dirac Delta function is found in Ref.[1], but the final form is given here as

$$q(\xi) = 2P\sum_{m=1}^{\infty} \sin m\pi u \, \sin m\pi\xi \qquad (1.22)$$

Eq. 1.22 presents q(ξ) having units of force per unit length. The force distribution is highly peaked at a distance u from the origin along the ξ-axis and exerts virtually no net force of moment elsewhere. Now with sufficient information about the boundaries and concentrated force, attention is turned back to solving the governing equation using the Lévy technique.

1.3 THE LÉVY - TYPE SOLUTION

In the early 18th century, scientist Navier presented to the French Academy of Sciences a technique in solving the bending of simply supported rectangular plates by double trigonometric series. Later on, a solution using a single Fourier series was introduced by another scientist M. Lévy. This powerful method, still in use in the present day, expresses the solution of the governing differential equation in the form

$$W(\xi,\eta) = \sum_{m=1,2}^{\infty} Y_m(\eta) \sin m\pi\xi \tag{1.23}$$

This equation represents the plate displacement function of a plate with two opposite edges simply supported in the η-direction along ξ=0 and ξ=1. Further inspection shows that each term in the series satisfies the boundary conditions, zero displacement and zero bending moment at ξ=0 and ξ=1. Substitution of (1.23) into the G.D.E. (1.4) yields

$$\frac{d^4Y_m(\eta)}{d\eta^4} + \alpha_1\frac{d^2Y_m(\eta)}{d\eta^2} + \alpha_2 Y_m(\eta) = 0 \tag{1.24}$$

For each value of m: $\alpha_1 = -2H/D_y\ \phi^2\ (m\pi)^2$

$$\alpha_2 = D_x/D_y\ \phi^4\ \{\ (m\pi)^4 - \lambda^4\}$$

can also introduce $DHY = H/D_y$

$DXY = D_x/D_y$

Being in the quadratic form, the roots of Eq1.24 can take on three possible formulations depending on the values of the parameters α_1 and α_2 as follows

$$R_{1,2,3,4} = \pm\left[\frac{-\alpha_1 \pm \sqrt{\alpha_1^2 - 4\alpha_2}}{2}\right]^{1/2}$$

$$let\ z = \alpha_1^2 - 4\alpha_2$$

It is at this stage that the analysis differs from that for the isotropic plates. It should be noted that the relationship holds for the special case of orthotropy: isotropic when DHY=DXY=1. The solutions of Equation 1.24 are (Ref. [6],[9]):

Case 1 - For $z > 0$ and $(\sqrt{z} + \alpha_1) \geq 0$

$$Y_m(\eta) = A_m \sinh \beta_m \eta + B_m \cosh \beta_m \eta + C_m \sin \gamma_m \eta + D_m \cos \gamma_m \eta \tag{1.25}$$

Case 2 - For $z > 0$ and $(\sqrt{z} + \alpha_1) < 0$

$$Y_m(\eta) = A_m \sinh \beta_m \eta + B_m \cosh \beta_m \eta + C_m \sinh \gamma_m \eta + D_m \cosh \gamma_m \eta \tag{1.26}$$

where

$$\beta_m^2 = \frac{1}{2}(\sqrt{z} - \alpha_1)$$

$$\gamma_m^2 = \frac{1}{2}(\sqrt{z} + \alpha_1) \quad or \quad \gamma_m^2 = -\frac{1}{2}(\sqrt{z} + \alpha_1)$$

whichever is positive

Case 3 - for $z<0$, this is the only case encountered in orthotropic analysis, more parameters have to be introduced.

Let $z_1 = -1/2\ \alpha_1$ $\quad z_2 = 1/2\ \sqrt{-z}$,

$z_3 = \tan^{-1}(z_2/z_1)$ $\quad z_4 = (z_1^2 + z_2^2)^{1/4}$

$R = z_4 \sin(z_3/2)$ $\quad S = z_4 \cos(z_3/2)$

$$Y_m(\eta) = A_m \sin R\eta \sinh S\eta + B_m \sin R\eta \cosh S\eta + C_m \cos R\eta \sinh S\eta + D_m \cos R\eta \cosh S\eta \tag{1.27}$$

A_m, B_m, C_m, and D_m are constants to be determined by enforcing the appropriate boundary constrains. It should be pointed out once again that the solution presented in Eq. 1.23 is only applicable only to rectangular plates whose two opposite edges are simply supported. However, it has been shown that by making use of the superposition method [1], the Lévy-type solution can be used to solve plate vibration problems of all possible combinations of classical boundary conditions and even with concentrated-force type of loading. One such example is the cantilever plate, one clamped edge and the other three edges being free. What follows is a review of methods used in past research and specifically in the case of cantilever plates.

1.4 LITERATURE REVIEW

In the publication "History of the Theory of Elasticity" by Todhunter and Pearson, it was noted that the development of structural mechanics started with the investigation of static problems. Euler was the first to have examined dynamic plate problems, specifically vibration using mathematical membrane theory [2]. The theory was further extended by noted scientists such as J. Bernoulli and Lagrange. The correct governing differential equation was credited to Navier (1785-1836) a civil engineer who, by using the Fourier trigonometry series, was able to provide an exact solution to this type of boundary value problems. The method was further applied and modified by Poisson and Lévy.

In the early 20th century, the mathematical theories were made practical by Russian scientists in the field of naval architecture. One noted researcher was Timoshenko [3] who presented to the engineers with an excellent classic text on the theory of plates and shells. This book covers most topics in plate vibration problems from the plates with classical-type edges to those with various types of loading; certain special and approximate methods used in plate analysis were also reviewed.

However, it was not till the 1950's that new methods of solution were made possible with the introduction of high-speed computers. Large memory capacity and fast computational rates allowed demanding and powerful methods to be used in plate vibration analysis such as finite element, finite difference, and the unique superposition method. Although considerable amounts of literature dealt with the problems of plate vibration, it was to the credit of Leissa of the Ohio State University that one single popular reference was published [5]. In this reference, information is available covering a wide range of studies from circular, elliptical, triangular, to rectangular plates. These plates can either be isotropic or orthotropic, or with inplane forces or variable thickness; the results include valuable lists of natural frequencies and mode shapes. However, it was noted in this reference that not all plate vibration solutions satisfied "exactly" the governing differential equation and prescribed boundary conditions. This difficulty lead D. Gorman to further refine the accuracy of vibration solution with the new method called

superposition. In Gorman's book, Ref.[1] an orderly collection of plate vibration analysis employing the superposition principle was presented. This technique is ideal because it breaks down complicated boundary conditions of an original problem into building blocks whose conditions are easier to obtain. Superposition requires that the summation of individual building blocks is the same as the original, for example $W(\xi,\eta)=W_1(\xi,\eta)+W_2(\xi,\eta)+W_3(\xi,\eta)$ if 3 building blocks were used. In his book and numerous other publications, Gorman solved for plates with different type of boundary conditions and with various types of loading, the cantilever plate is one of the problems. Saliba [2] further analysed the cantilever plate with symmetrically distributed point supports along the free edges and also internally in the plate. In doing so, he used different building blocks than those used by Gorman, this demonstrated the freedom in choosing the appropriate building blocks without altering the final results, even though the formulation of the problem might look different. In the case of point supports, Ohman [8] provided a detailed description in the analysis of plates with multiple point supports for six possible combination of classical boundary conditions; unfortunately, none dealt specifically with the cantilever plate. The cantilever plate problem dealt in [1] and [2] is the isotropic case, to the author's knowledge, the orthotropic cantilever plates have not been published or approached by any other researchers. Hence the purpose of this thesis is to completely solve this problem. Since the problem has not been solved before, the results of this study could not be compared or verified against any other sets of data except for the special case of orthotropy: isotropic.

The problem of vibration of orthotropic plates has received less attention than that given to isotropic plates. Since numerous engineering materials are orthotropic by nature or design ie. wood, plastic, stiffeners, reinforced concrete slabs etc.; vibration of orthotropic plates is of considerable importance. Notable contributions in this field have been made by Huffington and Hoppmann [13] who in the published paper, discussed the flexural vibration of rectangular orthotropic plates for a class of boundary value problems for which the classical Lévy-type solutions could be easily obtained. This lead to six particular cases being examined involving a combination of clamped, free, and simply supported edges; none of which remotely resembles the cantilever plate. The method of analysis is of the energy type, in which orthogonality properties and energy functions were fully discussed. In addition, formal aspects of forced

vibration were also presented.

Iyengar and Jagadish [14] solved the clamped-square-plate problem using the characteristics functions acquired from the vibrating beam problem. Their results were compared with those of previous researcher Kanazawa and Kawai, and the agreement has been found to be very good and more complete in the sense that more function approximations were included. Hearmon [15] also worked out a similar problem using the Rayleigh method, assuming that the deflections of the plates could be represented by suitable characteristic functions. It was noted in the article that the characteristic functions only satisfy the boundary conditions approximately for a free edge and inclusion of free edges would somewhat complicate the derivation and presentation of results. Later on, Hearmon did apply the Ritz modification to the Rayleigh method and found slight improvement in the estimates of the frequencies but noted that the Rayleigh-Ritz procedure would not yield simple closed formulas.

Dickinson [16] investigated the vibration of orthotropic plates using the sine series solution for isotropic plates developed by Dill and Pister [17]. A note of interest is that the roots of the determinants of the dynamic matrix converge more rapidly for simple-supported plates than those with free edges. Dickinson's first three natural frequencies are lower that Hearmon's upper bounds. Marangoni [18] employed the Rayleigh-Ritz technique, using clamped beam eigenfunctions to determine the upper and lower bounds of the natural frequencies for clamped orthotropic plates. The upper-bound estimates were evaluated for all modes by not imposing any restriction on the symmetry conditions, while the lower bounds were based on decomposition technique by Bazely and Fox [19] in which the governing differential equation got decomposed into two or more equations that are individually solvable. The results of Marangoni and Dickinson were further validated by Gorman's recent work - clamped orthotropic plate free vibration using the superposition technique [9]. All three sets of results agree remarkably well, almost to fourth significant digit accuracy, the agreement is quite impressive considering the great differences in the techniques employed - the sine-series, Rayleigh-Ritz, and the superposition methods. Confidence in the use of superposition method as applied to orthotropic plates lead to another investigation - "analysis of completely free orthotropic plates" [6], it is this reference that

provided great assistance to the present thesis work since the building blocks used in [6] are very similar to what would be required for cantilever plate.

Many other references also contribute good insight to studies in orthotropy. References [20], [21] studied vibration of plates under inplane forces and those which possess rotational flexibility edges. Medwadowski [22] gave a refined theory of elastic, orthotropic plates. Laminated orthotropic plates are of related interest, these studies are found in [23], [24], [25], [26] which covered many topics from general theories to buckling effects.

Chapter 2

The Orthotropic Cantilever Plate

In Chapter one the general theory as applicable to orthotropic plates was discussed and the method of superposition was introduced. The application of this powerful method is further demonstrated here in details by solving the problem of orthotropic cantilever plates. The cantilever plate has received little attention by researchers in the vibration field except by Gorman [1] and Saliba [2]; this is due to difficulties encountered in trying to satisfy its free edge conditions. Solution for this particular problem is presented in this chapter.

Figure 2.1 shows the cantilever plate with dimensions 2b x a. The length of the clamped edge is 2b, and the other length is designated as a. The x, or non-dimensionalised ξ axis runs along the centerline of the plate starting from the clamped side, while the y or η axis originates from the midpoint. All free vibration modes of this plate are either symmetric or antisymmetric with respect to the ξ axis. Hence only half of the plate needs to be analysed since the other half either take on the same or opposite displacement. The method of analysing the vibration modes is the superposition technique which involves using the Lévy-type solution developed in section 1.3 for each required building block and combine the solutions in such a way that an eigenvalue matrix could be created and solved. The symmetric family of modes is investigated first.

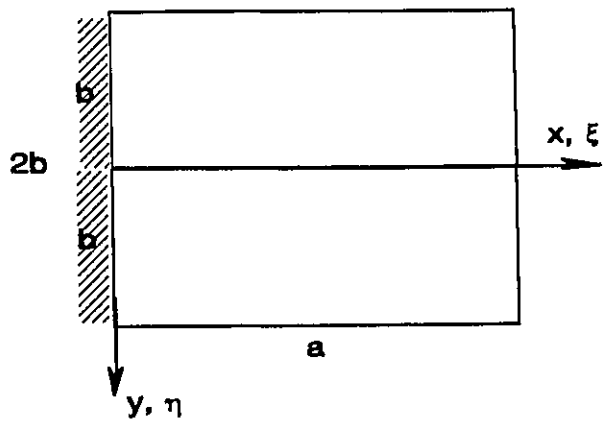

Figure 2-1 The Cantilever Plate

2.1 SYMMETRIC MODES

The half plate under consideration is shown in Figure 2.2. The superposition principle allows this plate to be the equivalent of three building blocks whose combination has the same characteristic conditions as the original. Each building block has its own intrinsic boundary conditions. Series of small semicircles with arrows along the edge of a building block refer to the *enforcing slope* $\partial w/\partial \eta$ normal to that edge. The prescribed slope varies cyclicly with time at the same frequency as the plate vibration. It should be pointed out that bending moment could be enforced in place of the prescribed slope but the solution would take on different form and could lead to rejection modes [1]. A small pair of circles attached to an edge indicates that along that edge, the plate has zero vertical edge reaction and its normal slope is also zero; this condition is referred to as *slip shear*, correspond to the centreline reaction of the full plate 2b x a undergoing symmetric mode vibrations. Symbol *s.s.* means simple support. The symmetric mode solution can be obtained by superimposing the three building blocks. Attention is now turned to formulating the Lévy-type solution for the first block.

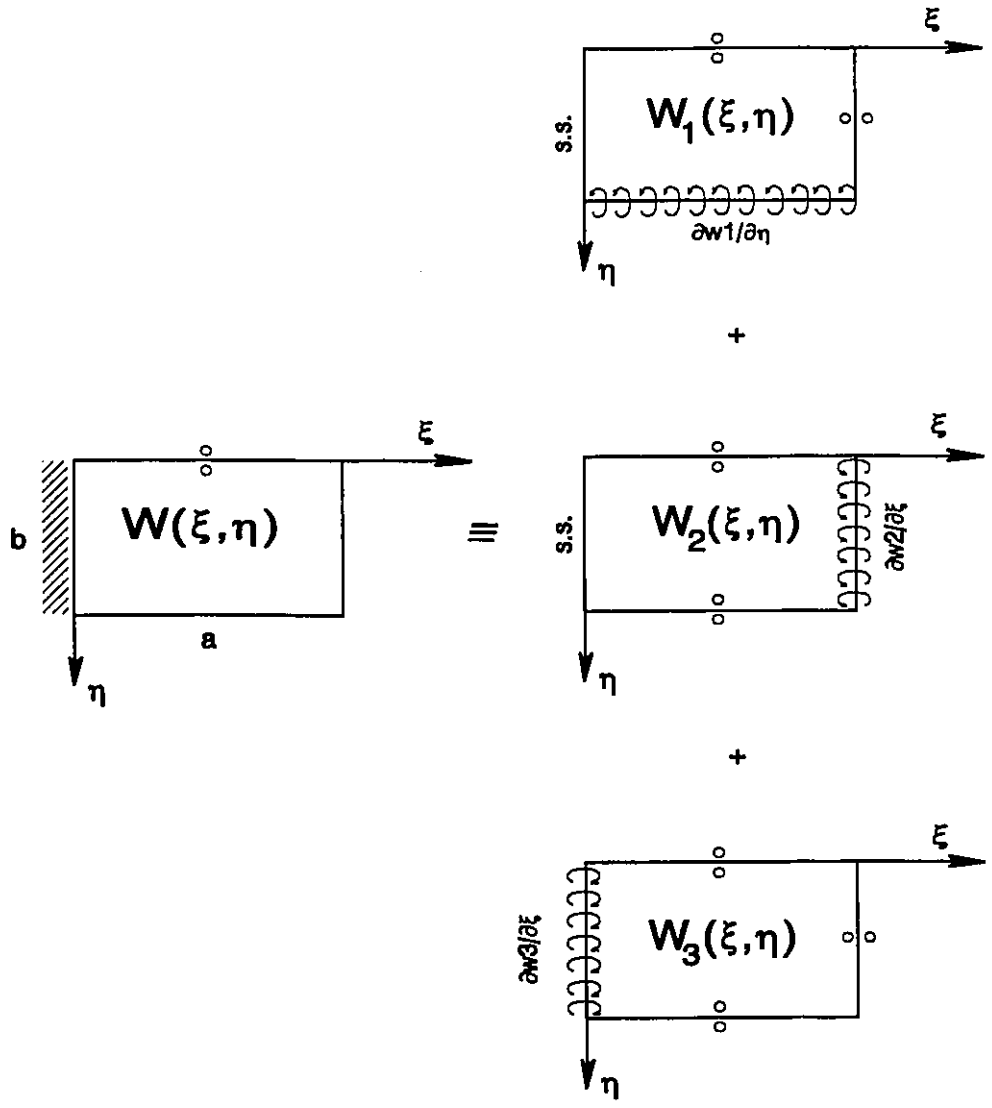

Figure 2.2 Building Blocks utilized in analyzing the free vibration symmetric modes of the orthotropic cantilever plate

2.1.1 Solution of the first building block

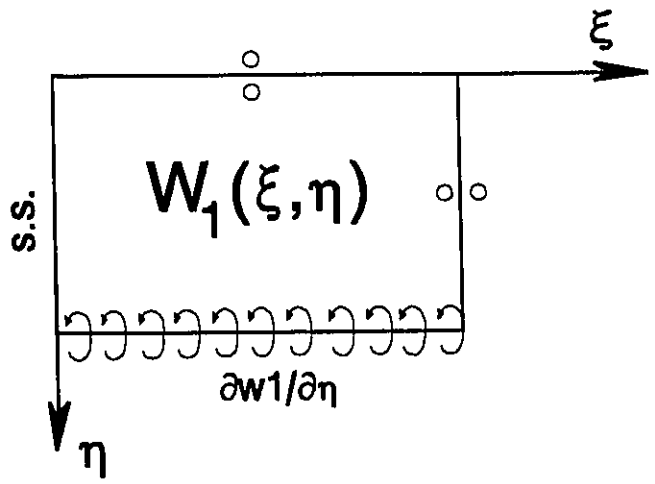

Figure 2.3 Building Block #1

The first building block, Figure 2.3 has slip shear conditions imposed along the edges η=0, ξ=1 and simple support conditions on edge ξ=0. Edge η=1 has zero vertical edge reactions and is enforced by a prescribed slope $\partial W_1/\partial\eta$. Equation 2.1 constitutes a Lévy type solution for this block. It should be noted that this series satisfy the boundary conditions at ξ=0,1; another feature is that only odd terms were used in the summation because if Fourier expansion is taken, $Y_m(\eta)$ would be zero for all even values of m (Ref.[1]).

$$W_1(\xi,\eta) = \sum_{m=1,3}^{\infty} Y_m(\eta)\sin\frac{m\pi\xi}{2} \qquad (2.1)$$

Substitute (2.1) into the governing differential equation (1.4) of Chapter 1.1, solutions are obtained in the form of Equations 1.25, 1.26, and 1.27 depending on values of α_1 and α_2.

where: $\alpha_1 = -2DHY\ \phi^2\ (m\pi/2)^2$

$\alpha_2 = Dxy\ \phi^4\ \{\ (m\pi/2)^4 - \lambda^4\}$

β_m, γ_m, R, and S are defined as in Chapter 1.3

For symmetric mode analysis, antisymmetric terms are deleted due to slip shear condition along edge $\eta=0$. Therefore, the complete solution for the three possible cases is (A_m and B_m were previously denoted as B_m and D_m)

$$W_1(\xi,\eta) = \sum_{m=1,3}^{k^*} \{A_m \cosh \beta_m\eta + B_m \cos \gamma_m\eta\} \sin\frac{m\pi\xi}{2} + \sum_{k^*+2}^{\infty} \{A_m \cosh \beta_m\eta + B_m \cosh \gamma_m\eta\} \sin\frac{m\pi\xi}{2} \quad (2.2)$$

or

$$\{A_m \sin R\eta \sinh S\eta + B_m \cos R\eta \cosh S\eta\} \sin\frac{m\pi\xi}{2}$$

The first summation relates to case $1 - z > 0$ and $(\sqrt{z} + \alpha_1) \geq 0$. The second refers to case $2 - z > 0$ and $(\sqrt{z} + \alpha_1) \leq 0$. The third term involves case 3 where $z< 0$ which is not a summation but can enter into the solution depending on values of m ie. some values in the range $1 - \infty$ are of this type. Even though the boundary conditions at edges $\xi= 0,1$ and $\eta=0$ are satisfied, the two boundary conditions along edge $\eta=1$ remained to be enforced. This would lead to unique expressions for A_m and B_m.

Solutions for A_m and B_m coefficients

On edge $\eta=1$, the vertical edge reaction V_y is zero. This condition is used in conjunction with the imposing distributed harmonic rotation (slope) at $\eta=1$ in developing the final expressions for the displacement $W_1(\xi,\eta)$. Respectively,

$$\frac{V_y b^3}{aD_y} = -\left\{\frac{\partial^3 W(\xi,\eta)}{\partial\eta^3} + \nu_x^* \phi^2 \frac{\partial^3 W(\xi,\eta)}{\partial\eta\partial\xi^2}\right\} \quad (2.3)$$

$$\frac{\partial W_1}{\partial\eta}\Big|_{\eta=1} = \sum_{m=1,3,5}^{\infty} E_m \sin\frac{m\pi\xi}{2} \quad (2.4)$$

For Case 1 - For $z > 0$ and $(\sqrt{z} + \alpha_1) \geq 0$

The first summation of Equation 2.2 is substituted into the shear force Eq.(2.3) and enforcing the vertical edge reaction to 0 at η=1. This will result in an expression of B_m in terms of A_m.

$$W_1(\xi,\eta) = (A_m \cosh \beta_m\eta + B_m \cos \gamma_m\eta) \sin\frac{m\pi\xi}{2} \tag{2.5}$$

$$\frac{\partial^3 w}{\partial\eta^3}|_{\eta=1} = (A_m\beta_m^3 \sinh \beta_m + B_m\gamma^3 \sin \gamma_m) \sin\frac{m\pi\xi}{2} \tag{a}$$

$$\frac{\partial^3 w}{\partial\eta\partial\xi^2}|_{\eta=1} = -(\frac{m\pi}{2})^2[A_m\beta_m \sinh \beta_m - B_m\gamma_m \sin \gamma_m] \sin\frac{m\pi\xi}{2} \tag{b}$$

(a) + (b) = 0, cancel out the common $\sin(m\pi\xi/2)$ term and solve for B_m in terms of A_m

$$B_m = A_m \{\frac{-\beta_m[\beta_m^2 - \upsilon_x^*\phi^2(\frac{m\pi}{2})^2] \sinh\beta_m}{\gamma_m[\gamma_m^2 + \upsilon_x^*\phi^2(\frac{m\pi}{2})^2] \sin\gamma_m}\}$$

$$Let \quad ZZ1 = -\beta_m[\beta_m^2 - \upsilon_x^*\phi^2(\frac{m\pi}{2})^2]$$

$$ZZ2 = \gamma_m[\gamma_m^2 + \upsilon_x^*\phi^2(\frac{m\pi}{2})^2]$$

$$With \quad B_m = \theta_{1m} A_m \qquad where \quad \theta_{1m} = \frac{ZZ1 \sinh\beta_m}{ZZ2 \sin\gamma_m}$$

Equation 2.5 is now,

$$\therefore W_1(\xi,\eta) = A_m [\cosh \beta_m\eta + \theta_{1m} \cos \gamma_m\eta) \sin\frac{m\pi\xi}{2} \tag{2.6}$$

Next step is to impose distributed harmonic rotation (slope) at η=1, represented by the sine series. Substitute Eq. (2.6) into (2.4).

$$\frac{\partial W_1}{\partial \eta}\Big|_{\eta=1} = \sum_{m=1,3,5}^{K} E_m \sin\frac{m\pi\xi}{2}$$

$$LHS = A_m\,[\beta_m \sinh\beta_m - \theta_{1m}\gamma_m \sin\gamma_m]\,\sin\frac{m\pi\xi}{2}$$

$$RHS = E_m \sin\frac{m\pi\xi}{2}$$

Once again, cancel out the common $\sin(m\pi\xi/2)$ term and solve for A_m in terms of E_m

$$A_m = \frac{E_m}{[\beta_m - \frac{zz1}{zz2}\gamma_m]\,\sinh\beta_m}$$

$$A_m\theta_{1m} = \frac{zz1}{zz2}\,\frac{E_m}{[\beta_m - \frac{zz1}{zz2}\gamma_b]\,\sin\gamma_m}$$

$$Let\quad \theta_{11m} = \frac{1}{[\beta_m - \frac{zz1}{zz2}\gamma_m]}$$

$$\theta_{13m} = \frac{zz1}{zz2}\,\frac{E_m}{[\beta_m - \frac{zz1}{zz2}\gamma_m]} = \frac{zz1}{zz2}\,\theta_{11m}$$

Now that the A_m and B_m coefficients are solved in terms of the imposing rotational variable E_m, θ_{11m}, and θ_{13m} the final form of W_1 (case 1) is:

$$W_1(\xi,\eta) = E_m\{\theta_{11m}\,\frac{\cosh\beta_m\eta}{\sinh\beta_m} + \theta_{13m}\frac{\cos\gamma_m\eta}{\sin\gamma_m}\}\,\sin\frac{m\pi\xi}{2} \qquad (2.7)$$

For Case 2 and 3 - [$z > 0$ and $(\sqrt{z} + \alpha_1) \leq 0$], and [$z < 0$] respectively

The procedures in solving for A_m and B_m are the same as those applied in case 1. Firstly, the zero shear force condition at $\eta=1$ (Eq. 2.3) is enforced to get B_m in terms of A_m: $B_m = \theta_{\#m} A_m$. Secondly, by enforcing the prescribed slope (Eq. 2.4) A_m is replaced by the rotational variable E_m ie. $A_m = \theta_{\#\#m} E_m$. Detailed derivations of the expressions for case 2 and 3 are provided in Appendix A. All $\theta_{\#\#m}$ coefficient are in terms of β_m, γ_m, R, and S.

The final combined form of W_1 covering all three cases for the first building block is:

$$W_1(\xi,\eta) = \sum_{m=1,3}^{k^*} E_m \left\{\theta_{11m}\frac{\cosh \beta_m\eta}{\sinh\beta_m} + \theta_{13m}\frac{\cos \gamma_m\eta}{\sin\gamma_m}\right\} \sin\frac{m\pi\xi}{2} + \sum_{k^*+2}^{k^{**}} E_m \left\{\theta_{22m}\frac{\cosh \beta_m\eta}{\sinh\beta_m} + \theta_{23m}\frac{\cosh \gamma_m\eta}{\sinh\gamma_m}\right\} \sin\frac{m\pi\xi}{2} + \sum_{k^{**}+2}^{\infty} E_m \left[\theta_{33m}\sin R\eta \sinh S\eta + \theta_{333m}\cos R\eta \cosh S\eta\right] \sin\frac{m\pi\xi}{2} \quad (2.8)$$

2.1.2 Solution of the second building block

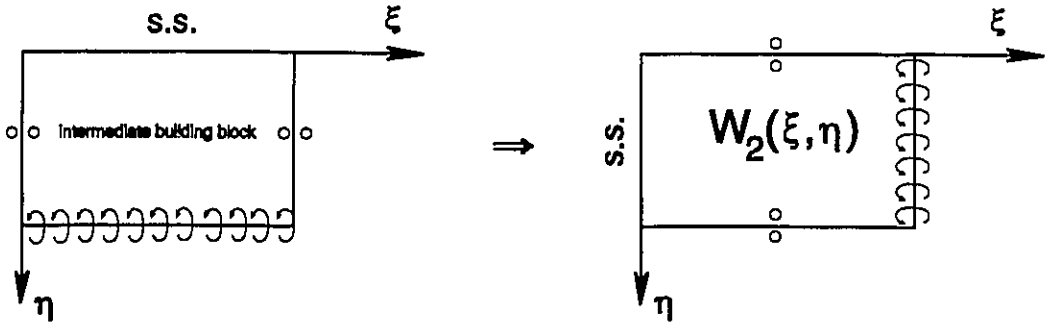

Figure 2.4 Intermediate block used in the solution of the second building block

Inspection of Figure 2.4 shows that the trigonometric part of the solution runs in the η axis direction. Solution for this building block could be obtained easier if one can take advantage of the forms of solutions already developed previously. One can begin by solving for the intermediate building block. Then an interchange of the ξ and η coordinates will result in the solution of the original second building block. In order to avoid repetitions in showing derivations, only final forms of certain expressions are written.

The Lévy type solution for the intermediate block is:

$$W_2^*(\xi,\eta) = \sum_{m=0,1,2}^{\infty} Y_m(\eta) \cos m\pi\xi \tag{2.9}$$

Following the same procedures as before to obtain the solutions for $Y_m(\eta)$, they are given as Equations 2.5, 2.6, and 2.7. Due to the simple support conditions along edge η, only odd functions are considered. Hence W_2^* becomes

$$W_2^*(\xi,\eta) = \sum_{m=0,1,2}^{k^*} \{A_m \sinh\beta_m\eta + B_m \sin\gamma_m\eta\} \cos m\pi\xi + \sum_{k^*+1}^{\infty} \{A_m \sinh\beta_m\eta + B_m \sinh\gamma_m\eta\} \cos m\pi\xi + \{A_m \sin R\eta \cosh S\eta + B_m \cos R\eta \sinh S\eta\} \cos m\pi\xi \quad (2.10)$$

Once again β_m, γ_m, R, and S are defined as in Chapter 1. The first summation applies to Case 1 - For $z > 0$ and $(\sqrt{z} + \alpha_1) \geq 0$. The second relates to Case 2 - for $\sqrt{z} > 0$ and $(\sqrt{z} + \alpha_1) \leq 0$. The third is to Case 3 - $z<0$.

The steps used to solve for the A_m and B_m coefficients are similar to those carried out for the first building block. Firstly, the shear force along edge $\eta=1$ is enforced to be zero (Eq2.3), secondly the prescribed slope is expanded in a cosine series. The process eliminates the two unknowns A_m and B_m. Detailed derivations and expressions are found in Appendix A.

The solution of the original second building block is then extracted from that of the intermediate block. The coordinates ξ and η are interchanged. In addition, since the eigenvalue λ^2 was dimensionalised with respect to side length a, it is necessary to replace the aspect ratio by its inverse and to multiply λ^2 by the square of the aspect ratio. For clarity, subscript m is replaced with n to distinguish the solution from that of the first building block. Accordingly, the solution is

$$W_2(\xi,\eta) = \sum_{n=0,1,2}^{k^*} E_n\{\theta_{11n} \frac{\sinh\beta_n\xi}{\cosh\beta_n} + \theta_{13n} \frac{\sin\gamma_n\xi}{\cos\gamma_n}\} \cos n\pi\eta + \sum_{k^*+1}^{\infty} E_n\{\theta_{22n} \frac{\sinh\beta_n\xi}{\cosh\beta_n} + \theta_{23n} \frac{\sinh\gamma_m\xi}{\cosh\gamma_n}\} \cos n\pi\eta + E_n\{\theta_{33n} \sin R\xi \cosh S\xi + \theta_{333n} \cos R\xi \sinh S\xi\} \cos n\pi\eta \quad (2.11)$$

And the enforcing rotation along edge ξ=1 is

$$\frac{\partial W_2}{\partial \xi}\Big|_{\xi=1} = \sum_{n=0,1,2}^{\infty} E_n \cos n\pi\xi \qquad (2.12)$$

2.1.3 Solution of the third building block

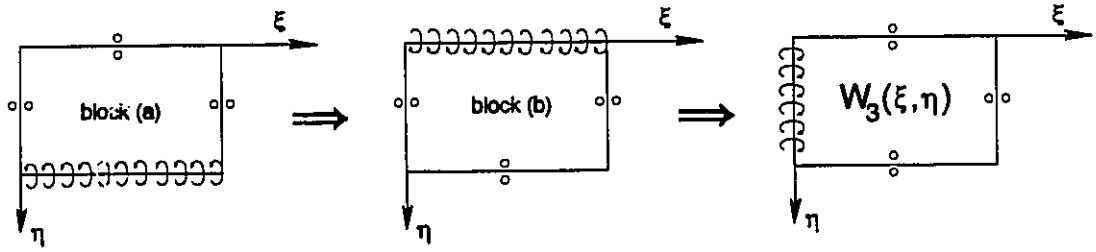

Figure 2.5 Intermediate blocks used in the solution of building block #3

The building block (a) of Figure 2.5 is noted to have the Lévy-type solution as shown in Eq. 2.13. This solution is selected to satisfy the slip shear conditions along edges ξ = 0, 1.

$$W_3^*(\xi,\eta) = \sum_{m=0,1,2}^{\infty} Y_m(\eta) \cos m\pi\xi \qquad (2.13)$$

Substitute (2.13) into the equilibrium GDE, this results in Equations 1.25, 1.26, 1.27 and delete the antisymmetric terms to satisfy the additional boundary condition on edge η=0. In order to obtain expressions for the A_m and B_m coefficients in the solution of this building block, it is necessary to enforce the zero - displacement condition at η=1 and enforcing harmonic slope. Respectively, they are

$$W(\xi,1) = 0 \tag{2.14}$$

$$\frac{\partial W_3^a}{\partial \eta}\Big|_{\eta=1} = \sum_{m=0,1,2}^{\infty} E_m \cos m\pi\xi \tag{2.15}$$

The solution of building block (b) is then extracted from the solution for block (a) by replacing η with 1-η. The prescribed slope will also change sign. Finally, to arrive at the solution of block (c) or original third building block, variables ξ and η have to be interchanged. Following the same logic in variable transformation as before, the aspect ratio is now the its inverse and λ^2 is multiplied by ϕ^2. The final solution for the third building block is:

$$W_3(\xi,\eta) = \sum_{p=0,1,2}^{k^*} E_p \{\theta_{11p}\cosh\beta_p(1-\xi) + \theta_{13p}\cos\gamma_p(1-\xi)\}\cos p\pi\eta + \sum_{k^*+1}^{k^{**}} E_p \{\theta_{22p}\cosh\beta_p(1-\xi) + \theta_{23p}\cosh\gamma_p(1-\xi)\}\cos p\pi\eta \tag{2.16}$$

or

$$E_p \{\theta_{33p}\sin R(1-\xi)\sinh S(1-\xi) + \theta_{333p}\cos R(1-\xi)\cosh S(1-\xi)\}\cos p\pi\eta$$

The prescribed slope will be:

$$\frac{\partial W_3}{\partial \xi}\Big|_{\xi=0} = \sum_{p=0,1,2}^{\infty} -E_p \cos m\pi\eta \tag{2.17}$$

With the solutions for all three building blocks available, the next step is to create an eigenvalue matrix for vibration mode study.

2.1.4 Generation of Eigenvalue Matrix for the Symmetric Modes

The Lévy-type solutions of the first, second, and third building blocks of Figure 2.2 are Equations 2.8, 2.11, 2.16 respectively. These solutions have to be superimposed so the combined effects of the building blocks will satisfy the boundary conditions of the cantilevered plate. The conditions are: bending moments along edges $\xi=1$ and $\eta=1$ must be set to zero, slope in the ξ direction along edge $\xi=0$ must also be zero. Since the solutions $W_1(\xi,\eta)$, $W_2(\xi,\eta)$, $W_3(\xi,\eta)$ satisfy the governing differential equation, their summation will also be satisfied. Firstly, one has to determine the individual contributions of each block to these bending moments and slope.

1.1 Contribution of the first building block, $W_1(\xi,\eta)$ to bending moment along edge $\eta=1$ of the cantilever plate. By using Equation 2.18, differentiations were carried out and terms were collected resulting in Equations 2.19, 2.20, 2.21 for each mth term

$$\frac{M_y b^2}{aD_y}\Big|_{\eta=1} = -\left\{\frac{\partial^2 W(\xi,\eta)}{\partial\eta^2} + \upsilon_x\phi^2\,\frac{\partial^2 W(\xi,\eta)}{\partial\xi^2}\right\} \tag{2.18}$$

case 1

$$E_m\left\{\begin{array}{l}[\upsilon_x\phi^2(\frac{m\pi}{2})^2 - \beta_m^2]\;\theta_{11m}\dfrac{\cosh\beta_m}{\sinh\beta_m} \\ \qquad + \quad [\upsilon_x\phi^2(\frac{m\pi}{2})^2 + \gamma_m^2]\;\theta_{13m}\dfrac{\cos\gamma_m}{\sin\gamma_m}\end{array}\right\}\sin\frac{m\pi\xi}{2} \tag{2.19}$$

case 2

$$E_m\left\{\begin{array}{l}[\upsilon_x\phi^2(\frac{m\pi}{2})^2 - \beta_m^2]\;\theta_{22m}\dfrac{\cosh\beta_m}{\sinh\beta_m} \\ \qquad + \quad [\upsilon_x\phi^2(\frac{m\pi}{2})^2 - \gamma_m^2]\;\theta_{23m}\dfrac{\cosh\gamma_m}{\sinh\gamma_m}\end{array}\right\}\sin\frac{m\pi\xi}{2} \tag{2.20}$$

case 3

$$E_m \left\{ \begin{array}{l} -\left[(\theta_{33m}(S^2-R^2) - 2RS\theta_{333m}) - \upsilon_x\phi^2(\frac{m\pi}{2})^2\theta_{33m}\right] \sin R \sinh S \\ -\left[(\theta_{33m}2RS + \theta_{333m}(S^2-R^2) - \upsilon_x\phi^2(\frac{m\pi}{2})^2\theta_{333m}\right] \cos R \cosh S \end{array} \right\} \sin\frac{m\pi\xi}{2} \qquad (2.21)$$

[1,2] Contribution of $W_1(\xi,\eta)$ to bending moment along edge $\xi=1$ of the cantilever plate. By using Equation 2.22, The following are obtained:

$$\frac{M_\xi a}{D_x}\Big|_{\xi=1} = -\left\{\frac{\partial^2 W(\xi,\eta)}{\partial\xi^2} + \frac{\upsilon_y}{\phi^2}\frac{\partial^2 W(\xi,\eta)}{\partial\eta^2}\right\} \qquad (2.22)$$

case 1

$$E_m \left\{ \begin{array}{l} \left[(\frac{m\pi}{2})^2 - \frac{\upsilon_y}{\phi^2}\beta_m^2\right] \theta_{11m}\frac{\cosh\beta_m\eta}{\sinh\beta_m} \\ + \left[(\frac{m\pi}{2})^2 + \frac{\upsilon_y}{\phi^2}\gamma_m^2\right] \theta_{13m}\frac{\cos\gamma_m\eta}{\sin\gamma_m} \end{array} \right\} \sin\frac{m\pi}{2} \qquad (2.23)$$

case 2

$$E_m \left\{ \begin{array}{l} \left[(\frac{m\pi}{2})^2 - \frac{\upsilon_y}{\phi^2}\beta_m^2\right] \theta_{22m}\frac{\cosh\beta_m\eta}{\sinh\beta_m} \\ + \left[(\frac{m\pi}{2})^2 - \frac{\upsilon_y}{\phi^2}\gamma_m^2\right] \theta_{23m}\frac{\cosh\gamma_m\eta}{\sinh\gamma_m} \end{array} \right\} \sin\frac{m\pi}{2} \qquad (2.24)$$

case 3

$$E_m \left\{ \begin{array}{l} \left[(\frac{m\pi}{2})^2\theta_{33m} - \frac{\upsilon_y}{\phi^2}(\theta_{33m}(S^2-R^2) - 2RS\theta_{333m})\right] \sin R\eta \sinh S\eta \\ + \left[(\frac{m\pi}{2})^2\theta_{333m} - \frac{\upsilon_y}{\phi^2}(\theta_{33m}2RS + \theta_{333m}(S^2-R^2))\right] \cos R\eta \cosh S\eta \end{array} \right\} \sin\frac{m\pi}{2} \qquad (2.25)$$

[1.3] Contribution of $W_1(\xi,\eta)$ to the slope along edge $\xi=0$ of the cantilever plate.

case 1

$$\frac{\partial W_1}{\partial \xi}\Big|_{\xi=0} = E_m\left(\frac{m\pi}{2}\right)\left\{\theta_{11m}\frac{\cosh\beta_m\eta}{\sinh\beta_m} + \theta_{13m}\frac{\cos\gamma_m\eta}{\sin\gamma_m}\right\} \tag{2.26}$$

case 2

$$\frac{\partial W_1}{\partial \xi}\Big|_{\xi=0} = E_m\left(\frac{m\pi}{2}\right)\left\{\theta_{22m}\frac{\cosh\beta_m\eta}{\sinh\beta_m} + \theta_{23m}\frac{\cosh\gamma_m\eta}{\sinh\gamma_m}\right\} \tag{2.27}$$

case 3

$$\frac{\partial W_1}{\partial \xi}\Big|_{\xi=0} = E_m\left(\frac{m\pi}{2}\right)\left\{\theta_{33m}\sin R\eta\sinh S\eta + \theta_{333m}\cos R\eta\cosh S\eta\right\} \tag{2.28}$$

[2.1] Contribution of the second building block, $W_2(\xi,\eta)$ to bending moment along edge $\eta=1$ of the cantilever plate. Using Eq. 2.18, for each nth term of the three cases of solution respectively

$$E_n\left\{\begin{array}{l}[(n\pi)^2 - \upsilon_x\phi^2\beta_n^2]\;\theta_{11n}\dfrac{\sinh\beta_n\xi}{\cosh\beta_n} \\ \qquad + \quad [(n\pi)^2 + \upsilon_x\phi^2\gamma_n^2]\;\theta_{13n}\dfrac{\sin\gamma_n\xi}{\cos\gamma_n}\end{array}\right\}\cos n\pi \tag{2.29}$$

$$E_n\left\{\begin{array}{l}[(n\pi)^2 - \upsilon_x\phi^2\beta_n^2]\;\theta_{22n}\dfrac{\sinh\beta_n\xi}{\cosh\beta_n} \\ \qquad + \quad [(n\pi)^2 - \upsilon_x\phi^2\gamma_n^2]\;\theta_{23n}\dfrac{\sinh\gamma_n\xi}{\cosh\gamma_n}\end{array}\right\}\cos n\pi \tag{2.30}$$

$$E_n \left\{ \begin{array}{l} [(n\pi)^2 - \upsilon_x\phi^2 (\theta_{33n}(S^2-R^2) - 2RS\theta_{333n})] \sin R\xi \cosh S\xi \\ \quad + [(n\pi)^2 - \upsilon_x\phi^2 (\theta_{33n}2RS + \theta_{333n}(S^2-R^2))] \cos R\xi \sinh S\xi \end{array} \right\} \cos n\pi \qquad (2.31)$$

2.2 Contribution of $W_2(\xi,\eta)$ to bending moment along edge $\xi=1$ for case 1,2,3 respectively.

$$E_n \left\{ \begin{array}{l} [-\beta_n^2 + \frac{\upsilon_y}{\phi^2}(n\pi)^2] \theta_{11n} \frac{\sinh\beta_n}{\cosh\beta_n} \\ \quad + [\gamma_n^2 + \frac{\upsilon_y}{\phi^2}(n\pi)^2] \theta_{13n} \frac{\sin\gamma_n}{\cos\gamma_n} \end{array} \right\} \cos n\pi\eta \qquad (2.32)$$

$$E_n \left\{ \begin{array}{l} [-\beta_n^2 + \frac{\upsilon_y}{\phi^2}(n\pi)^2] \theta_{22n} \frac{\sinh\beta_n}{\cosh\beta_n} \\ \quad + [-\gamma_n^2 + \frac{\upsilon_y}{\phi^2}(n\pi)^2] \theta_{23n} \frac{\sinh\gamma_n}{\cosh\gamma_n} \end{array} \right\} \cos n\pi\eta \qquad (2.33)$$

$$E_n \left\{ \begin{array}{l} [- (\theta_{33n}(S^2-R^2) - 2RS\theta_{333n}) + \frac{\upsilon_y}{\phi^2}(n\pi)^2] \sin R\cosh S \\ \quad + [-(\theta_{33n}2RS + \theta_{333n}(S^2-R^2)) + \frac{\upsilon_y}{\phi^2}(n\pi)^2] \cos R\sinh S \end{array} \right\} \cos n\pi\eta \qquad (2.34)$$

2.3 Contribution of $W_2(\xi,\eta)$ to the slope along edge $\xi=0$ for three cases,

$$\frac{\partial W_2}{\partial \xi}|_{\xi=0} = E_n \left\{ \theta_{11n} \frac{\beta_n}{\cosh\beta_n} + \theta_{13n} \frac{\gamma_n}{\cos\gamma_n} \right\} \cos n\pi\eta \qquad (2.35)$$

$$\frac{\partial W_2}{\partial \xi}|_{\xi=0} = E_n \left\{ \theta_{22n} \frac{\beta_n}{\cosh\beta_n} + \theta_{23n} \frac{\gamma_n}{\cosh\gamma_n} \right\} \cos n\pi\eta \qquad (2.36)$$

$$\frac{\partial W_2}{\partial \xi}|_{\xi=0} = E_n \{ \theta_{33n} R + \theta_{333n} S \} \cos n\pi\eta \tag{2.37}$$

3.1 Contribution of the third building block, $W_3(\xi,\eta)$ to bending moment along edge $\eta=1$. Using Eq. 2.18, for each pth term of this solution the results of case 1,2,3 are respectively

$$E_p \left\{ \begin{array}{l} [(p\pi)^2 - \upsilon_x \phi^2 \beta_p^2] \ \theta_{11p} \cosh\beta_p(1-\xi) \\ \qquad + \quad [(p\pi)^2 + \upsilon_x \phi^2 \gamma_p^2] \ \theta_{13p} \cos\gamma_p(1-\xi) \end{array} \right\} \cos p\pi \tag{2.38}$$

$$E_p \left\{ \begin{array}{l} [(p\pi)^2 - \upsilon_x \phi^2 \beta_p^2] \ \theta_{22p} \cosh\beta_p(1-\xi) \\ \qquad + \quad [(p\pi)^2 - \upsilon_x \phi^2 \gamma_p^2] \ \theta_{23p} \cosh\gamma_p(1-\xi) \end{array} \right\} \cos p\pi \tag{2.39}$$

$$E_p \left\{ \begin{array}{l} [(p\pi)^2 \theta_{33p} - \upsilon_x \phi^2 \ (\theta_{33p}(S^2 - R^2) - 2RS\theta_{333p}) \ ] \ \sin R(1-\xi) \sinh S(1-\xi) \\ + \ [(p\pi)^2 \theta_{333p} - \upsilon_x \phi^2 \ (\theta_{33p} 2RS + \theta_{333p}(S^2 - R^2))] \ \cos R(1-\xi) \cosh S(1-\xi) \end{array} \right\} \cos p\pi \tag{2.40}$$

3.2 Contribution of $W_3(\xi,\eta)$ to bending moment along edge $\xi=1$.

$$E_p \left\{ [-\beta_p^2 + \frac{\upsilon_y}{\phi^2}(p\pi)^2] \ \theta_{11p} \quad + \quad [\gamma_p^2 + \frac{\upsilon_y}{\phi^2}(p\pi)^2] \ \theta_{13p} \right\} \cos p\pi\eta \tag{2.41}$$

$$E_p \left\{ [-\beta_p^2 + \frac{\upsilon_y}{\phi^2}(p\pi)^2] \ \theta_{22p} \quad + \quad [-\gamma_p^2 + \frac{\upsilon_y}{\phi^2}(p\pi)^2] \ \theta_{23p} \right\} \cos p\pi\eta \tag{2.42}$$

$$E_p \left\{ [-(\theta_{33p} 2RS + \theta_{333p}(S^2 - R^2)) + \frac{\upsilon_y}{\phi^2}(p\pi)^2 \theta_{333p}] \right\} \cos p\pi\eta \tag{2.43}$$

[3.3] Contribution of $W_3(\xi,\eta)$ to the slope along edge $\xi=0$.

$$\frac{\partial W_3}{\partial \xi}\Big|_{\xi=0} = E_p \{ -\theta_{11p}\beta_p \sinh\beta_p + \theta_{13p}\gamma_p \sin\gamma_p \} \cos p\pi\eta \tag{2.44}$$

$$\frac{\partial W_3}{\partial \xi}\Big|_{\xi=0} = E_p \{ -\theta_{22p}\beta_p \sinh\beta_p - \theta_{23p}\gamma_p \sinh\gamma_p \} \cos p\pi\eta \tag{2.45}$$

$$\frac{\partial W_3}{\partial \xi}\Big|_{\xi=0} = E_p \left\{ \begin{array}{l} -(\theta_{33p}R + S\theta_{333p})\cos R \sinh S \\ \qquad + (-S\theta_{33p} + \theta_{333p}R)\sin R \cosh S \end{array} \right\} \cos p\pi\eta \tag{2.46}$$

It should be noted that the bracketed terms in three above expressions equal to -1 since the slope must be equal to the enforcing slope.

I. Along edge $\eta=1$ of the cantilever plate, the net contributions of the three building blocks to the bending moment must be zero in order to satisfy the free edge condition. One can write,

$$Equation \begin{Bmatrix} 2.19 \\ 2.20 \\ 2.21 \end{Bmatrix} + Equation \begin{Bmatrix} 2.29 \\ 2.30 \\ 2.31 \end{Bmatrix} + Equation \begin{Bmatrix} 2.38 \\ 2.39 \\ 2.40 \end{Bmatrix} = 0 \tag{2.47}$$

Since the net effect must satisfy the boundary condition of zero net moment along the plate edge $\eta=1$, the Fourier coefficients in all of the moment expressions of Eq. 2.47 must be constrained. Reexamination of Eq. 2.47 shows that its first term (Eq. 2.19 - 2.21) involves trigonometric functions $\sin(m\pi\xi/2)$. Now once the second and third term of Eq. 2.47 are expanded in the same type of series, then the constraint that the sum of the coefficients equalling zero is readily imposed. For each term, the expansion is carried out as follows:

$$f(\xi) = \sum_{m=1,3}^{\infty} A_m \sin\frac{m\pi\xi}{2}$$

$$A_m = 2\int_0^1 f(\xi) \sin\frac{m\pi\xi}{2}\, d\xi \tag{2.48}$$

For better insight into the idea of constraint under study, consider the moment along edge $\eta=1$ as a series of analytical functions of Eq. 2.47; for any mth term

$$\frac{M_\eta b^2}{aD_y} = \{E_m C_m \sin\frac{m\pi\xi}{2}\} + \{E_{n=1} f_{n=1}(\xi) + E_2 f_2(\xi)+.....\} + \{E_{p=1} f_{p=1}(\xi) + E_2 f_2(\xi)+.....\}$$

Where C_m, $f_n(\xi)$, $f_p(\xi)$ are coefficients of the three terms of Equation 2.47 respectively. Expand the above equation using Eq. 2.48 and set moment equal zero, resulting in

$$\{E_m C_m\} + \{2E_{n=1}\int_0^1 f_{n=1}(\xi)\sin(\frac{m\pi\xi}{2})d\xi + 2E_2\int_0^1 f_2(\xi)\sin(\frac{m\pi\xi}{2})d\xi + ...\}$$
$$+ \{2E_{p=1}\int_0^1 f_{p=1}(\xi)\sin(\frac{m\pi\xi}{2})d\xi + 2E_2\int_0^1 f_2(\xi)\sin(\frac{m\pi\xi}{2})d\xi + ...\} = 0$$

This is a homogeneous algebraic equation relating E_m, E_n, and E_p together. If k terms are used in the moment expansion, then this equation would allow k linear homogeneous equations to be written.

II. Focusing on the edge $\xi=1$ of the plate, the combined bending moment contributions must be set to zero to satisfy the free edge condition.

$$Equation \begin{Bmatrix} 2.23 \\ 2.24 \\ 2.25 \end{Bmatrix} + Equation \begin{Bmatrix} 2.32 \\ 2.33 \\ 2.34 \end{Bmatrix} + Equation \begin{Bmatrix} 2.41 \\ 2.42 \\ 2.43 \end{Bmatrix} = 0 \qquad (2.49)$$

Equations 2.32-2.34 and 2.41-2.43 involve cosine functions $\cos(n\pi\eta)$ and $\cos(p\pi\eta)$, note that the two functions are identical since n = p = 0, 1, 2.... Equations 2.23-2.25 then have to be expanded in the same type of cosine series. The coefficients are obtained by multiplying the expressions by $2\cos(n\pi\eta)$ and integrating from 0 to 1.

$$f(\eta) = \sum_{n=0,1}^{\infty} A_n \cos(n\pi\eta)$$

$$A_n = \begin{cases} \int_0^1 f(\eta)\, d\eta & \text{for } n = 0 \\ 2\int_0^1 f(\eta)\cos(n\pi\eta)\, d\eta & n \neq 0 \end{cases} \tag{2.50}$$

III. The contributions to the slope along the clamp edge of the plate ξ=0 must also be set to zero

$$\textit{Equation} \begin{Bmatrix} 2.26 \\ 2.27 \\ 2.28 \end{Bmatrix} + \textit{Equation} \begin{Bmatrix} 2.35 \\ 2.36 \\ 2.37 \end{Bmatrix} + \textit{Equation} \begin{Bmatrix} 2.44 \\ 2.45 \\ 2.46 \end{Bmatrix} = 0 \tag{2.51}$$

Following the same reasoning as before, the first term of Eq. 2.51 involve cosine function. Eq. 2.26-2.28 expressions are multiplied by $2\cos(n\pi\eta)$ and integrated from 0 to 1.

If k terms are used in each series, Equations 2.47, 2.49, and 2.51 in their properly expanded form produce 3k homogeneous algebraic equations relating 3k unknown coefficients E_m's, E_n's, and E_p's. A matrix is then generated by the computer. Figure 2.6 is a simple representation of an eigenvalue matrix of 3 terms. As indicated in the figure, the first three rows of this matrix result from enforcing the requirement of zero net bending moment along edge η=1, the second three rows from the zero moment condition at the edge ξ=1, and the last three arise from the condition of zero net slope on edge ξ=0. By trial and error, a value of λ^2 is entered into the coefficient matrix and its determinant is established, a determinant of zero indicates that a nontrivial solution exists for E_m's, E_n's, and E_p's and hence the associated λ^2 is an eigenvalue.

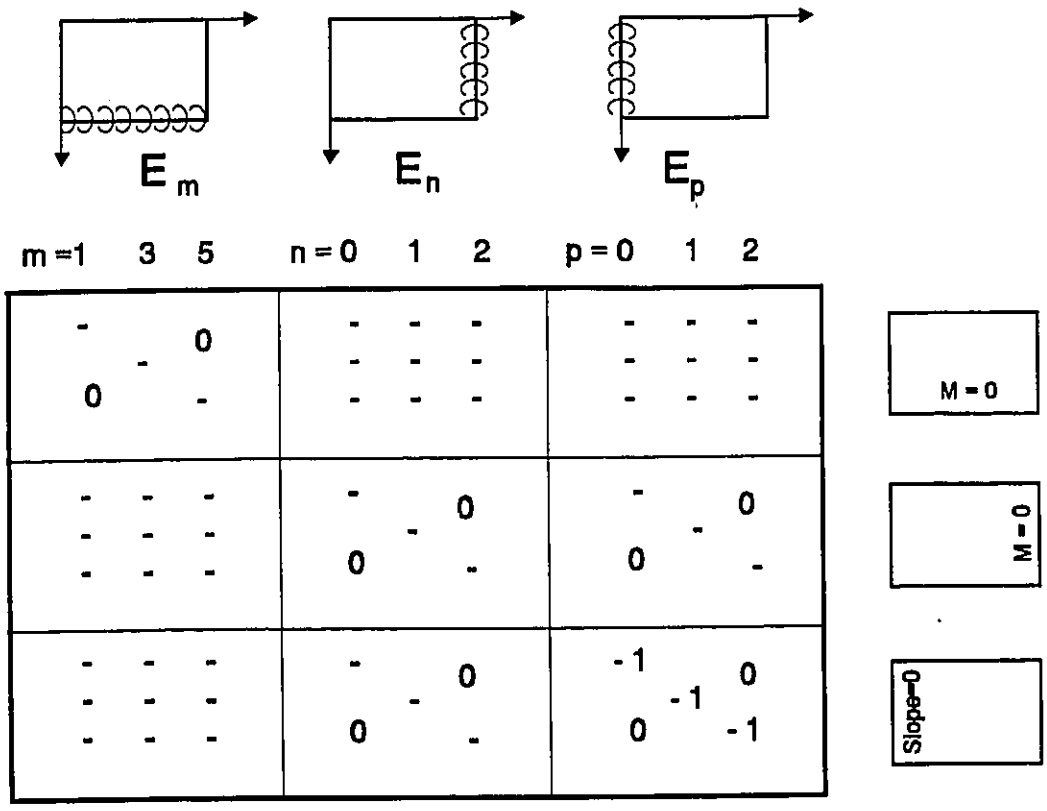

Figure 2.6 Eigenvalue Matrix used in the analysis of the Symmetric Modes of the Orthotropic Cantilever Plate

The segments of the matrix are referred to by pairs of numbers (x,y), the elements within each are as follows:

Segment (1,1)

$$A\left(\frac{m+1}{2},\frac{m+1}{2}\right) = \textit{Equation } 2.19 \textit{ or } 2.20 \textit{ or } 2.21$$
$$\textit{for } m = 1, 3, 5, \ldots\ldots, 2k-1$$

Segment (1,2)

$$A\left(\frac{m+1}{2},k+n+1\right) = 2\int\{\textit{Equation } 2.29 \textit{ or } 2.30 \textit{ or } 2.31\}\sin\frac{m\pi\xi}{2}d\xi$$
$$\textit{for } n = 0, 1, 2, \ldots\ldots, k-1$$

Segment (1,3)

$$A\left(\frac{m+1}{2}, 2k+p+1\right) = 2\int \{Equation\ 2.38\ or\ 2.39\ or\ 2.40\} \sin\frac{m\pi\xi}{2} d\xi$$
$$for\ p = 0,\ 1,\ 2,\ .....,\ k-1$$

Segment (2,1)

$$A\left(k+n+1, \frac{m+1}{2}\right) = 2\int \{Equation\ 2.23\ or\ 2.24\ or\ 2.25\} \cos n\pi\eta\, d\eta$$
$$for\ n = 0,1,2,.....,k-1\ ;\ m = 1,3,5,...,2k-1$$

Segment (2,2)

$$A\ (k+n+1, k+n+1) = Equation\ 2.32\ or\ 2.33\ or\ 2.34$$
$$for\ n = 0,1,2,.....,k-1$$

Segment (2,3)

$$A\ (k+p+1, k+p+1) = Equation 2.41\ or\ 2.42\ or\ 2.43$$
$$for\ p = 0,1,2,.....,k-1$$

Segment (3,1)

$$A\left(2k+n+1, \frac{m+1}{2}\right) = 2\int \{Equation\ 2.26\ or\ 2.27\ or\ 2.28\} \cos n\pi\eta\, d\eta$$
$$for\ n = 0,1,2,.....,k-1\ ;\ m = 1,3,5,...,2k-1$$

Segment (3,2)

$$A\ (2k+n+1, k+n+1) = Equation\ 2.35\ or\ 2.36\ or\ 2.37$$
$$for\ n = 0,1,2,.....,k-1$$

Segment (3,3)

$$A\ (2k+p+1, 2k+p+1) = -1$$
$$for\ p = 0,1,2,.....,k-1$$

The above information is fed into the computer program 1 of Appendix A to generate eigenvalues for the first four modes and their appropriate mode shapes. The results are tabulated and discussed in the section 2.3. The antisymmetric modes are next examined.

2.2 ANTISYMMETRIC MODES

The procedures followed in the analysis of antisymmetric modes are the same as those carried out in the case of symmetric modes. Only half of the full plate needs to be considered as shown in Figure 2.7. Three building blocks are required with their appropriate boundary conditions. The main difference between these blocks and those in symmetric analysis is that along edge η=0 simple supports are enforced instead of slip shear conditions due to antisymmetric with respect to the ξ-axis.

2.2.1 Solution of the first building block

The first building block employs simple support boundaries along the edges ξ=0, and η=0; and slip shear condition imposed on edge ξ=1. The prescribed slope which varies cyclicly with time at the same frequency as the plate vibration is enforced along the free edge η=1. The Lévy type solution for this block can be written as

$$W_1(\xi,\eta) = \sum_{m=1,3,5}^{\infty} Y_m(\eta) \sin\frac{m\pi\xi}{2} \tag{2.52}$$

Substitute (2.52) into the GDE in order to obtain expressions for $Y_m(\eta)$ (Eq. 1.25 - 27), the symmetric terms are deleted so simple support condition @ η=0 is satisfied. By enforcing the condition of zero vertical edge reaction along the edge η=1 (Equation 1.15) and the harmonic slope, the solution can therefore be expressed as (derivation is found in Appendix A):

$$W_1(\xi,\eta) = \sum_{m=1,3}^{k^*} E_m \{\theta_{11m}\sinh \beta_m\eta + \theta_{13m}\sin \gamma_m\eta\} \sin\frac{m\pi\xi}{2} + \sum_{k^*+2}^{\infty} E_m \{\theta_{22m}\sinh \beta_m\eta + \theta_{23m}\sinh \gamma_m\eta\} \sin\frac{m\pi\xi}{2} \tag{2.53}$$

or

$$E_m [\theta_{33m}\sin R\eta \cosh S\eta + \theta_{333m}\cos R\eta \sinh S\eta] \sin\frac{m\pi\xi}{2}$$

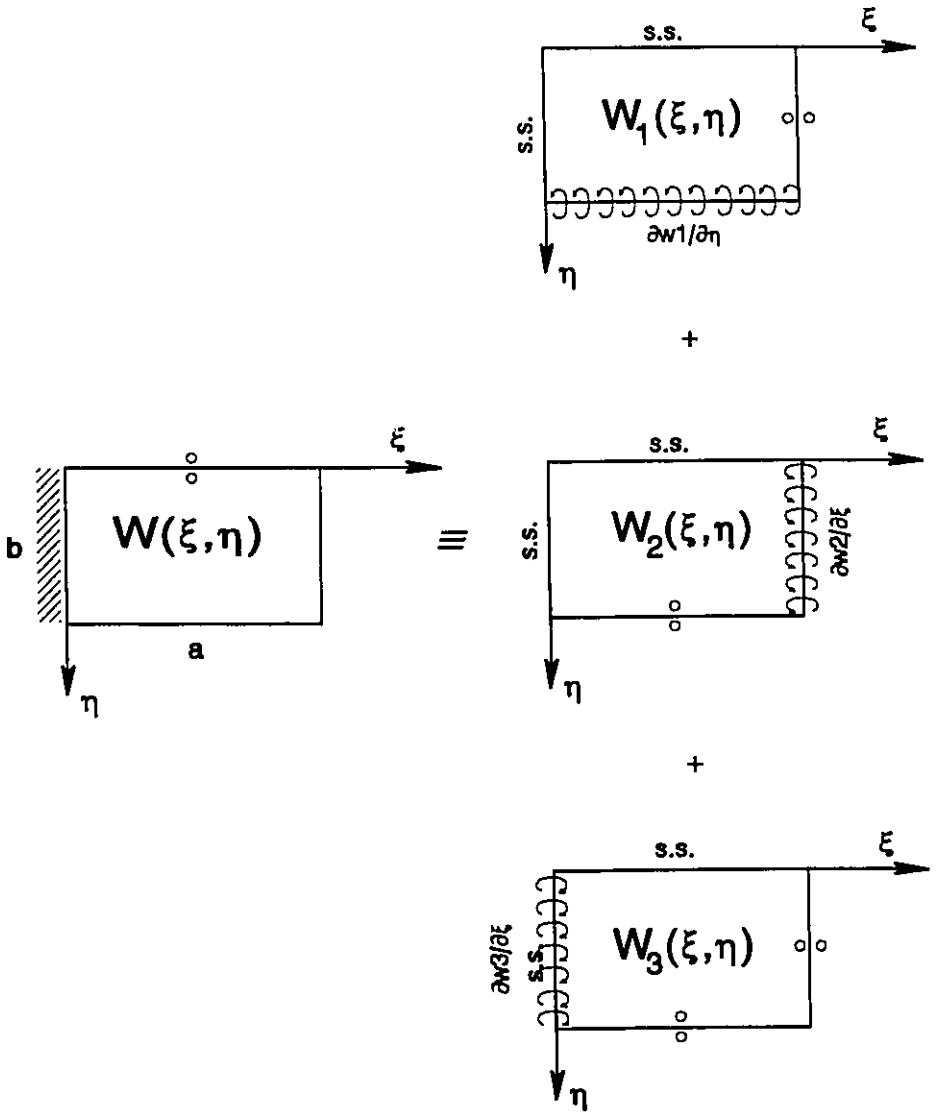

Figure 2.7 Building Blocks utilized in analyzing the free vibration antisymmetric modes of the orthotropic cantilever plate

2.2.2 Solution of the second building block

Examination of building block #2 reveals that it is exactly identical to the first building block with the coordinates ξ and η interchanged. Therefore, the solution for this building block is derived from the solution of section 2.2.1 by following the transformation rules - multiply eigenvalue λ^2 by ϕ^2 and change ϕ into $1/\phi$. Subscript m is replaced with n to distinguish the solution from that of the first building block. In addition, the moment imposed along edge $\xi=1$ is expanded with respect to η. Accordingly, the solution is

$$W_2(\xi,\eta) = \sum_{n=1,3}^{k^*} E_n \{\theta_{11n}\sinh \beta_n\xi + \theta_{23n}\sin \gamma_n\xi\} \sin\frac{n\pi\eta}{2} + \sum_{k^*+2}^{\infty} E_n \{\theta_{22n}\sinh \beta_n\xi + \theta_{23n}\sinh \gamma_n\xi\} \sin\frac{n\pi\eta}{2} \quad (2.54)$$

or

$$E_n [\theta_{33n}\sin R\xi \cosh S\xi + \theta_{333n}\cos R\xi \sinh S\xi] \sin\frac{n\pi\eta}{2}$$

2.2.3 Solution of the third building block

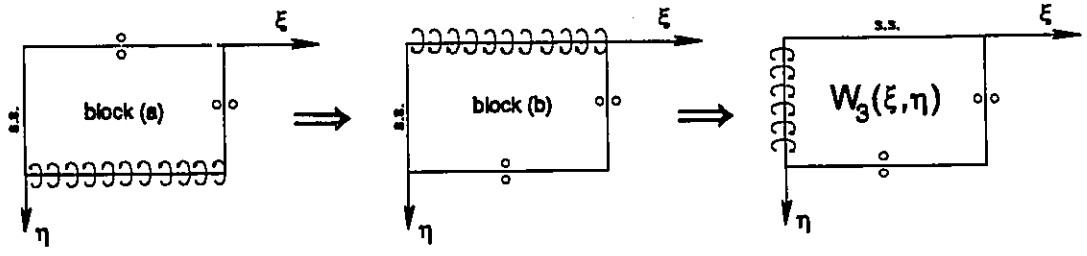

Figure 2.8 Intermediate blocks used in the solution of building block #3

The task of finding the third building block solution is made easier by using intermediate blocks which resemble those used previously. Firstly, building block (a) of Figure 2.8 is solved, then by changing variable η into $(1-\eta)$ leads to solution for block (b). Finally, the required third block solution is obtained by interchanging the ξ and η coordinates and following all the transformation rules. Appendix A contains all solutions of these blocks, only the final solution is given here

$$W_3(\xi,\eta) = \sum_{p=1,3,5}^{k^*} E_p \{\theta_{11p}\cosh\beta_p(1-\xi) + \theta_{13p}\cos\gamma_p(1-\xi)\}\sin\frac{p\pi\eta}{2} + \sum_{k^*+2}^{\infty} E_p \{\theta_{22p}\cosh\beta_p(1-\xi) + \theta_{23p}\cosh\gamma_p(1-\xi)\}\sin\frac{p\pi\eta}{2} \quad (2.55)$$

or

$$E_p \{\theta_{33p}\sin R(1-\xi)\sinh S(1-\xi) + \theta_{333p}\cos R(1-\xi)\cosh S(1-\xi)\}\sin\frac{p\pi\eta}{2}$$

2.2.4 Generation of Eigenvalue Matrix for Antisymmetric Modes

Now that the solutions for each building block of Figure 2.7, Equations 2.53, 2.54, and 2.55 are found, the next step is to superimpose these solutions and adjust their unknown coefficients so the prescribed boundary conditions of the orthotropic cantilever plate are satisfied so an eigenvalue matrix could be generated. This section will describe such procedures. Examination of the contributions of individual block to the final constrained boundary conditions must first be done.

1.1 Contribution of the first building block, $W_1(\xi,\eta)$ to bending moment along edge $\eta=1$ of the cantilever plate. By using Equation 2.56, performing the necessary differentiations and collecting terms yields Equations 2.57, 2.58, 2.59 for each *m*th term

$$\frac{M_y b^2}{aD_y}\Big|_{\eta=1} = -\left\{\frac{\partial^2 W(\xi,\eta)}{\partial\eta^2} + \upsilon_x\phi^2\,\frac{\partial^2 W(\xi,\eta)}{\partial\xi^2}\right\} \tag{2.56}$$

case 1

$$E_m\left\{\begin{array}{l}[\upsilon_x\phi^2(\frac{m\pi}{2})^2 - \beta_m^2]\;\theta_{11m}\sinh\beta_m \\ \qquad + \quad [\upsilon_x\phi^2(\frac{m\pi}{2})^2 + \gamma_m^2]\;\theta_{13m}\sin\gamma_m\end{array}\right\}\sin\frac{m\pi\xi}{2} \tag{2.57}$$

case 2

$$E_m\left\{\begin{array}{l}[\upsilon_x\phi^2(\frac{m\pi}{2})^2 - \beta_m^2]\;\theta_{22m}\sinh\beta_m \\ \qquad + \quad [\upsilon_x\phi^2(\frac{m\pi}{2})^2 - \gamma_m^2]\;\theta_{23m}\sinh\gamma_m\end{array}\right\}\sin\frac{m\pi\xi}{2} \tag{2.58}$$

$$E_m\left\{\begin{array}{l}-[(\theta_{33m}(S^2-R^2) - 2RS\theta_{333m}) - \upsilon_x\phi^2(\frac{m\pi}{2})^2\theta_{33m}]\;\sin R\cosh S \\ -[(\theta_{33m}2RS + \theta_{333m}(S^2-R^2)) - \upsilon_x\phi^2(\frac{m\pi}{2})^2\theta_{333m}]\;\cos R\sinh S\end{array}\right\}\sin\frac{m\pi\xi}{2} \tag{2.59}$$

[1.2] Contribution of $W_1(\xi,\eta)$ to bending moment along edge $\xi=1$ of the cantilever plate. Using Equation 2.60, The followings are obtained for the three cases respectively:

$$\frac{M_\xi a}{D_x}\Big|_{\xi=1} = -\left\{\frac{\partial^2 W(\xi,\eta)}{\partial\xi^2} + \frac{\upsilon_y}{\phi^2}\,\frac{\partial^2 W(\xi,\eta)}{\partial\eta^2}\right\} \tag{2.60}$$

$$E_m\left\{\begin{array}{l}[(\frac{m\pi}{2})^2 - \frac{\upsilon_y}{\phi^2}\beta_m^2]\;\theta_{11m}\sinh\beta_m\eta \\ \qquad + \quad [(\frac{m\pi}{2})^2 + \frac{\upsilon_y}{\phi^2}\gamma_m^2]\;\theta_{13m}\sin\gamma_m\eta\end{array}\right\}\sin\frac{m\pi}{2} \tag{2.61}$$

$$E_m \left\{ \begin{array}{l} [(\frac{m\pi}{2})^2 - \frac{\upsilon_y}{\phi^2}\beta_m^2]\ \theta_{22m}\sinh\beta_m\eta \\ \qquad + \quad [(\frac{m\pi}{2})^2 - \frac{\upsilon_y}{\phi^2}\gamma_m^2]\ \theta_{23m}\sinh\gamma_m\eta \end{array} \right\} \sin\frac{m\pi}{2} \tag{2.62}$$

$$E_m \left\{ \begin{array}{l} [(\frac{m\pi}{2})^2\theta_{33m} - \frac{\upsilon_y}{\phi^2}\ (\theta_{33m}(S^2-R^2) - 2RS\theta_{333m})\ ]\ \sin R\eta\ \cosh S\eta \\ \quad + \ [(\frac{m\pi}{2})^2\theta_{333m} - \frac{\upsilon_y}{\phi^2}\ (\theta_{33m}2RS + \theta_{333m}(S^2-R^2))]\ \cos R\eta\ \sinh S\eta \end{array} \right\} \sin\frac{m\pi}{2} \tag{2.63}$$

[1.3] Contribution of $W_1(\xi,\eta)$ to the slope along edge $\xi=0$ of cantilever plate.

$$\frac{\partial W_1}{\partial \xi}|_{\xi=0} = E_m(\frac{m\pi}{2})\ \{\ \theta_{11m}\ \sinh\ \beta_m\eta\ +\ \theta_{13m}\ \sin\ \gamma_m\eta\ \} \tag{2.64}$$

$$\frac{\partial W_1}{\partial \xi}|_{\xi=0} = E_m(\frac{m\pi}{2})\ \{\ \theta_{22m}\ \sinh\ \beta_m\eta\ +\ \theta_{23m}\ \sinh\ \gamma_m\eta\ \} \tag{2.65}$$

$$\frac{\partial W_1}{\partial \xi}|_{\xi=0} = E_m(\frac{m\pi}{2})\ \{\ \theta_{33m}\ \sin R\eta\ \cosh S\eta\ +\ \theta_{333m}\cos R\eta\ \sinh S\eta\ \} \tag{2.66}$$

[2.1] Contribution of the second building block, $W_2(\xi,\eta)$ to bending moment along edge $\eta=1$ of the cantilever plate. Using Eq. 2.56, for each nth term of this solution,

$$E_n \left\{ \begin{array}{l} [(\frac{n\pi}{2})^2 - \upsilon_x\phi^2\beta_n^2]\ \theta_{11n}\sinh\beta_n\xi \\ \qquad + \quad [(\frac{n\pi}{2})^2 + \upsilon_x\phi^2\gamma_n^2]\ \theta_{13n}\sin\gamma_n\xi \end{array} \right\} \sin\frac{n\pi}{2} \tag{2.67}$$

$$E_n \left\{ \begin{array}{l} [(\frac{n\pi}{2})^2 - \upsilon_x\phi^2\beta_n^2]\ \theta_{22n}\sinh\beta_n\xi \\ \qquad + \quad [(\frac{n\pi}{2})^2 - \upsilon_x\phi^2\gamma_n^2]\ \theta_{23n}\sinh\gamma_n\xi \end{array} \right\} \sin\frac{n\pi}{2} \tag{2.68}$$

$$E_n \left\{ \begin{array}{l} [(\frac{n\pi}{2})^2 - \upsilon_x\phi^2\ (\theta_{33n}(S^2-R^2) - 2RS\theta_{333n})\ ]\ \sin R\xi\cosh S\xi \\ \quad + \quad [(\frac{n\pi}{2})^2 - \upsilon_x\phi^2\ (\theta_{33n}2RS + \theta_{333n}(S^2-R^2)\ )\ ]\ \cos R\xi\sinh S\xi \end{array} \right\} \sin\frac{n\pi}{2} \tag{2.69}$$

2.2 Contribution of $W_2(\xi,\eta)$ to bending moment along edge $\xi=1$. Equation 2.60 provides

$$E_n \left\{ \begin{array}{l} [-\beta_n^2 + \frac{\upsilon_y}{\phi^2}(\frac{n\pi}{2})^2]\ \theta_{11n}\sinh\beta_n \\ \qquad + \quad [\ \gamma_n^2 + \frac{\upsilon_y}{\phi^2}(\frac{n\pi}{2})^2]\ \theta_{13n}\sin\gamma_n \end{array} \right\} \sin\frac{n\pi\eta}{2} \tag{2.70}$$

$$E_n \left\{ \begin{array}{l} [-\beta_n^2 + \frac{\upsilon_y}{\phi^2}(\frac{n\pi}{2})^2]\ \theta_{22n}\sinh\beta_n \\ \qquad + \quad [\ -\gamma_n^2 + \frac{\upsilon_y}{\phi^2}(\frac{n\pi}{2})^2]\ \theta_{23n}\sinh\gamma_n \end{array} \right\} \sin\frac{n\pi\eta}{2} \tag{2.71}$$

$$E_n \left\{ \begin{array}{l} [\ -(\theta_{33n}(S^2-R^2) - 2RS\theta_{333n}) + \frac{\upsilon_y}{\phi^2}(\frac{n\pi}{2})^2\ ]\ \sin R\cosh S \\ \quad + \quad [\ -(\theta_{33n}2RS + \theta_{333n}(S^2-R^2)\ ) + \frac{\upsilon_y}{\phi^2}(\frac{n\pi}{2})^2\ ]\ \cos R\sinh S \end{array} \right\} \sin\frac{n\pi\eta}{2} \tag{2.72}$$

[2.3] Contribution of $W_2(\xi,\eta)$ to the slope along edge $\xi=0$.

$$\frac{\partial W_2}{\partial \xi}\Big|_{\xi=0} = E_n \left\{ \theta_{11n}\, \beta_n + \theta_{13n}\, \gamma_n \right\} \sin\frac{n\pi\eta}{2} \tag{2.73}$$

$$\frac{\partial W_2}{\partial \xi}\Big|_{\xi=0} = E_n \left\{ \theta_{22n}\, \beta_n + \theta_{23n}\, \gamma_n \right\} \sin\frac{n\pi\eta}{2} \tag{2.74}$$

$$\frac{\partial W_2}{\partial \xi}\Big|_{\xi=0} = E_n \left\{ \theta_{33n} R + \theta_{333n} S \right\} \sin\frac{n\pi\eta}{2} \tag{2.75}$$

[3.1] Contribution of the third building block, $W_3(\xi,\eta)$ to bending moment along edge $\eta=1$. Equation 2.56 provides, for each pth term of this solution

$$E_p \left\{ \begin{array}{l} [(\frac{p\pi}{2})^2 - \upsilon_x \phi^2 \beta_p^2]\ \theta_{11p} \cosh\beta_p (1-\xi) \\ \qquad + \quad [(\frac{p\pi}{2})^2 + \upsilon_x \phi^2 \gamma_p^2]\ \theta_{13p} \cos\gamma_p (1-\xi) \end{array} \right\} \sin\frac{p\pi}{2} \tag{2.76}$$

$$E_p \left\{ \begin{array}{l} [(\frac{p\pi}{2})^2 - \upsilon_x \phi^2 \beta_p^2]\ \theta_{22p} \cosh\beta_p (1-\xi) \\ \qquad + \quad [(\frac{p\pi}{2})^2 - \upsilon_x \phi^2 \gamma_p^2]\ \theta_{23p} \cosh\gamma_p (1-\xi) \end{array} \right\} \sin\frac{p\pi}{2} \tag{2.77}$$

$$E_p \left\{ \begin{array}{l} [(\frac{p\pi}{2})^2 \theta_{33p} - \upsilon_x \phi^2\ (\theta_{33p}(S^2 - R^2) - 2RS\theta_{333p})\ ]\ \sin R(1-\xi) \sinh S(1-\xi) \\ + [(\frac{p\pi}{2})^2 \theta_{333p} - \upsilon_x \phi^2\ (\theta_{33p} 2RS + \theta_{333p}(S^2 - R^2))]\ \cos R(1-\xi) \cosh S(1-\xi) \end{array} \right\} \sin\frac{p\pi}{2}$$

(2.78)

[3.2] Contribution of $W_3(\xi,\eta)$ to bending moment along edge $\xi=1$. Using Eq. 2.60

$$E_p \left\{ \left[-\beta_p^2 + \frac{\upsilon_y}{\phi^2}\left(\frac{p\pi}{2}\right)^2 \right] \theta_{11p} + \left[\gamma_p^2 + \frac{\upsilon_y}{\phi^2}\left(\frac{p\pi}{2}\right)^2 \right] \theta_{13p} \right\} \sin\frac{p\pi\eta}{2} \tag{2.79}$$

$$E_p \left\{ \left[-\beta_p^2 + \frac{\upsilon_y}{\phi^2}\left(\frac{p\pi}{2}\right)^2 \right] \theta_{22p} + \left[-\gamma_p^2 + \frac{\upsilon_y}{\phi^2}\left(\frac{p\pi}{2}\right)^2 \right] \theta_{23p} \right\} \sin\frac{p\pi\eta}{2} \tag{2.80}$$

$$E_p \left\{ \left[-(\theta_{33p} 2RS + \theta_{333p}(S^2 - R^2)) + \frac{\upsilon_y}{\phi^2}\left(\frac{p\pi}{2}\right)^2 \theta_{333p} \right] \right\} \sin\frac{p\pi\eta}{2} \tag{2.81}$$

[3.3] Contribution of $W_3(\xi,\eta)$ to the slope along edge $\xi=0$.

$$\frac{\partial W_3}{\partial \xi}\Big|_{\xi=0} = - E_p \sin\frac{p\pi\eta}{2} \tag{2.82}$$

$$\frac{\partial W_3}{\partial \xi}\Big|_{\xi=0} = - E_p \sin\frac{p\pi\eta}{2} \tag{2.83}$$

$$\frac{\partial W_3}{\partial \xi}\Big|_{\xi=0} = - E_p \sin\frac{p\pi\eta}{2} \tag{2.84}$$

I. Along edge $\eta=1$ of the cantilever plate, the net contributions of the three building blocks to the bending moment must be zero in order to satisfy the free edge condition. One can write,

$$Equation \begin{Bmatrix} 2.57 \\ 2.58 \\ 2.59 \end{Bmatrix} + Equation \begin{Bmatrix} 2.67 \\ 2.68 \\ 2.69 \end{Bmatrix} + Equation \begin{Bmatrix} 2.76 \\ 2.77 \\ 2.78 \end{Bmatrix} = 0 \tag{2.85}$$

The second and third term of Eq. 2.85 must be expanded in the series $\sin(m\pi\xi/2)$.

II. Focusing on the edge $\xi=1$ of the plate, the combined bending moment contributions must be set to zero to satisfy the free edge condition.

$$Equation \begin{Bmatrix} 2.61 \\ 2.62 \\ 2.63 \end{Bmatrix} + Equation \begin{Bmatrix} 2.70 \\ 2.71 \\ 2.72 \end{Bmatrix} + Equation \begin{Bmatrix} 2.79 \\ 2.80 \\ 2.81 \end{Bmatrix} = 0 \qquad (2.86)$$

The first term of Eq. 2.86 has to be expanded in the series $\sin(n\pi\eta/2)$.

III. The contributions to the slope along the clamp edge of the plate $\xi=0$ is

$$Equation \begin{Bmatrix} 2.64 \\ 2.65 \\ 2.66 \end{Bmatrix} + Equation \begin{Bmatrix} 2.73 \\ 2.74 \\ 2.75 \end{Bmatrix} + Equation \begin{Bmatrix} 2.82 \\ 2.83 \\ 2.84 \end{Bmatrix} = 0 \qquad (2.87)$$

The first term of Eq. 2.87 is multiplied by $2\sin(n\pi\eta/2)$ and integrated from 0 to 1.

The matrix relating unknown coefficients E_m's, E_n's, and E_p's is similar to that in Figure 2.6 for the symmetric mode analysis except that m = 1,3,5. A matrix is then generated by the computer.

The segments of the matrix are as follows:

Segment (1,1)

$$A\left(\frac{m+1}{2},\frac{m+1}{2}\right) = Equation 2.57 \ or \ 2.58 \ or \ 2.59$$
$$for\ m = 1, 3, 5, \ldots\ldots, 2k-1$$

Segment (1,2)

$$A\left(\frac{m+1}{2},\frac{n+1}{2}+k\right) = 2\int_0^1 \{Equation\ 2.67\ or\ 2.68\ or\ 2.69\} \sin\frac{m\pi\xi}{2} d\xi$$
$$for\ m\ and\ n = 1, 3, 5, \ldots\ldots, 2k-1$$

Segment (1,3)

$$A\left(\frac{m+1}{2},\frac{p+1}{2}+2k\right) = 2\int_0^1 \{\textit{Equation } 2.76 \textit{ or } 2.77 \textit{ or } 2.78\} \sin\frac{m\pi\xi}{2} d\xi$$

$$\textit{for } m \textit{ and } p = 1, 3, 5, \ldots\ldots, 2k-1$$

Segment (2,1)

$$A\left(\frac{n+1}{2}+k,\frac{m+1}{2}\right) = 2\int_0^1 \{\textit{Equation } 2.61 \textit{ or } 2.62 \textit{ or } 2.63\} \sin\frac{n\pi\eta}{2} d\eta$$

$$\textit{for } m \textit{ and } n = 1,3,5,\ldots\ldots,2k-1$$

Segment (2,2)

$$A\left(\frac{n+1}{2}+k,\frac{n+1}{2}+k\right) = \textit{Equation } 2.70 \textit{ or } 2.71 \textit{ or } 2.72$$

$$\textit{for } n = 1,3,5,\ldots\ldots,2k-1$$

Segment (2,3)

$$A\left(\frac{p+1}{2}+k,\frac{p+1}{2}+2k\right) = \textit{Equation } 2.79 \textit{ or } 2.80 \textit{ or } 2.81$$

$$\textit{for } p = 1,3,5,\ldots\ldots,2k-1$$

Segment (3,1)

$$A\left(\frac{n+1}{2}+2k,\frac{m+1}{2}\right) = 2\int_0^1 \{\textit{Equation } 2.64 \textit{ or } 2.65 \textit{ or } 2.66\} \sin\frac{n\pi\eta}{2} d\eta$$

$$\textit{for } m \textit{ and } n = 1,3,5,\ldots,2k-1$$

Segment (3,2)

$$A\left(\frac{n+1}{2}+2k,\frac{n+1}{2}+k\right) = \textit{Equation } 2.73 \textit{ or } 2.74 \textit{ or } 2.75$$

$$\textit{for } n = 1,3,5,\ldots\ldots,2k-1$$

Segment (3,3)

$$A\left(\frac{p+1}{2}+2k,\frac{p+1}{2}+2k\right) = -1$$
$$for\ p = 1,3,5,.....,2k-1$$

The above information is fed into a specially written computer program to generate eigenvalues for the first four modes and their appropriate mode shapes. The results are tabulated and discussed in the next section.

2.3 RESULTS AND DISCUSSION

In summary, as a result of the prescribed boundary conditions, the superposition allows a set of 3k homogeneous algebraic equations relating the 3k unknown coefficients E_m's, E_n's, and E_p's. The eigenvalues for the orthotropic cantilever plates are determined by the following procedure.

1. A trial value is selected for the parameter λ^2, this must be small enough so the first mode eigenvalue could be found.
2. By substituting this value into the expressions developed, the matrix is generated.
3. The determinant of the matrix is evaluated and stored.
4. The trial value is increased by a specified increment (typically 0.1) and steps 1 to 3 are repeated until the determinant undergoes a sign change ie. zero crossing. The eigenvalue is then obtained by reducing the increment to make the determinant vanish, the associated λ^2 is the eigenvalue. The procedure can be repeated for higher eigenvalues.
5. Coefficients E_m's, E_n's, and E_p's are then solved by arbitrarily setting one of them to unity; it is customary to set the last coefficient of the matrix to unity. Then the remaining 3k-1 non-homogeneous equations are solved using the standard elimination technique.
6. $W_1(\xi,\eta)$, $W_2(\xi,\eta)$, $W_3(\xi,\eta)$ are determined using the computed E_m's, E_n's, and E_p's values. Hence the mode shape, $W(\xi,\eta)= W_1 + W_2 + W_3$, associated with the λ^2 eigenvalue is found.

An eigenvalue search was conducted for the orthotropic cantilever plate using a specially designed computer program. The results are tabulated in Appendix B. The eigenvalues were computed to four significant digit accuracy. In order to achieve this kind of accuracy, the number of terms k, used in each of the Fourier series involved in the solution, must be determined. Convergence tests were conducted as shown in Figure 2.9 and 2.10. Inspection of these figures show that four digit accuracy in the eigenvalues is achieved with 8 or more terms; computation of eigenvalues was carried out with 15 terms to insure the required accuracy. In order to save computer running time , the preliminary computer runs (steps 1-3 in the procedure) were performed with 8 terms and the final passes (step 4) utilized 15 terms.

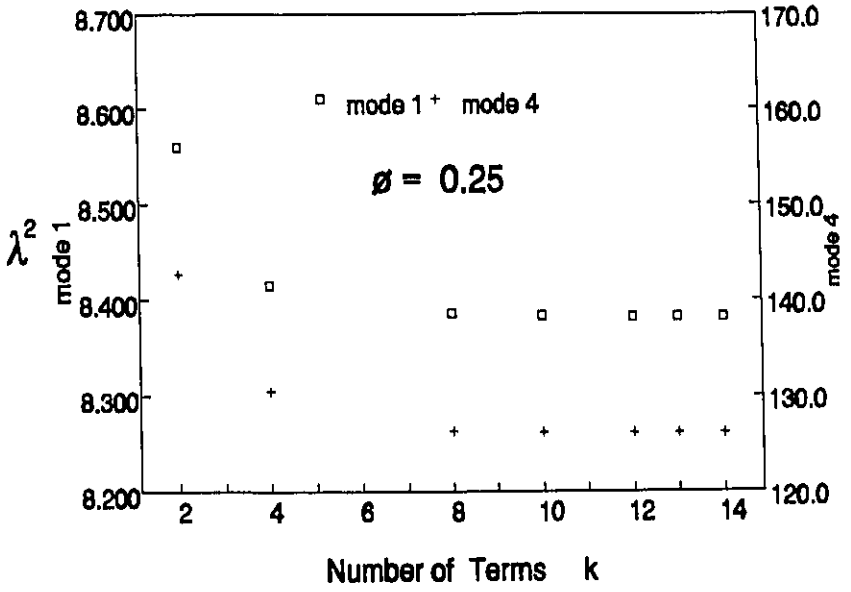

Figure 2.9 Convergence test (antisymmetric mode DHY=0.5, DHX=0.5)

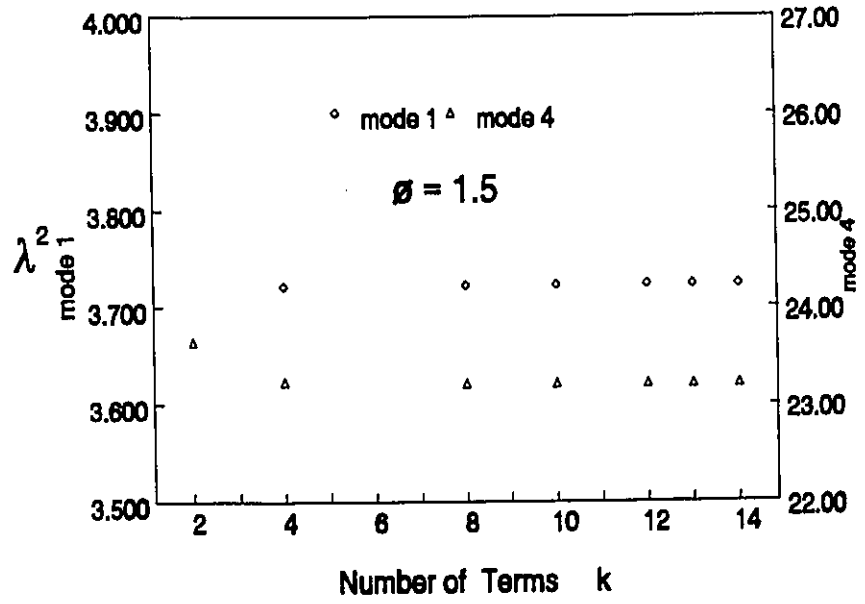

Figure 2.10 Convergence test (antisymmetric mode DHY=0.5, DHX=0.5)

Tables B1.1 - B1.25 contains eigenvalues for the first four symmetric modes of the orthotropic cantilever plates. These eigenvalue tables covered a wide range of aspect ratios, $\phi(b/a)=0.25$ to 1.5 (full plate $\phi=2b/a$), the material constants DHY and DHX ranges from 0.5 to 2.0. Tables B2.1 - B2.25 includes eigenvalues for the first four antisymmetric modes with the same plate geometry range and material constants.

Even though the analysis is valid for any combination of plate geometries and material properties, it is impossible to cover all orthotropic materials so it was decided to restrict eigenvalue compilation to a particular subset of these problems. Timoshenko [3] and Szilard [4] point out that H can be approximated to be $\sqrt{D_x D_y}$, this approximation is most closely applied to thin reinforced concrete, and the product $\upsilon_x\upsilon_y$ is defined as $\sqrt{\upsilon_x\upsilon_y}=0.333$. It should be pointed out that the accuracy of the analysis of orthotropic plates depends, to a large extent, on the expressions used for the sectional properties, direct tests if possible, should be applied to determine the actual flexural and torsional rigidities.

Since the analysis of orthotropic cantilever plates, to the author's knowledge, has never been performed by other researchers, no published data are available for comparison in the accuracy of results. However, for a special case of orthotropy DHY=1.0 and DHX=1.0 - isotropic case, the problem was solved by Gorman [1] and Saliba [2]. The results were found to be identical with those in [1] and [2], insignificant differences in some of the higher modes are due to computational errors and/or difference in the number of terms used. The agreement increases confidence in the method of analysis.

Researchers and designers not only appreciate the vast number of eigenvalue tables included but also how the results could be envisioned. Pictorial representation can provide an intuitive understanding of data and points out specific behavioural patterns which are almost impossible to discover in numerical information. Figures B1.1 - B1.10 in Appendix B include the first four mode shapes and associated contour plots for symmetric case. The plots associate with square plates with full aspect ratio of one ($2\phi=1$) and various levels of orthotropy (DHY and DHX=0.5, 1.0, and 2.0). Similarly, Figure B2.1 - B2.10 are plots of the antisymmetric case. It is observed that the lower the directional rigidity (high values of DHY or DHX, note that $DHY=H/D_y$) is, the more the plate tends to "curve" in that direction. For instance, a low value

of DHY (0.5) and a high value of DHX (2.0) - Figure B1.3 shows that the cantilever plate acts almost as a cantilever beam ie. very little deflection in the y-direction; this can be compared with Figure B1.7 for the opposite case of DHY=2.0 and DHX=0.5, These figures confirm the validity of results, in other words the 3-D plots disclose that the boundary & continuity conditions are satisfied and whether symmetry or antisymmetry are revealed. These mode shapes and contour pictures also enable the analysts to locate the areas of a plate, when vibrating in a specific mode, that most likely to undergo high displacement and bending stresses.

The analysis of orthotropic cantilever plates using the method of superposition is now completed. Attention is next turned to analysing the plates with internal point supports.

Chapter 3

Orthotropic Cantilever Plate With Lateral Point Supports

Free vibration analysis of orthotropic cantilever plate was fully carried out in Chapter 2. In this chapter, internal supports are introduced to the plate as shown in Figure 3.1. The point supports are symmetric with respect to the ξ axis and take on coordinates of u and v where lateral movement of the plate is forbidden. There now exists two conditions that must be satisfied to ensure solutions of the Lévy type are obtainable and also that the method of superposition is applicable:

- The governing differential equation for orthotropic plates is satisfied.
- The lateral loadings - due to point supports and imposed boundary conditions do not present any nonlinearities into the analysis.

When the plate is assumed to vibrate in one of its vibration modes with circular frequency ω, then the lateral motion at the fixed point support (u,v) must be restrained by an opposing time varying force, represented as $P\sin\omega t$ where P is the amplitude of the harmonic force. Solution of this type of lateral loading is presented in Ref. [1]. As before, the examination of vibration modes will be divided into two families - Symmetric and Antisymmetric. Due to symmetry of the point supports only half of the plate is analysed.

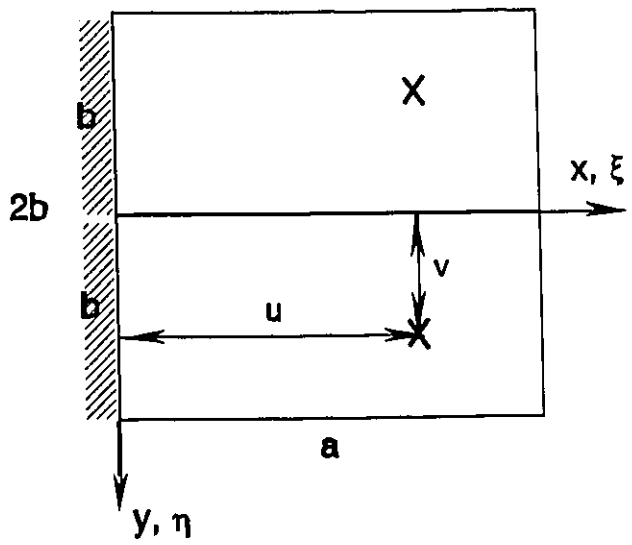

Figure 3.1 Cantilever Plate with Point Supports

3.1 SYMMETRIC MODES

The building blocks used in the analysis of symmetric family of modes are shown in Figure 3.2. The first three blocks are identical to those employed in Chapter 2.1 whose solutions are already developed. The fourth building block is the additional one to represent the forcing condition. This block is divided into two segments I and II, division line between segments is parallel to the ξ axis at $\eta = v$ as shown in Figure 3.3; in addition, it should be noted that each segment has its own coordinate system.

SOLUTION OF THE FOURTH BUILDING BLOCK:

This building block was used by Saliba [Ref.2] in his analysis of isotropic cantilever plate with point supports. A similar block was also used by Gorman [Ref.1] in the analysis of symmetric ξ - antisymmetric η axis for rectangular plate with symmetrically distributed point supports. Although parts of the solution are readily available, it is necessary to develop a complete solution for the orthotropic case.

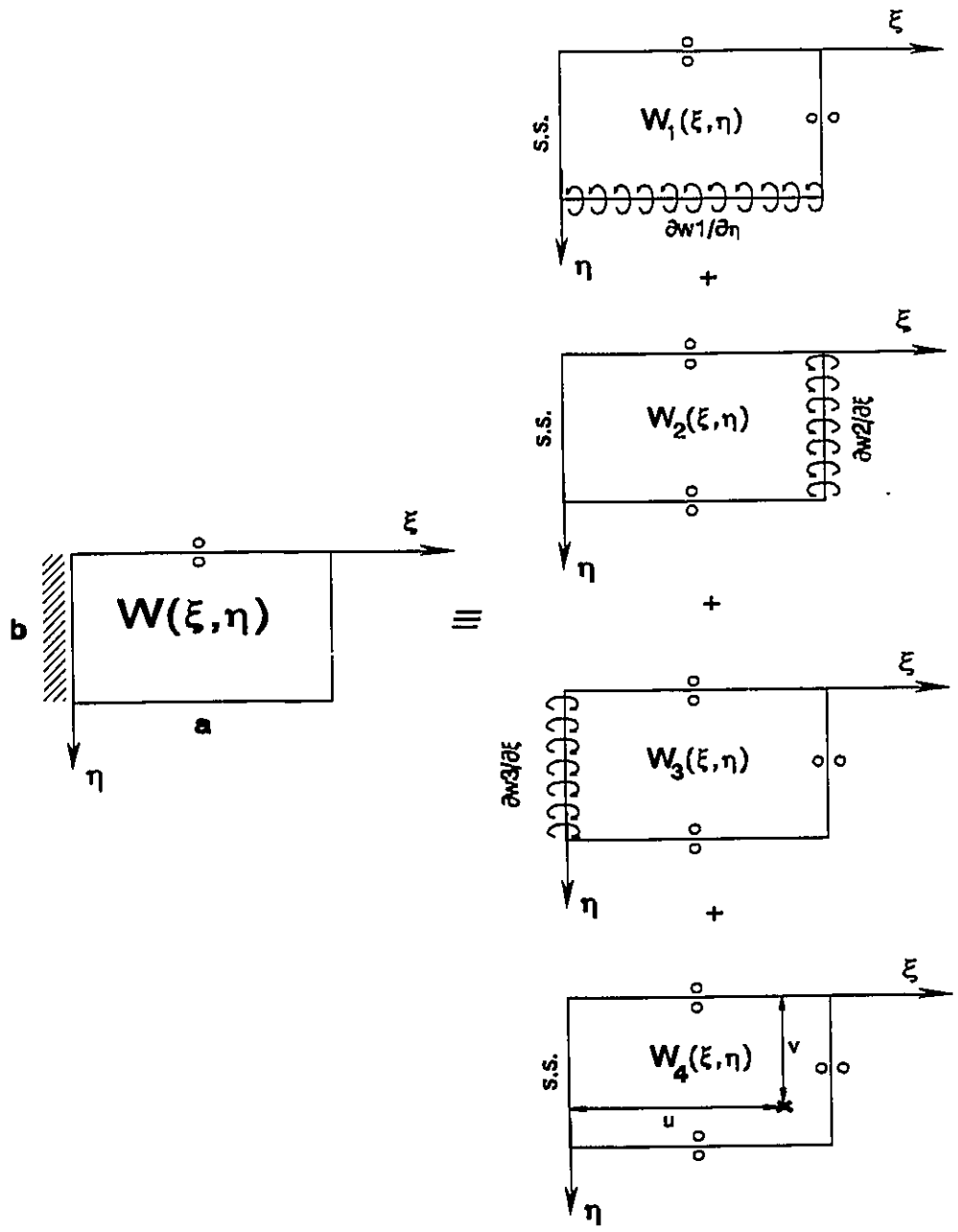

Figure 3.2 Building Blocks used in analyzing free vibration symmetric modes of the orthotropic plate with lateral point supports

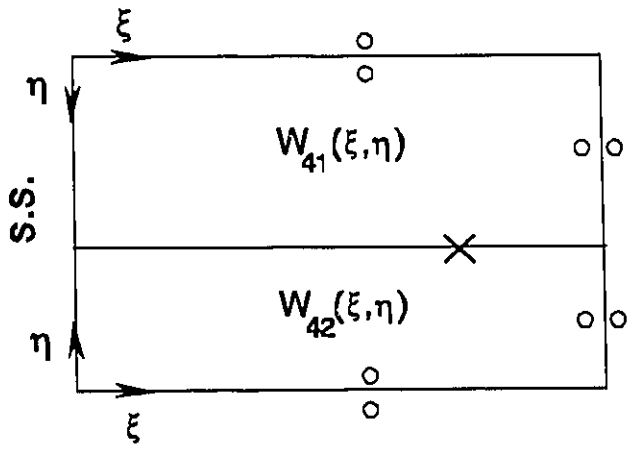

Figure 3.3 Fourth building block divided into two segments

With respect to the boundary conditions, the Lévy-type solution may be written for each segment as follows (subscripts 1,2 refer to solutions applicable to segment I and II respectively):

Segment I:

$$W_{41}(\xi,\eta) = \sum_{m=1,3}^{k^*} \{A_{1m}\cosh\beta_m\eta + B_{1m}\cos\gamma_m\eta\}\sin\frac{m\pi\xi}{2} + \sum_{k^*+2}^{\infty} \{A_{2m}\cosh\beta_m\eta + B_{2m}\cosh\gamma_m\eta\}\sin\frac{m\pi\xi}{2} \quad \textit{or} \quad \{A_{3m}\sin R\eta\sinh S\eta + B_{3m}\cos R\eta\cosh S\eta\}\sin\frac{m\pi\xi}{2} \tag{3.1}$$

and for segment II:

$$W_{42}(\xi,\eta) = \sum_{m=1,3}^{k^*} \{C_{1m}\cosh\beta_m\eta + D_{1m}\cos\gamma_m\eta\}\sin\frac{m\pi\xi}{2} + \sum_{k^*+2}^{\infty} \{C_{2m}\cosh\beta_m\eta + D_{2m}\cosh\gamma_m\eta\}\sin\frac{m\pi\xi}{2} \quad \textit{or} \quad \{C_{3m}\sin R\eta\sinh S\eta + D_{3m}\cos R\eta\cosh S\eta\}\sin\frac{m\pi\xi}{2} \tag{3.2}$$

Where β_m, γ_m, R, and S are defined as in Chapter 1. The concentrated force is represented as

$$P(\xi) = \sum_{1,3}^{\infty} P^*\sin\frac{m\pi u}{2}\sin\frac{m\pi\xi}{2} \tag{3.3}$$

The four unknowns A_m, B_m, C_m, and D_m can be determined by enforcing the conditions of continuity and force equilibrium along the segment division line. The continuity conditions are:

1. The plate displacement must be continuous across the boundary between the two segments.

$$Y_1(\eta)\,|_{\eta=v} = Y_2(\eta)\,|_{\eta=v'} \tag{3.4}$$

2. The slope of the plate taken in the direction normal to the boundary must be continuous.

$$\frac{dY_1(\eta)}{d\eta}\,|_{\eta=v} = -\frac{dY_2(\eta)}{d\eta}\,|_{\eta=v'} \tag{3.5}$$

3. The bending moment M_η across the boundary must also be continuous.

$$\frac{d^2Y_1(\eta)}{d\eta^2}\,|_{\eta=v} = \frac{d^2Y_2(\eta)}{d\eta^2}\,|_{\eta=v'} \tag{3.6}$$

4. There must be an equilibrium force balance between the applied force $P^*\sin\omega t$ and the vertical edge reactions taken along the edges of the plate segments along the boundary.

$$\frac{d^3Y_1(\eta)}{d\eta^3}\,|_{\eta=v} + \frac{d^3Y_2(\eta)}{d\eta^3}\,|_{\eta=v'} = P^*\sin m\pi u \tag{3.7}$$

where $v^*=2-v$ and $P^* = -2Pb^3/D_y a^2$.

The right hand side of the fourth condition constitutes the series expansion for the Dirac function representing the driving force amplitude imparted by the point support. A detailed description of the development of these condition can be found in Ref.[1].

Now it is necessary to enforce the above four conditions. Three sets of equations can then be obtained so the four unknowns could be solved simultaneously. Due to the complexity of the equations involved, it is best not to solve for A_m, B_m, C_m, and D_m symbolically but rather

solving them numerically whenever required using the usual Gaussian-elimination computer subroutine. By substituting Equations 3.1 and 3.2 into each of the continuity conditions, the results are:

Case 1 - for $z>0$ and $(\sqrt{z}+\alpha_1)\geq 0$

$$A_{1m}\cosh\beta_m v + B_{1m}\cos\gamma_m v - C_{1m}\cosh\beta_m v^* - D_{1m}\cos\gamma_m v^* = 0$$

$$A_{1m}\beta_m\sinh\beta_m v - B_{1m}\gamma_m\sin\gamma_m v + C_{1m}\beta_m\sinh\beta_m v^* - D_{1m}\gamma_m\sin\gamma_m v^* = 0$$

$$A_{1m}\beta_m^2\cosh\beta_m v - B_{1m}\gamma_m^2\cos\gamma_m v - C_{1m}\beta_m^2\cosh\beta_m v^* + D_{1m}\gamma_m^2\cos\gamma_m v^* = 0$$

$$A_{1m}\beta_m^3\sinh\beta_m v + B_{1m}\gamma_m^3\sin\gamma_m v + C_{1m}\beta_m^3\sinh\beta_m v^* + D_{1m}\gamma_m^3\sin\gamma_m v^* = P^*\sin\frac{m\pi u}{2}$$

Case 2 - for $z>0$ and $(\sqrt{z}+\alpha_1)\leq 0$

$$A_{2m}\cosh\beta_m v + B_{2m}\cosh\gamma_m v - C_{2m}\cosh\beta_m v^* - D_{2m}\cosh\gamma_m v^* = 0$$

$$A_{2m}\beta_m\sinh\beta_m v + B_{2m}\gamma_m\sinh\gamma_m v - C_{2m}\beta_m\sinh\beta_m v^* + D_{2m}\gamma_m\sinh\gamma_m v^* = 0$$

$$A_{2m}\beta_m^2\cosh\beta_m v + B_{2m}\gamma_m^2\cosh\gamma_m v - C_{2m}\beta_m^2\cosh\beta_m v^* - D_{2m}\gamma_m^2\cosh\gamma_m v^* = 0$$

$$A_{2m}\beta_m^3\sinh\beta_m v + B_{2m}\gamma_m^3\sinh\gamma_m v + C_{2m}\beta_m^3\sinh\beta_m v^* + D_{2m}\gamma_m^3\sinh\gamma_m v^* = P^*\sin\frac{m\pi u}{2}$$

Case 3 - for $z<0$

$$A_{3m}x_1 + B_{3m}x_2 - C_{3m}x_3 - D_{3m}x_4 = 0$$

$$A_{3m}x_5 + B_{3m}x_6 + C_{3m}x_7 + D_{3m}x_8 = 0$$

$$A_{3m}x_9 + B_{3m}x_{10} - C_{3m}x_{11} - D_{3m}x_{12} = 0$$

$$A_{3m}x_{13} + B_{3m}x_{14} + C_{3m}x_{15} + D_{3m}x_{16} = P^*\sin\frac{m\pi u}{2}$$

Where $x_1 \Rightarrow x_{16}$ are defined as:

$$x_1 = \sin Rv \sinh Sv$$
$$x_2 = \cos Rv \cosh Sv$$
$$x_3 = \sin Rv^* \sinh Sv^*$$
$$x_4 = \cos Rv^* \cosh Sv^*$$

$$x_5 = R\cos Rv \sinh Sv + S\sin Rv \cosh Sv$$
$$x_6 = -R\sin Rv \cosh Sv + S\cos Rv \sinh Sv$$
$$x_7 = R\cos Rv^* \sinh Sv^* + S\sin Rv^* \cosh Sv^*$$
$$x_8 = -R\sin Rv^* \cosh Sv^* + S\cos Rv^* \sinh Sv^*$$

$$x_9 = [(S^2-R^2) \sin Rv \sinh Sv + 2RS\cos Rv \cosh Sv]$$
$$x_{10} = [(S^2-R^2) \cos Rv \cosh Sv - 2RS\sin Rv \sinh Sv]$$
$$x_{11} = [(S^2-R^2) \sin Rv^* \sinh Sv^* + 2RS\cos Rv^* \cosh Sv^*]$$
$$x_{12} = [(S^2-R^2) \cos Rv^* \cosh Sv^* - 2RS\sin Rv^* \sinh Sv^*]$$

$$x_{13} = [R(3S^2-R^2) \cos Rv \sinh Sv + S(S^2-3R^2) \sin Rv \cosh Sv]$$
$$x_{14} = [S(S^2-3R^2) \cos Rv \sinh Sv - R(3S^2-R^2) \sin Rv \cosh Sv]$$
$$x_{15} = [R(3S^2-R^2) \cos Rv^* \sinh Sv^* + S(S^2-3R^2) \sin Rv^* \cosh Sv^*]$$
$$x_{16} = [S(S^2-3R^2) \cos Rv^* \sinh Sv^* - R(3S^2-R^2) \sin Rv^* \cosh Sv^*]$$

The solution for the fourth building block is now complete. However, the contributions of this block to the bending moment along edge ξ=1, and the slope along ξ=0, could be obtained much easier by having another solution with intersegment line running parallel to the η axis, as shown in Figure 3.4. This approach is not necessary but has been found to provide more rapid convergence.

Solutions for the two segments of Figure 3.4 can be easily inferred from existing solutions (Eq. 3.1 and 3.2) by interchanging ξ and η variables and following the already established transformation rules. Furthermore, the quantities u and v are changed to u^* and v^*, the A_m, B_m,

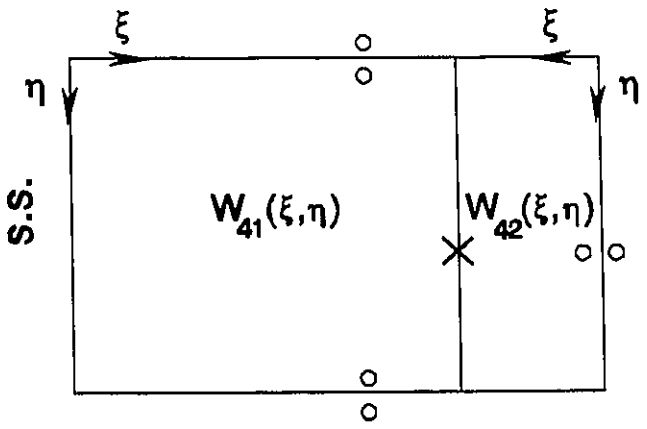

Figure 3.4 Alternative representation of the fourth building block

C_m, and D_m coefficients must be divided by ϕ^4 to leave unchanged the definition for P^*. The solutions are represented in Equations 3.8 and 3.9.

for segment I:

$$W_{41}(\xi,\eta) = \begin{cases} \sum_{n=0,1}^{k^*} \{A_{1n} \sinh \beta_n\xi + B_{1n} \sin \gamma_n\xi) \cos n\pi\eta \\ + \\ \sum_{k^*+1}^{\infty} \{A_{2n} \sinh \beta_n\xi + B_{2n} \sinh \gamma_n\xi) \cos n\pi\eta \\ \{A_{3n} \sin R\xi \cosh S\xi + B_{3n} \cos R\xi \sinh S\xi) \cos n\pi\eta \end{cases} \quad (3.8)$$

or

and for segment II:

$$W_{42}(\xi,\eta) = \begin{cases} \sum_{n=0,1}^{k^*} \{C_{1n} \cosh \beta_n\xi + D_{1n} \cos \gamma_n\xi) \cos n\pi\eta \\ + \\ \sum_{k^*+1}^{\infty} \{C_{2n} \cosh \beta_n\xi + D_{2n} \cosh \gamma_n\xi) \cos n\pi\eta \\ \{C_{3n} \sin R\xi \sinh S\xi + D_{3n} \cos R\xi \cosh S\xi) \cos n\pi\eta \end{cases} \quad (3.9)$$

or

Where β_n, γ_n, R, and S are defined as in Chapter 1 with transformation rules applied to each variable. The concentrated force is represented as

$$P(\xi) = \sum_{0,1}^{\infty} \frac{P^*}{\delta_m} \cos m\pi u \cos m\pi\xi \qquad (3.10)$$

$$\text{Where } \delta_m = \begin{matrix} 2 & if\ m=0 \\ 1 & if\ m\neq 0 \end{matrix}$$

Now that the solutions of the final building block are fully developed, the next step is to derive expressions for the contribution to the boundary conditions of the cantilever plate. Contributions of the first three blocks are already in Chapter 2.1.4, only the contribution of the fourth block is needed here.

[1.1] Contribution of the fourth building block, $W_{42}(\xi,\eta)$ to bending moment along edge $\eta=1$ of the cantilever plate. By substituting Eq3.2 into the moment expression,

$$\frac{M_\eta b^2}{aD_y}\Big|_{\eta=1} = -\left\{\frac{\partial^2 W(\xi,\eta)}{\partial\eta^2} + \upsilon_x\phi^2 \frac{\partial^2 W(\xi,\eta)}{\partial\xi^2}\right\}$$

$$\frac{M_\eta b^2}{aD_y}\Big|_{\eta=1} = \left\{\begin{array}{l} case1 \\ \quad [\upsilon_x\phi^2(\frac{m\pi}{2})^2 - \beta_m^2]\ C_{1m} + [\upsilon_x\phi^2(\frac{m\pi}{2})^2 + \gamma_m^2]\ D_{1m} \\ case2 \\ \quad [\upsilon_x\phi^2(\frac{m\pi}{2})^2 - \beta_m^2]\ C_{2m} + [\upsilon_x\phi^2(\frac{m\pi}{2})^2 - \gamma_m^2]\ D_{2m} \\ case3 \\ \quad \left[\begin{array}{l} -[(C_{3m}(S^2-R^2) - 2RSD_{3m}) - \upsilon_x\phi^2(\frac{m\pi}{2})^2 C_{3m}]\ \sin R\sinh S \\ \quad -[(C_{3m}2RS + D_{3m}(S^2-R^2) - \upsilon_x\phi^2(\frac{m\pi}{2})^2 D_{3m}]\ \cos R\cosh S \end{array}\right] \end{array}\right\} \sin\frac{m\pi\xi}{2} \qquad (3.11)$$

[1.2] Contribution of $W_{42}(\xi,\eta)$ to bending moment along edge $\xi=1$ of the cantilever plate. Using the following moment equation and Eq. 3.9,

$$\frac{M_\xi a}{D_x}\Big|_{\xi=1} = -\left\{\frac{\partial^2 W(\xi,\eta)}{\partial\xi^2} + \frac{\upsilon_y}{\phi^2}\frac{\partial^2 W(\xi,\eta)}{\partial\eta^2}\right\}$$

$$\frac{M_\xi a^2}{D_x}\Big|_{\xi=1} = \left\{\begin{array}{l} case1 \\ \quad [\upsilon_y\phi_T^2(n\pi)^2 - \beta_n^2]\ C_{1n} + [\upsilon_y\phi_T^2(n\pi)^2 + \gamma_n^2]\ D_{1n} \\ case2 \\ \quad [\upsilon_y\phi_T^2(n\pi)^2 - \beta_n^2]\ C_{2n} + [\upsilon_y\phi_T^2(n\pi)^2 - \gamma_n^2]\ D_{2n} \\ case3 \\ \left[\begin{array}{l} -\ [\,(C_{3n}(S^2-R^2) - 2RSD_{3n}) - \upsilon_y\phi_T^2(n\pi)^2 C_{3n}]\ \sin R\sinh S \\ \quad -\ [\,(C_{3n}2RS + D_{3n}(S^2-R^2) - \upsilon_y\phi_T^2(n\pi)^2 D_{3n}]\ \cos R\cosh S \end{array}\right] \end{array}\right\} \cos n\pi\eta$$

(3.12)

[1.3] Contribution of Equation 3.8, $W_{41}(\xi,\eta)$ to the slope along edge $\xi=0$ of the plate.

$$\frac{\partial W_{41}}{\partial \xi}\Big|_{\xi=0} = \left\{\begin{array}{l} case1 \\ \quad [A_{1n}\beta_n + B_{1n}\gamma_n] \\ case2 \\ \quad [A_{2n}\beta_n + B_{2n}\gamma_n] \\ case3 \\ \quad [A_{3n}R + B_{3n}S] \end{array}\right\} \cos n\pi\eta$$

(3.13)

[1.4] Contribution of Equation 3.1, $W_{41}(\xi,\eta)$ to the displacement at $\xi=u$ and $\eta=v$

$$W_{41}(\xi,\eta) = \sum_{m=1,3}^{k^*} \{A_{1m}\cosh\beta_m v + B_{1m}\cos\gamma_m v\}\sin\frac{m\pi u}{2} + \sum_{k^*+2}^{\infty} \{A_{2m}\cosh\beta_m v + B_{2m}\cosh\gamma_m v\}\sin\frac{m\pi u}{2}$$

or

$$\{A_{3m}\sin Rv\sinh Sv + B_{3m}\cos Rv\cosh Sv\}\sin\frac{m\pi u}{2}$$

(3.14)

With the contribution expressions established, the eigenvalue matrix can be generated in the same manner as described in Chapter 2.1.4. The same boundary conditions apply; that the superimposed solutions should have zero net bending moment along edges $\xi=1$ and $\eta=1$ and zero

slope along the clamped edge. For the analysis of point supports, the coefficient matrix must include one extra column to the right for the contribution of the fourth block, the matrix now relates together quantities E_m,E_n,E_p,and P^*. In addition, the matrix also has one added-on row which satisfies the condition that there be zero net displacement of the superimposed blocks at the point support location. Hence the size of the matrix is (3K+1,3K+1) if K terms are used.

The above information is fed into a specially written computer program. The eigenvalues are obtained, as before by searching for those values of λ^2 for which the determinant of the coefficient matrix is zero. The corresponding mode shape data for each eigenvalue are obtained by setting one of the unknowns equal to unity and solving for others. The results are discussed in section 3.3.

3.2 ANTISYMMETRIC MODES

The building blocks used in the analysis of antisymmetric family of modes are shown in Figure 3.5. The solutions for the first three blocks are already available in Chapter 2.2 and do not require any further consideration here. The fourth building block is the required additional one to represent the forcing condition. This block is divided into two segments I and II, division line between segments is parallel to the ξ axis at $\eta = v$ as shown in Figure 3.6; in addition, it should be noted that each segment has its own coordinate system.

SOLUTION OF THE FOURTH BUILDING BLOCK:

This building block was used by Gorman [Ref.1] & Saliba [Ref.2] in their analysis of plates with internal point supports. Although parts of the solution are readily available, it is necessary to develop a complete solution for the orthotropic case.

With respect to the boundary conditions, the Lévy-type solution may be written for each segment as follows (subscripts 1,2 refer to solutions applicable to segment I and II respectively):

$$W_{41}(\xi,\eta) = \sum_{m=1,3}^{k^*} \{A_{1m} \sinh \beta_m\eta + B_{1m} \sin \gamma_m\eta\} \sin\frac{m\pi\xi}{2} + \sum_{k^*+2}^{\infty} \{A_{2m} \sinh \beta_m\eta + B_{2m} \sinh \gamma_m\eta\} \sin\frac{m\pi\xi}{2} \quad \textbf{or} \quad \{A_{3m} \sin R\eta \cosh S\eta + B_{3m} \cos R\eta \sinh S\eta\} \sin\frac{m\pi\xi}{2} \tag{3.15}$$

and for segment II:

$$W_{42}(\xi,\eta) = \sum_{m=1,3}^{k^*} \{C_{1m} \cosh \beta_m\eta + D_{1m} \cos \gamma_m\eta\} \sin\frac{m\pi\xi}{2} + \sum_{k^*+2}^{\infty} \{C_{2m} \cosh \beta_m\eta + D_{2m} \cosh \gamma_m\eta\} \sin\frac{m\pi\xi}{2} \quad \textbf{or} \quad \{C_{3m} \sin R\eta \sinh S\eta + D_{3m} \cos R\eta \cosh S\eta\} \sin\frac{m\pi\xi}{2} \tag{3.16}$$

Where β_m, γ_m, R, and S are defined as in Chapter 1. The concentrated force is represented as in Equation 3.3.

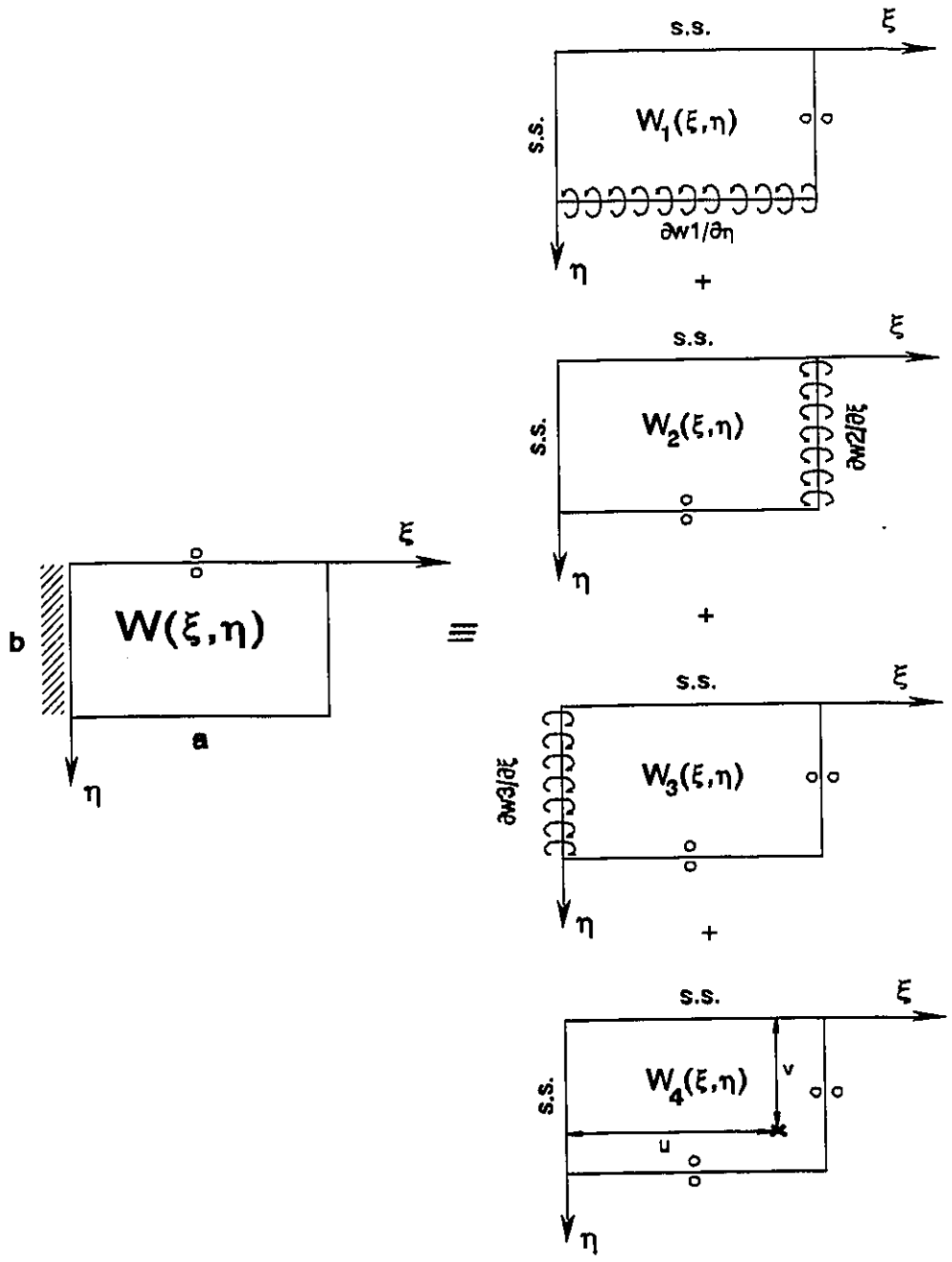

Figure 3.5 Building Blocks used in analyzing free vibration antisymmetric modes of the orthotropic plate with lateral point supports

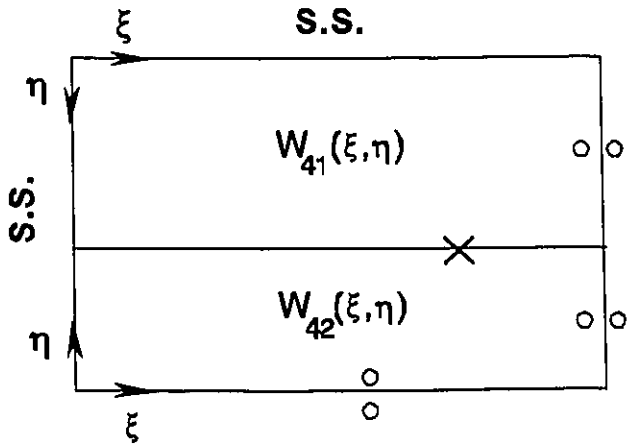

Figure 3.6 Fourth building block divided into two segments

The four unknowns A_m, B_m, C_m, and D_m can be determined by enforcing the conditions of continuity and force equilibrium along the segment division line. The continuity conditions are the same as those described in the analysis of the symmetric modes. The continuity equations can be obtained by substituting Equations 3.15 and 3.16 into Eq. 3.4 - 3.7, the resultant equations are apparent therefore are not included here to avoid unnecessary repetition. Three sets of equations allow the constants A_m, B_m, C_m, and D_m to be solved numerically whenever required using the usual Gaussian-elimination computer subroutine.

The solution for the fourth building block is now available. However, as in the analysis for the symmetric modes, another solution of the fourth block is required with the partition line running parallel to the η axis as shown in Figure 3.7.

Solutions for the two segments of Figure 3.7 can be derived from the solution of the block in Figure 3.6 (Eq. 3.15 and 3.16) by interchanging ξ and η variables and following the already established transformation rules. Furthermore, the subscript m is replaced by n, the quantities u and v are changed to u^* and v^*, the A_m, B_m, C_m, and D_m coefficients must be divided by ϕ^4 to leave unchanged the definition for P^*. The new solutions are represented in Equations 3.17 and 3.18.

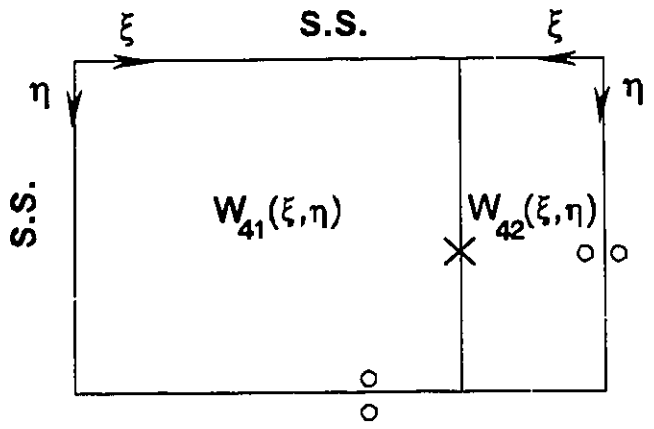

Figure 3.7 Alternative representation of the fourth building block

for segment I:

$$W_{41}(\xi,\eta) = \sum_{n=0,1}^{k^*} \{A_{1n} \sinh \beta_n\xi + B_{1n} \sin \gamma_n\xi\} \sin\frac{n\pi\eta}{2} + \sum_{k^*+1}^{\infty} \{A_{2n} \sinh \beta_n\xi + B_{2n} \sinh \gamma_n\xi\} \sin\frac{n\pi\eta}{2} \quad \textit{or} \quad \{A_{3n} \sin R\xi \cosh S\xi + B_{3n} \cos R\xi \sinh S\xi\} \sin\frac{n\pi\eta}{2} \tag{3.17}$$

and for segment II:

$$W_{42}(\xi,\eta) = \sum_{n=0,1}^{k^*} \{C_{1n} \cosh \beta_n\xi + D_{1n} \cos \gamma_n\xi\} \sin\frac{n\pi\eta}{2} + \sum_{k^*+1}^{\infty} \{C_{2n} \cosh \beta_n\xi + D_{2n} \cosh \gamma_n\xi\} \sin\frac{n\pi\eta}{2} \quad \textit{or} \quad \{C_{3n} \sin R\xi \sinh S\xi + D_{3n} \cos R\xi \cosh S\xi\} \sin\frac{n\pi\eta}{2} \tag{3.18}$$

Where β_n, γ_n, R, and S have the same definitions as in Chapter 1 with transformation rules applied to each variable. The concentrated force as usual is expanded in the Dirac function form.

As before, one can proceed to determine expressions for the contribution to the boundary conditions of the cantilever plate. Contributions of the first three blocks are already in Chapter 2.1.4, only the contribution of the fourth block is needed here.

1.1 Contribution of the fourth building block, $W_{42}(\xi,\eta)$ to bending moment along edge $\eta=1$ of the cantilever plate. By substituting Eq3.16 into the moment expression,

$$\frac{M_1 b^2}{aD_y}\Big|_{\eta=1} = -\left\{\frac{\partial^2 W(\xi,\eta)}{\partial\eta^2} + \upsilon_x\phi^2\,\frac{\partial^2 W(\xi,\eta)}{\partial\xi^2}\right\}$$

$$\frac{M_\eta b^2}{aD_y}\Big|_{\eta=1} = \left\{\begin{array}{l} case1 \\ \quad [\upsilon_x\phi^2(\frac{m\pi}{2})^2 - \beta_m^2]\ C_{1m} + [\upsilon_x\phi^2(\frac{m\pi}{2})^2 + \gamma_m^2]\ D_{1m} \\ case2 \\ \quad [\upsilon_x\phi^2(\frac{m\pi}{2})^2 - \beta_m^2]\ C_{2m} + [\upsilon_x\phi^2(\frac{m\pi}{2})^2 - \gamma_m^2]\ D_{2m} \\ case3 \\ \quad \left[\begin{array}{l} -[(C_{3m}(S^2-R^2) - 2RSD_{3m}) - \upsilon_x\phi^2(\frac{m\pi}{2})^2 C_{3m}]\ \sin R\sinh S \\ \quad -[(C_{3m}2RS + D_{3m}(S^2-R^2) - \upsilon_x\phi^2(\frac{m\pi}{2})^2 D_{3m}]\ \cos R\cosh S \end{array}\right] \end{array}\right\} \sin\frac{m\pi\xi}{2}$$

(3.19)

1.2 Contribution of $W_{42}(\xi,\eta)$ to bending moment along edge $\xi=1$ of the cantilever plate. Using the following moment equation and Eq3.18,

$$\frac{M_\xi a}{D_x}\Big|_{\xi=1} = -\left\{\frac{\partial^2 W(\xi,\eta)}{\partial\xi^2} + \frac{\upsilon_y}{\phi^2}\,\frac{\partial^2 W(\xi,\eta)}{\partial\eta^2}\right\}$$

$$\frac{M_\xi a^2}{D_x}\Big|_{\xi=1} = \left\{\begin{array}{l} case1 \\ \quad [\upsilon_y\phi_I^2(n\pi)^2 - \beta_n^2]\ C_{1n} + [\upsilon_y\phi_I^2(n\pi)^2 + \gamma_n^2]\ D_{1n} \\ case2 \\ \quad [\upsilon_y\phi_I^2(n\pi)^2 - \beta_n^2]\ C_{2n} + [\upsilon_y\phi_I^2(n\pi)^2 - \gamma_n^2]\ D_{2n} \\ case3 \\ \quad \left[\begin{array}{l} -[(C_{3n}(S^2-R^2) - 2RSD_{3n}) - \upsilon_y\phi_I^2(n\pi)^2 C_{3n}]\ \sin R\sinh S \\ \quad -[(C_{3n}2RS + D_{3n}(S^2-R^2) - \upsilon_y\phi_I^2(n\pi)^2 D_{3n}]\ \cos R\cosh S \end{array}\right] \end{array}\right\} \sin\frac{n\pi\eta}{2}$$

(3.20)

1.3 Contribution of Equation 3.17, $W_{41}(\xi,\eta)$ to the slope along edge $\xi=0$ of the plate.

$$\frac{\partial W_{41}}{\partial \xi}\Big|_{\xi=0} = \begin{Bmatrix} case1 & [A_{1n}\beta_n + B_{1n}\gamma_n] \\ case2 & [A_{2n}\beta_n + B_{2n}\gamma_n] \\ case3 & [A_{3n}R + B_{3n}S] \end{Bmatrix} \sin\frac{n\pi\eta}{2} \tag{3.21}$$

1.4 Contribution of Equation 3.15, $W_{41}(\xi,\eta)$ to the displacement at ξ=u and η=v

$$W_{41}(\xi,\eta) = \sum_{m=1,3}^{k^*} \{A_{1m}\sinh\beta_m u + B_{1m}\sin\gamma_m u\}\sin\frac{m\pi v}{2} + \sum_{k^*+2}^{\infty} \{A_{2m}\sinh\beta_m u + B_{2m}\sinh\gamma_m u\}\sin\frac{m\pi v}{2}$$

or

$$\{A_{3m}\sin Ru\sinh Su + B_{3m}\cos Ru\cosh Su\}\sin\frac{m\pi v}{2} \tag{3.22}$$

With the contribution expressions established, the eigenvalue matrix can be generated in the same manner as described in Chapter 2.2.4. The same boundary conditions of a cantilever plate apply. As in section 3.1, the size of coefficient matrix must contains one extra column and one row to account for the contribution of the fourth block. The method to obtain the eigenvalues and their corresponding mode shapes are the same, the procedures were implemented into an in-house computer program.

Having carried out the necessary analysis using the method of superposition, the results produced from the computer programs are then examined in the next section.

3.3 RESULTS AND DISCUSSIONS

The eigenvalues for the orthotropic cantilever plates with point supports are determined using the same procedure as that for plates without supports Chapter 2.3. A comprehensive set of results is included in Appendix B. Tables B3.1 - B3.5 contain eigenvalues of the symmetric case. Convergence tests have shown that in order to achieve four significant digit accuracy, 25 or more terms in the Fourier expansions must be used. The flexural rigidities DHY and DHX range from 0.5 to 2.0, the point supports are located at u=v=0.5 or u=v=0.75. Eigenvalue Tables B4.1 - B4.5 are of the antisymmetric case for the same ranges of parameters. Overally, it was observed that the eigenvalues (hence natural frequencies) increase for plates with point supports than of those without. This was expected since the point supports act as additional constraints to the plates. This effect is most noticeable for the first modes because the natural frequencies tend to small and the displacements are the highest compared to other modes. The eigenvalues for the cases of u=v=0.5 and u=v=0.75 only differ slightly, more significantly for the first modes. Hence only the cases of extreme ends in the rigidity range (For example, DHY=0.5 DHX=2.0) were considered for both support positions. It would seem that the stiffening effects of point supports are more pronounced as the supports move away from the clamped edge (u=v=0.75), however the results do not verify this claim ie. the suspected trend in eigenvalues was undetectable. This is probably due to overlapping effects of all the variables involved, especially the directional rigidities or because the distance difference is small.

The associated mode shapes have been represented as three-dimensional plots of the vibrating plates at their natural frequencies. Figures B3.1-12 of Appendix B show the first four associated mode shapes and contour plots for the symmetric and antisymmetric cases. From these pictorial representations, information is available on the areas of high displacements and nodal lines of the plate. The mode shapes also confirm that the plate boundary and continuity conditions are satisfied; the clamped edge is noted to have zero displacement, zero slope, and the point supports locations have zero displacement. As observed earlier, the displacements for plates with the presence of point supports are less significant because the natural frequencies are higher.

Conclusions

The free vibration analysis of orthotropic cantilever plates with internal point supports has been solved using the method of superpostion. The solution was obtained by superimposing a number of building blocks whose individual Lévy-type solutions are known. With the solutions made available by enforcing necessary boundary conditions, an eigenvalue matrix could be generated. The plate eigenvalues and mode shapes could then be determined using standard computer techniques.

Eigenvalues, mode shapes and contour plots have been documented for both the symmetric and antisymmetric modes of vibration. The plates studied cover a wide range of aspect ratios and various degrees of flexural rigidities. All the computed eigenvalues are accurate to four significant digits. In order to achieve this level of accuracy, fifteen terms were used in the Fourier expansion in the solutions for plates without point supports; and for plates with point supports, thirty terms were required. The mode shapes and contour plots showed that the boundary and continuity conditions were satisfied to any desired degree of exactitude.

Review of literature revealed that highly accurate solutions for many plate vibration problems were available but none has dealt directly with the problem of orthotropic cantilever plates. Consequently no comparisons of results were made. However, for a special case of orthotropy: isotropic, this specific problem has been solved by Gorman [1] and Saliba [2]. The results are in excellent agreement with those in Ref.[1] & [2], but this was expected since both used the same superposition method. The analytical solution presented in this thesis may be considered as an extension of the use of superposition method into the area of analysis of orthotropic plates.

The results from this study are hoped to be of help to future researchers for comparison of results whether they use the same technique or other analysis methods. In addition, the data presented could enable design engineers to optimize their products in order to minimize the dynamic excitation and hence extending the operating life of industrial structures.

Bibliography

[1] D.J. Gorman — *Free Vibration Analysis of Rectangular Plates*, Elsvier North Holland , New York 1982.

[2] H.T. Saliba — *Free Vibration Analysis of Rectangular Cantilever Plates with Symmetrically Distributed Point Supports*, M.A.Sc. thesis, University of Ottawa, 1982.

[3] S. Timoshenko Woinowsky — *Theory of Plates and Shells*, Second Edition, McGraw-Hill Inc., U.S.A. 1959.

[4] R. Szilard — *Theory and Analysis of Plates Classical and Numerical Methods*, Prentice-Hill Inc., New Jersey U.S.A 1974.

[5] A.W. Leissa — *Vibration of Plates*, National Aeronautics and Space Administration, NASA SP-160, 1969.

[6] D.J. Gorman — *Accurate Free Vibration Analysis of the Completely Free Orthotropic Rectangular Plates by the Method of Superposition*, Journal of Sound and Vibration, Volume 165 No.3 Pg.409-420, 1993.

[7] D. Gorman R. Singal — *Analytical and Experimental Study of Vibrating Rectangular Plates on Rigid Point Supports*, AIAA Journal Volume 29 No. 5 Pg. 838-844, Washington DC.

[8] H. Ohman — *Free Vibration Analysis of Rectangular Plates with Internal Point Supports*, M.A.Sc. thesis, University of Ottawa, 1990.

[9] D.J.Gorman — *Accurate Free Vibration Analysis of Clamped Orthotropic Plates by the Method of Superposition*, Journal of Sound and Vibration, Volume 140 No.3 Pg. 391-411, 1990.

[10] I. Todhunter, K. Pearson — *A History of the Theory of Elasticity*, Dover Publications Inc., New York 1960.

[11] D.J.Gorman — *Free Vibration Analysis of Cantilever Plates by the Method of Superposition*, Journal of Sound and Vibration, Volume 49 No.4, Pg. 453-467, 1976.

[12] D.J.Gorman — *An Analytical Solution for the Free Vibration Analysis of Rectangular Plates Resting on Symmetrically Distributed Point Supports*, Journal of Sound and Vibration, Volume 79 No.4, 1981.

[13] N.J. Huffington, W.H. Hoppmann — *On the Transverse Vibration of Rectangular Orthotropic Plates*, Journal of Applied Mechanics, September 1958 pg. 389-395.

[14] S.R. Iyengar, K.S. Jagadish — *Vibration of Rectangular Orthotropic Plates*, Journal of Applied Mechanics, ASME 36 Pg.101-106, 1969.

[15] R.F. Hearmon — *The Frequency of Flexural Vibration of Rectangular Orthotropic Plates with Clamped or Supported Edges*, Journal of Applied Mechanics Pg. 537-540, 1959.

[16] S. Dickinson — *The Flexural Vibration of Rectangular Orthotropic Plates*, Journal of Applied Mechanics Pg. 101-106, March 1969.

[17] E.H. Hill, K.S. Pister — *Vibration of Rectangular Plates and Plate Systems*, Proc. 3rd. National Congress Applied Mechanics Pg.123-132, 1958.

[18] R. Marangoni, L. Cook — *Upper and Lower Bounds to the Natural Frequencies of Vibration of Clamped Rectangular Orthotropic Plates*, International Journal of Solids and Structures Volume 14 Pg. 611-623, 1978.

[19] N.W. Bazely, D.W. Fox — *Upper and Lower Bounds for Frequencies of Rectangular Clamped Plates*, Applied Physics Laboratory, John Hopkins University, Report T6-609, 1965.

[20] S.R. Soni, Ambra Rao — *Vibration of Orthotropic Rectangular Plates under Inplane Forces*, Computers & Structures, Volume 4 Pg. 1105-1115, 1974.

[21] P. Laura, L. Luisoni — *Vibrations of Orthotropic Rectangular Plates with Edges Possessing Different Rotational Flexibility and Subjected to Inplane Forces*, Computers & Structures, Volume 9 Pg. 527-532, 1978.

[22] S.Medwadowski — *A Refined Theory of Elastic, Orthotropic Plates*, Journal of Applied Mechanics, Pg. 437-443, December 1958.

[23] R.B. Nelson, D.R. Lorch — *A Refined theory for Laminated Orthotropic Plates*, Journal of Applied Mechanics, Pg. 177-183, March 1974.

[24] S.B. Dong, R.B. Nelson — *On Natural Vibrations and Waves in Laminated Orthotropic Plates*, Journal of Applied Mechanics, September 1972.

[25] S. Srinivas, A.K. Rao — *Bending, Vibration and Buckling of Simply Supported Thick Orthotropic Rectangular Plates and Laminates*, International Journal of Solids & Structures, Volume 6 Pg.1463-1481, 1970.

[26] J.N. Reddy, N.D. Phan — *Stability and Vibration of Isotropic, Orthotropic and Laminated Plates According to a Higher-Order Shear Deformation Theory*, Journal of Sound and Vibration Volume 98 No.2 .Pg.157-170, 1985.

[27] A.W. Leissa — *Recent Research in Plate Vibrations 1973-1976: Complicating Effects*, Shock and Vibration Digest, Volume 10 No.12 Pg. 21-35, 1978.

[28] A.W. Leissa — *Recent Studies in Plate Vibrations 1981-1985: Part I Classical Theory*, Shock and Vibration Digest Volume 19 No.2 Pg.11-18, 1987.

[29] Y. Narita — *The Effects of Point Constraints on Transverse Vibration of Cantilever Plates*, Journal of Sound and Vibration, Volume 101 No.3 Pg.305-313, 1985.

[30] G. Isnor — *A Literature Survey of the Mathematical Formulations of Free Vibration Problems of Homogeneous Isotropic & Orthotropic Plates*, Masters of Engineering thesis, University of Ottawa 1992.

[31] R.K. Singal, D.J. Gorman — *Effects of Attached Masses on Free Vibration of Rigid Point Supported Rectangular Plates*, AIAA Journal, Volume 30 No.3 Pg.853-855, 1991.

Appendix A

Development of Equations

This appendix contains full description of the steps used in deriving expressions for the solutions in Chapter 2.

A.1 Symmetric Modes

A.1.1 Solution of the first building block - Section 2.1.1

For Case 1 - For $z > 0$ and $(\sqrt{z} + \alpha_1) \geq 0$

Full development of solution for this case was already done as an example in Chapter 2.1.1

For Case 2 - for $\sqrt{z} > 0$ and $(\sqrt{z} + \alpha_1) \leq 0$

Using the shear force condition at $\eta=1$, Substitute the second summation of Eq.(2.2) into Eq. (2.3)

$$W_1(\xi,\eta) = (A_m \cosh \beta_m\eta + B_m \cosh \gamma_m\eta) \sin\frac{m\pi\xi}{2}$$

$$\frac{\partial^3 w}{\partial\eta^3}|_{\eta=1} = (A_m B_m^3 \sinh \beta_m + B_m\gamma^3 \sinh \gamma_m) \sin\frac{m\pi\xi}{2} \qquad (a)$$

$$\frac{\partial^3 w}{\partial\eta\partial\xi^2}|_{\eta=1} = -(\frac{m\pi}{2})^2[A_m B_m \sinh \beta_m - B_m\gamma_m \sinh \gamma_m] \sin\frac{m\pi\xi}{2} \qquad (b)$$

(a) + (b) = 0, solve for B_m in terms of A_m

$$B_m = A_m \{\frac{-\beta_m[\beta_m^2 - \upsilon_x^*\phi^2(\frac{m\pi}{2})^2] \sinh\beta_m}{\gamma_m[\gamma_m^2 - \upsilon_x^*\phi^2(\frac{m\pi}{2})^2] \sinh\gamma_m}\}$$

$$Let\ ZZ1 = -\beta_m[\beta_m^2 - \upsilon_x^*\phi^2(\frac{m\pi}{2})^2]$$

$$ZZ2 = \gamma_m[\gamma_m^2 - \upsilon_x^*\phi^2(\frac{m\pi}{2})^2]$$

Now $B_m = \theta_{2m} A_m$

where $\theta_{2m} = \dfrac{ZZ1 \sinh\beta_m}{ZZ2 \sinh\gamma_m}$

$$\therefore W_1(\xi,\eta) = A_m [\cosh \beta_m\eta + \theta_{2m} \cosh \gamma_m\eta) \sin\frac{m\pi\xi}{2}$$

Next step is to impose distributed harmonic rotation (slope) at η=1, represented by the sine series, substitute the above equation into the following

$$\frac{\partial W_1}{\partial \eta}|_{\eta=1} = \sum_{m=1,3,5}^{\infty} E_m \sin \frac{m\pi\xi}{2}$$

$$LHS = A_m [\beta_m \sinh\beta_m - \theta_{2m}\gamma_m \sinh\gamma_m] \sin \frac{m\pi\xi}{2}$$

$$RHS = E_m \sin\frac{m\pi\xi}{2}$$

Solve for A_m in terms of E_m

$$A_m = \frac{E_m}{[\beta_m + \frac{zz1}{zz2}\gamma_m] \sinh\beta_m}$$

$$A_m\theta_{2m} = \frac{zz1}{zz2} \frac{E_m}{[\beta_m + \frac{zz1}{zz2}\gamma_m] \sinh\gamma_m}$$

$$Let \quad \theta_{22m} = \frac{1}{[\beta_m + \frac{zz1}{zz2}\gamma_m]}$$

$$\theta_{23m} = \frac{zz1}{zz2} \frac{E_m}{[\beta_m + \frac{zz1}{zz2}\gamma_m]} = \frac{zz1}{zz2} \theta_{22m}$$

Now that the A_m and B_m coefficients are solved in terms of the imposing rotational variable E_m,θ_{22m}, and θ_{23m} the final form of W_1 (case 2) is:

$$W_1(\xi,\eta) = E_m\{\theta_{22m}\frac{\cosh\beta_m\eta}{\sinh\beta_m} + \theta_{23m}\frac{\cos\gamma_m\eta}{\sinh\gamma_m}\}\sin\frac{m\pi\xi}{2}$$

Case 3 - z<0

Using the shear force condition at η=1, Substitute the third summation of Eq.(2.2) into Eq. (2.3)

$$W_1(\xi,\eta) = (A_m \sin R\eta \sinh S\eta + B_m \cos R\eta \cosh S\eta)\sin\frac{m\pi\xi}{2}$$

$$\frac{\partial^3 w}{\partial\eta^3}\Big|_{\eta=1} = \left\{\begin{matrix} A_m\,[R_1 \cos R \sinh S + R_2 \sin R \cosh S] \\ + \\ B_m\,[R_2 \cos R \sinh S - R_1 \sin R \cosh S] \end{matrix}\right\}\sin\frac{m\pi\xi}{2}$$

Where

$$R_1 = R(3S^2 - R^2)$$
$$R_2 = S(S^2 - 3R^2)$$

$$\frac{\partial^3 w}{\partial\eta\partial\xi^2}\Big|_{\eta=1} = -(\frac{m\pi}{2})^2\left\{\begin{matrix} A_m\,(R\cos R\sinh S + S\sin R\cosh S) \\ + \\ B_m\,(-R\sin R\cosh S + S\cos R\sinh S) \end{matrix}\right\}\sin\frac{m\pi\xi}{2}$$

Therefore, the shear force expression is

$$\frac{V_y a^3}{bD_y} = \left\{\begin{matrix} A_m\,\{R_3 \cos R sinh S + R_4 \sin R \cosh S\} \\ + \\ B_m\{R_5 \cos R \sinh S + R_6 \sin R \cosh S\} \end{matrix}\right\} = 0$$

Where

$$R_3 = [R_1 - \upsilon_x^* \phi^2 (\frac{m\pi}{2})^2 R] \qquad R_4 = [R_2 - \upsilon_x^* \phi^2 (\frac{m\pi}{2})^2 S]$$

$$R_5 = [R_2 - \upsilon_x^* \phi^2 (\frac{m\pi}{2})^2 S] \qquad R_6 = -[R_1 - \upsilon_x^* \phi^2 (\frac{m\pi}{2})^2 R]$$

Now $B_m = \theta_{3m} A_m$

where $$\theta_{3m} = \frac{-R_3 \cos R \sinh S - R_4 \sin R \cosh S}{R_5 \cos R \sinh S + R_6 \sin R \cosh S}$$

$$\therefore W_1(\xi,\eta) = A_m [\sin R \sinh S + \theta_{3m} \cos R \cosh S] \sin\frac{m\pi\xi}{2}$$

Next step is to impose distributed harmonic rotation (slope) at η=1, represented by the sine series, substitute the above equation into this slope series

$$\frac{\partial W_1}{\partial \eta}|_{\eta=1} = \sum_{m=1,3,5}^{\infty} E_m \sin\frac{m\pi\xi}{2}$$

$$LHS = A_m \left\{ \begin{array}{c} (R\cos R\sinh S + S\sin R\cosh S) \\ + \\ \theta_{3m} (S\cos R\sinh S - R\sin R\cosh S) \end{array} \right\} \sin\frac{m\pi\xi}{2}$$

$$RHS = E_m \sin\frac{m\pi\xi}{2}$$

Solve for A_m in terms of E_m

$A_m = \theta_{33m} E_m$

where

$$\theta_{33m} = \frac{1}{\{(R\cos R\sinh S + S\sin R\cosh S) + \theta_{3m} (S\cos R\sinh S - R\sin R\cosh S)\}}$$

Let $\theta_{333m} = \theta_{33m} \cdot \theta_{3m}$

Now that the A_m and B_m coefficients are solved in terms of the imposing rotational variable E_m, the final form of W_1 (case 3) is:

$$W_1(\xi,\eta) = E_m\,[\theta_{33m}\sin R\sinh S + \theta_{333m}\cos R\,\cosh S]\,\sin\frac{m\pi\xi}{2}$$

A.1.2 Solution of the second building block

$$W_2(\xi,\eta) = \sum_{m=0,1,2}^{k^*} \{A_m \sinh\beta_m\eta + B_m \sin\gamma_m\eta\}\cos m\pi\xi + \sum_{k^*+2}^{\infty} \{A_m \sinh\beta_m\eta + B_m \sinh\gamma_m\eta\}\cos m\pi\xi$$

or

$$\{A_m \sin R\eta\cos S\eta + B_m \cos R\eta\,\sinh S\eta\}\cos m\pi\xi$$

For this case $\alpha_1 = -2DHy\,\phi^2\,(M\pi)^2$

$\alpha_2 = Dxy\,\phi^4\,\{(M\pi)^4 - \lambda^4\}$

β_m, γ_m, R, and S are defined as in Chapter 1

Solutions for Am and Bm coefficients

The steps used upon arriving at the solutions are similar to those carried out for the first building block. Firstly, the shear force along edge $\eta=1$ is enforced to be zero (Eq. 2.3), secondly the prescribed slope is expanded in a cosine series as follows. The process eliminates the two unknowns A_m and B_m.

$$\frac{\partial W_2^*}{\partial\eta}\Big|_{\eta=1} = \sum_{m=0,1,2}^{\infty} E_m \cos m\pi\xi$$

where

$$\theta_{1m}^* = \frac{\beta_m[\beta_m^2 - \upsilon_x^*\phi^2(m\pi)^2]}{\gamma_m[\gamma_m^2 + \upsilon_x^*\phi^2(m\pi)^2]} \qquad \theta_{2m}^* = \frac{\beta_m[\beta_m^2 - \upsilon_x^*\phi^2(m\pi)^2]}{-\gamma_m[\gamma_m^2 - \upsilon_x^*\phi^2(m\pi)^2]}$$

$$\theta_{11m} = \frac{1}{[\beta_m + \gamma_m \theta^*_{1m}]} \qquad \theta_{22m} = \frac{1}{[\beta_m + \gamma_m \theta^*_{2m}]}$$

$$\theta_{13m} = \theta_{11m} \cdot \theta^*_{1m} \qquad \theta_{23m} = \theta_{22m} \cdot \theta^*_{2m}$$

And

$$R_1 = R(3S^2 - R^2)$$
$$R_2 = S(S^2 - 3R^2)$$

Where

$$R_3 = [R_1 - \upsilon_x^* \phi^2 (m\pi)^2 R] \qquad R_4 = [R_2 - \upsilon_x^* \phi^2 (m\pi)^2 S]$$
$$R_5 = [R_2 - \upsilon_x^* \phi^2 (m\pi)^2 S] \qquad R_6 = -[R_1 - \upsilon_x^* \phi^2 (m\pi)^2 R]$$

$$\theta_{3m} = -\frac{R_3 \cos R \cosh S + R_4 \sin R \sinh S}{R_5 \cos R \cosh S + R_6 \sin R \sinh S}$$

$$\theta_{33m} = \frac{1}{\{(R\cos R\cosh S + S\sin R\sinh S) + \theta_{3m}(S\cos R\cosh S - R\sin R\sinh S)\}}$$

$$\theta_{333m} = \theta_{33m} \cdot \theta_{3m}$$

The solution of the original second building block is then extracted from the newly developed equation. The subscript m is changed to n to avoid confusion with the first building block solution. Transformation of coordinates ξ and η gives the final solution as

$$W_2(\xi,\eta) = \sum_{n=0,1,2}^{k^*} E_n \{\theta_{11n} \frac{\sinh \beta_n \xi}{\cosh \beta_n} + \theta_{13n} \frac{\sin \gamma_n \xi}{\cos \gamma_n}\} \cos n\pi\eta$$

$$+ \sum_{k^*+1}^{\infty} E_n \{\theta_{22n} \frac{\sinh \beta_n \xi}{\cosh \beta_n} + \theta_{23n} \frac{\sinh \gamma_m \xi}{\cosh \gamma_n}\} \cos n\pi\eta$$

or

$$E_n \{\theta_{33n} \sin R\xi \cosh S\xi + \theta_{333n} \cos R\xi \sinh S\xi\} \cos n\pi\eta$$

where

$$\phi_1 = 1/\phi$$

$$\theta^*_{1n} = \frac{\beta_n[\beta_n^2 - \upsilon_y * \phi_1^2(n\pi)^2]}{\gamma_n[\gamma_n^2 + \upsilon_y^* \phi_1^2(n\pi)^2]} \qquad \theta^*_{2n} = \frac{\beta_n[\beta_n^2 - \upsilon_y^* \phi_1^2(n\pi)^2]}{-\gamma_n[\gamma_n^2 - \upsilon_y^* \phi_1^2(n\pi)^2]}$$

$$\theta_{11n} = \frac{1}{[\beta_n + \gamma_n \theta^*_{1n}]} \qquad \theta_{22n} = \frac{1}{[\beta_n + \gamma_m \theta^*_{2m}]}$$

$$\theta_{13n} = \theta_{11n} \cdot \theta^*_{1n} \qquad \theta_{23n} = \theta_{22n} \cdot \theta^*_{2n}$$

And $\alpha_1 = -2DHx\ \phi_1^2\ (n\pi)^2$

$\alpha_2 = 1/Dxy\ \phi_1^4\ \{(n\pi)^4 - \lambda^4\phi^4\}$

$$R_1 = R(3S^2 - R^2)$$
$$R_2 = S(S^2 - 3R^2)$$

And

$$R_3 = [R_1 - \upsilon_y^* \phi_1^2(n\pi)^2 R] \qquad R_4 = [R_2 - \upsilon_y^* \phi_1^2(n\pi)^2 S]$$
$$R_5 = [R_2 - \upsilon_y^* \phi_1^2(n\pi)^2 S] \qquad R_6 = -[R_1 - \upsilon_y^* \phi_1^2(n\pi)^2 R]$$

θ_{3n}, θ_{33n}, θ_{333n} *are the same as* θ_{3m}, θ_{33m}, θ_{333m}

The enforcing rotation along edge ξ=1 is

$$\frac{\partial W_2}{\partial \xi}\Big|_{\xi=1} = \sum_{n=0,1,2}^{\infty} E_n \cos n\pi\xi$$

A.1.3 Solution of the third building block

The building block (a) of Figure 2.5 is noted to have the Lévy-type solution as

$$W_3^*(\xi,\eta) = \sum_{m=0,1,2}^{\infty} Y_m(\eta)\cos m\pi\xi$$

$$\sum_{m=0,1,2}^{k^*} \{A_m \cosh\beta_m\eta + B_m \cos\gamma_m\eta\} \cos m\pi\xi$$

$$+$$

$$W_3''(\xi,\eta) = \sum_{k^*+1}^{\infty} \{A_m \cosh\beta_m\eta + B_m \cosh\gamma_m\eta\} \cos m\pi\xi$$

$$\textit{or}$$

$$\{A_m \sin R\eta \sinh S\eta + B_m \cos R\eta \cosh S\eta\} \cos m\pi\xi$$

β_m, γ_m, R, and S are defined as in Chapter 1.

For this building block, it is necessary to enforce the zero - displacement condition at η=1. For all three cases, respectively

$$W(\eta,1) = 0$$

$$A_m \cosh\beta_m + B_m \cos\gamma_m = 0$$

$$A_m \cosh\beta_m + B_m \cosh\gamma_m = 0$$

$$A_m \sin R \sinh S + B_m \cos R \cosh S = 0$$

Solve each equation for B_m in terms of A_m as before

$$B_m = \theta_{\#m} \cdot A_m$$

$$\Theta_{1m} = -\frac{\cosh\beta_m}{\cos\gamma_m} \qquad \Theta_{2m} = -\frac{\cosh\beta_m}{\cosh\gamma_m} \qquad \Theta_{3m} = -\frac{\sin R \sinh S}{\cos R \cosh s}$$

Enforce harmonic slope at edge $\eta=1$

$$\frac{\partial W_3^a}{\partial \eta}\Big|_{\eta=1} = \sum_{m=0,1,2}^{\infty} E_m \cos m\pi\xi$$

Equate the LHS to the RHS, cancel the common terms $\cos(m\pi\xi)$, and finally solve for A_m in terms of E_m. This results in solutions of building block (a) as follows

$$W_3^a(\xi,\eta) = \sum_{m=0,1,2}^{k^*} E_m \{\theta_{11m}\cosh\beta_m\eta + \theta_{13m}\cos\gamma_m\eta\}\cos m\pi\xi$$

$$+$$

$$\sum_{k^*+1}^{\infty} E_m \{\theta_{22m}\cosh\beta_m\eta + \theta_{23m}\cosh\gamma_m\eta\}\cos m\pi\xi$$

$$\textit{or}$$

$$E_m \{\theta_{33m}\sin R\eta\sinh S\eta + \theta_{333m}\cos R\eta\cosh S\eta\}\cos m\pi\xi$$

Where

$$\theta_{11m} = \frac{1}{[\beta_m\sinh\beta_m - \gamma_m\theta_{1m}\sin\gamma_m]} \qquad \theta_{22m} = \frac{1}{[\beta_m\cosh\beta_m + \gamma_m\theta_{2m}\cosh\gamma_m]}$$

$$\theta_{33m} = \frac{1}{\{(R\cos R\sinh S + S\sin R\cosh S) + \theta_{3m}(S\cos R\sinh S - R\sin R\cosh S)\}}$$

And

$$\theta_{13m} = \theta_{11m}\cdot\theta_{1m} \qquad \theta_{23m} = \theta_{22m}\cdot\theta_{2m} \qquad \theta_{333m} = \theta_{33m}\cdot\theta_{3m}$$

The solution of building block (b) is then extracted from solution of block (a) by replacing η with $1-\eta$. The prescribed slope will also change sign.

$$\frac{\partial W_3^b}{\partial \eta}\Big|_{\eta=0} = \sum_{m=0,1,2}^{\infty} -E_m \cos m\pi\xi$$

Building block (b) has solutions as:

$$W_3^b(\xi,\eta) = \sum_{m=0,1,2}^{k^*} E_m \{\theta_{11m}\cosh\beta_m(1-\eta) + \theta_{13m}\cos\gamma_m(1-\eta)\}\cos m\pi\xi$$

$$+$$

$$\sum_{k^*+1}^{\infty} E_m \{\theta_{22m}\cosh\beta_m(1-\eta) + \theta_{23m}\cosh\gamma_m(1-\eta)\}\cos m\pi\xi$$

or

$$E_m \{\theta_{33m}\sin R(1-\eta)\sinh S(1-\eta) + \theta_{333m}\cos R(1-\eta)\cosh S(1-\eta)\}\cos m\pi\xi$$

To arrive at the solution of block (c) or original third building block, variables ξ and η have to be interchanged. Following the same logic in variable transformation as before, the aspect ratio is now the its inverse and λ^2 is multiplied by ϕ^2. Subscript m is changed to p to avoid confusion with previous solutions. The final solution for the third building block is:

$$W_3(\xi,\eta) = \sum_{p=0,1,2}^{k^*} E_p \{\theta_{11p}\cosh\beta_p(1-\xi) + \theta_{13p}\cos\gamma_p(1-\xi)\}\cos p\pi\eta$$

$$+$$

$$\sum_{k^*+1}^{\infty} E_p \{\theta_{22p}\cosh\beta_p(1-\xi) + \theta_{23p}\cosh\gamma_p(1-\xi)\}\cos p\pi\eta$$

or

$$E_p \{\theta_{33p}\sin R(1-\xi)\sinh S(1-\xi) + \theta_{333p}\cos R(1-\xi)\cosh S(1-\xi)\}\cos p\pi\eta$$

Where

$\phi_I = 1/\phi$

$\alpha_1 = -2DHY\ \phi_I^2\ (p\pi)^2$

$\alpha_2 = Dxy\ \phi_I^4\ \{(p\pi)^4 - \lambda^4\phi^4\}$

And

$$\Theta_{1p} = -\frac{\cosh\beta_p}{\cos\gamma_p} \qquad \Theta_{2p} = -\frac{\cosh\beta_p}{\cosh\gamma_p} \qquad \Theta_{3p} = -\frac{\sin R \sinh S}{\cos R \cosh s}$$

$$\theta_{11p} = \frac{1}{[\beta_p \sinh\beta_p - \gamma_p \theta_{1p} \sin\gamma_p]} \qquad \theta_{22p} = \frac{1}{[\beta_p \cosh\beta_p + \gamma_p \theta_{2p} \cosh\gamma_p]}$$

$$\theta_{33p} = \frac{1}{\{(R\cos R\sinh S + S\sin R\cosh S) + \theta_{3p}(S\cos R\sinh S - R\sin R\cosh S)\}}$$

$$\theta_{13p} = \theta_{11p} \cdot \theta_{1p} \qquad \theta_{23p} = \theta_{22p} \cdot \theta_{2p} \qquad \theta_{333p} = \theta_{33p} \cdot \theta_{3p}$$

The prescribed slope will be:

$$\frac{\partial W_3}{\partial \xi}\Big|_{\xi=0} = \sum_{p=0,1,2}^{\infty} - E_p \cos m\pi\eta$$

A.2 Antisymmetric Modes

A.2.1 Solution of the first building block

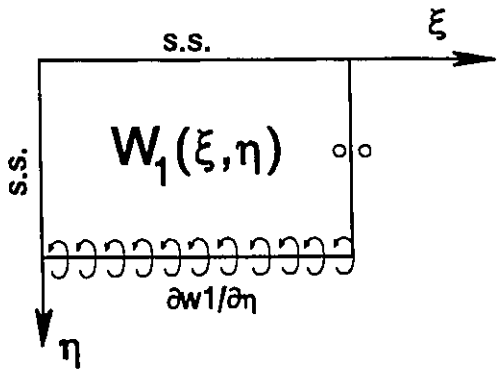

The Lévy type solution for this block can be written as

$$\sum_{m=1,3}^{k^*} \{A_m \sinh \beta_m\eta + B_m \sin \gamma_m\eta\} \sin\frac{m\pi\xi}{2}$$

$$+$$

$$W_1(\xi,\eta) = \sum_{k^*+2}^{\infty} \{A_m \sinh \beta_m\eta + B_m \sinh \gamma_m\eta\} \sin\frac{m\pi\xi}{2}$$

or

$$\{A_m \sin R\eta \cosh S\eta + B_m \cos R\eta \sinh S\eta\} \sin\frac{m\pi\xi}{2}$$

The condition of zero vertical edge reaction along the edge η=1 must be satisfied

$$\frac{V_y a^3}{bD_y} = -\left\{\frac{\partial^3 W(\xi,\eta)}{\partial\eta^3} + \nu_x^* \phi^2 \frac{\partial^3 W(\xi,\eta)}{\partial\eta\partial\xi^2}\right\}$$

Substitute W_1 into the above and set equal to zero. After carrying out the differentiations and

solving B_m in terms of A_m, the results are

$$B_m = \theta_{\#m} A_m$$

$$\theta_{1m} = \frac{\beta_m[\beta_m^2 - \upsilon_x^{*}\phi^2(\frac{m\pi}{2})^2]\cosh\beta_m}{\gamma_m[\gamma_m^2 + \upsilon_x^{*}\phi^2(\frac{m\pi}{2})^2]\cos\gamma_m}$$

$$\theta_{2m} = \frac{-\beta_m[\beta_m^2 - \upsilon_x^{*}\phi^2(\frac{m\pi}{2})^2]\cosh\beta_m}{\gamma_m[\gamma_m^2 - \upsilon_x^{*}\phi^2(\frac{m\pi}{2})^2]\cosh\gamma_m}$$

$$\theta_{3m} = -\frac{R_3\cos R\cosh S + R_4\sin R\sinh S}{R_5\cos R\cosh S + R_6\sin R\sinh S}$$

Now the slope along $\eta=1$ is expanded in the series

$$\frac{\partial W_1}{\partial \eta}\Big|_{\eta=1} = \sum_{m=1,3,5}^{\infty} E_m \sin\frac{m\pi\xi}{2}$$

Substitute W_1 (with $\theta_{\#m}A_m$ in place of B_m) into the slope equation, solve for A_m in terms of E_m.

$$\theta_{11m} = \frac{1}{[\beta_m\cosh\beta_m + \gamma_m\theta_{1m}\cos\gamma_m]}$$

$$\theta_{22m} = \frac{1}{[\beta_m\cosh\beta_m + \gamma_m\theta_{2m}\cosh\gamma_m]}$$

$$\theta_{33m} = \frac{1}{\{(R\cos R\cosh S + S\sin R\sinh S) + \theta_{3m}(S\cos R\cosh S - R\sin R\sinh S)\}}$$

where

$$R_1 = R(3S^2 - R^2)$$
$$R_2 = S(S^2 - 3R^2)$$

$$R_3 = [R_1 - \upsilon_x^* \phi^2 (\frac{m\pi}{2})^2 R] \qquad R_4 = [R_2 - \upsilon_x^* \phi^2 (\frac{m\pi}{2})^2 S]$$
$$R_5 = [R_2 - \upsilon_x^* \phi^2 (\frac{m\pi}{2})^2 S] \qquad R_6 = -[R_1 - \upsilon_x^* \phi^2 (\frac{m\pi}{2})^2 R]$$

Let

$\theta_{13m} = \theta_{11m} \cdot \theta_{1m}$
$\theta_{23m} = \theta_{22m} \cdot \theta_{2m}$
$\theta_{333m} = \theta_{33m} \cdot \theta_{3m}$

After the boundary conditions of the first building block is enforced, variables A_m and B_m are solved in terms of E_m and the newly introduced variable $\theta_{\#m}$. The final solution can therefore be expressed as:

$$W_1(\xi,\eta) = \sum_{m=1,3}^{k^*} E_m \{\theta_{11m}\sinh \beta_m\eta + \theta_{13m}\sin \gamma_m\eta\} \sin\frac{m\pi\xi}{2}$$

$$+$$

$$\sum_{k^*+2}^{\infty} E_m \{\theta_{22m}\sinh \beta_m\eta + \theta_{23m}\sinh \gamma_m\eta\} \sin\frac{m\pi\xi}{2}$$

or

$$E_m [\theta_{33m}\sin R\eta \cosh S\eta + \theta_{333m}\cos R\eta \sinh S\eta] \sin\frac{m\pi\xi}{2}$$

A.2.2 Solution of the second building block

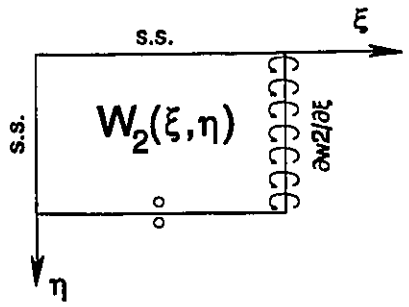

Second building block

Examination of building block #2 reveals that it is exactly identical to the first building block with the coordinates ξ and η interchanged. By following the transformation rules the solution is

$$W_2(\xi,\eta) = \sum_{n=1,3}^{k^*} E_n \{\theta_{11n}\sinh \beta_n\xi + \theta_{23n}\sin \gamma_n\xi\} \sin\frac{n\pi\eta}{2} + \sum_{k^*+2}^{\infty} E_n \{\theta_{22n}\sinh \beta_n\xi + \theta_{23n}\sinh \gamma_n\xi\} \sin\frac{n\pi\eta}{2}$$

or

$$E_n [\theta_{33n}\sin R\xi \cosh S\xi + \theta_{333n}\cos R\xi \sinh S\xi] \sin\frac{n\pi\eta}{2}$$

$$\theta_{1n} = \frac{\beta_n[\beta_n^2 - \upsilon_y^*\phi_I^2(\frac{n\pi}{2})^2] \cosh\beta_n}{\gamma_n[\gamma_n^2 + \upsilon_y^*\phi_I^2(\frac{n\pi}{2})^2] \cos\gamma_n}$$

$$\theta_{2n} = \frac{\cdot\cdot\beta_n[\beta_n^2 - \upsilon_y^*\phi_I^2(\frac{n\pi}{2})^2]\cosh\beta_n}{\gamma_n[\gamma_n^2 - \upsilon_y^*\phi_I^2(\frac{n\pi}{2})^2]\cosh\gamma_n}$$

$$\theta_{3n} = -\frac{R_3\cos R\cosh S + R_4\sin R\sinh S}{R_5\cos R\cosh S + R_6\sin R\sinh S}$$

Where: $\alpha_1 = -2DHy\ \phi_i^2\ (n\pi/2)^2$

$\alpha_2 = Dxy\ \phi_i^4\ \{(n\pi/2)^4 - \lambda^4\phi^4\}$

$z = \alpha_1^2 - 4\alpha_2$

$$\beta_m^2 = \frac{1}{2}(\sqrt{z} - \alpha_1)$$

$$\gamma_m^2 = \frac{1}{2}(\sqrt{z} + \alpha_1) \quad or \quad \gamma_m^2 = -\frac{1}{2}(\sqrt{z} + \alpha_1)$$

whichever is positive

And

$z_1 = -1/2\ \alpha_1$ $\qquad$ $z_2 = 1/2\ \sqrt{-z},$

$z_3 = \tan^{-1}(z_2/z_1)$ $\qquad$ $z_4 = (z_1^2 + z_2^2)^{1/4}$

$R = z_4 \sin(z_3/2)$ $\qquad$ $S = z_4 \cos(z_3/2)$

$$R_1 = R(3S^2 - R^2)$$
$$R_2 = S(S^2 - 3R^2)$$

$$R_3 = [R_1 - \upsilon_y^*\phi_I^2(\frac{n\pi}{2})^2 R] \qquad R_4 = [R_2 - \upsilon_y^*\phi_I^2(\frac{n\pi}{2})^2 S]$$

$$R_5 = [R_2 - \upsilon_y^*\phi_I^2(\frac{n\pi}{2})^2 S] \qquad R_6 = -[R_1 - \upsilon_y^*\phi_I^2(n\pi)^2 R]$$

$$\theta_{11n} = \frac{1}{[\beta_n\cosh\beta_n + \gamma_n\theta_{1n}\cos\gamma_n]}$$

$$\theta_{22n} = \frac{1}{[\beta_n \cosh\beta_n + \gamma_n \theta_{2n} \cosh\gamma_n]}$$

$$\theta_{33n} = \frac{1}{\{(R\cos R\cosh S + S\sin R\sinh S) + \theta_{3n}\,(S\cos R\cosh S - R\sin R\sinh S)\}}$$

$$\theta_{13n} = \theta_{11n} \cdot \theta_{1n}$$
$$\theta_{23n} = \theta_{22n} \cdot \theta_{2n}$$
$$\theta_{333n} = \theta_{33n} \cdot \theta_{3n}$$

The enforcing rotation along edge $\xi=1$ is

$$\frac{\partial W_2}{\partial \xi}\Big|_{\xi=1} = \sum_{n=1,3,5}^{\infty} E_n \sin\frac{n\pi\eta}{2}$$

A.2.3 Solution of the third building block

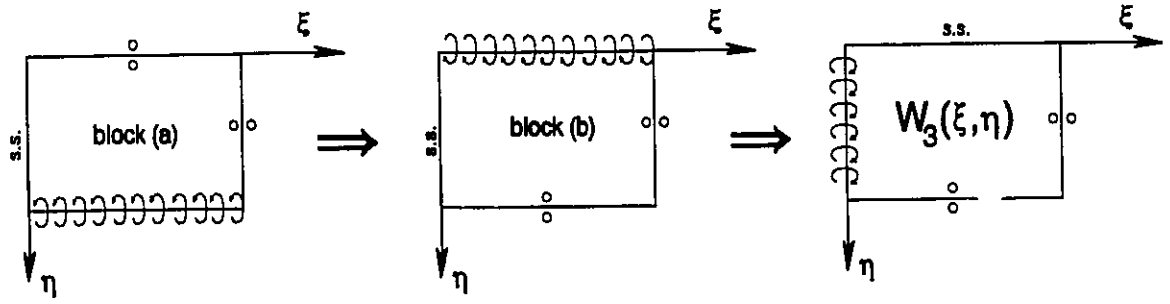

Building Block #3

The task of finding the third building block solution is made easier by using intermediate blocks which resemble those used previously. Firstly, building block (a) of Figure 2.11is solved,

then by changing variable η into $(1-\eta)$ leads to solution for block (b). Finally, the required third block solution is obtained by interchanging the ξ and η coodinates and following all the transformation rules.

Focusing on block (a), the Lévy-type solution is

$$W_3^a(\xi,\eta) = \sum_{m=1,3,5}^{\infty} Y_m(\eta) \sin\frac{m\pi\xi}{2}$$

Substituting this equation into the equilibrium GDE results in expressions for $Y_m(\eta)$. β_m, γ_m, R, and S are defined as in Chapter 1. Due to the slip shear condition along edge η, antisymmetric terms in $Y_m(\eta)$ are deleted. The solution is

$$\sum_{m=1,3,5}^{k^*} \{A_m \cosh\beta_m\eta + B_m \cos\gamma_m\eta\} \sin\frac{m\pi\xi}{2}$$

$$+$$

$$W_3^{''}(\xi,\eta) = \sum_{k^*+2}^{\infty} \{A_m \cosh\beta_m\eta + B_m \cosh\gamma_m\eta\} \sin\frac{m\pi\xi}{2}$$

$$\textit{or}$$

$$\{A_m \sin R\eta \sinh S\eta + B_m \cos R\eta \cosh S\eta\} \sin\frac{m\pi\xi}{2}$$

For this building block, it is necessary to enforce the zero - displacement condition at η=1.

$$W(\xi,1) = 0$$

For all three cases, respectively

$$A_m \cosh\beta_m + B_m \cos\gamma_m = 0$$

$$A_m \cosh\beta_m + B_m \cosh\gamma_m = 0$$

$$A_m \sin R \sinh S + B_m \cos R \cosh S = 0$$

Solve each for B_m in terms of A_m as before

$$B_m = \theta_{\#m} \cdot A_m$$

$$\Theta_{1m} = -\frac{\cosh\beta_m}{\cos\gamma_m} \qquad \Theta_{2m} = -\frac{\cosh\beta_m}{\cosh\gamma_m} \qquad \Theta_{3m} = -\frac{\sin R \sinh S}{\cos R \cosh s}$$

Next step is to enforce harmonic slope at edge $\eta=1$.

$$\frac{\partial W_3^a}{\partial \eta}\Big|_{\eta=1} = \sum_{m=1,3,5}^{\infty} E_m \sin\frac{m\pi\xi}{2}$$

Equate the first derivatives of Eq. W_3^a (with $\theta_{\#m}A_m$ in place of B_m) to the RHS of Eq. 2.76 cancel the common terms $\sin(m\pi\xi/2)$, and finally solve for A_m in terms of E_m. This results in solution of building block (a) as follows

$$W_3^a(\xi,\eta) = \sum_{m=1,3,5}^{k^*} E_m \{\theta_{11m}\cosh\beta_m\eta + \theta_{13m}\cos\gamma_m\eta\} \sin\frac{m\pi\xi}{2} + \sum_{k^*+2}^{\infty^{**}} E_m \{\theta_{22m}\cosh\beta_m\eta + \theta_{23m}\cosh\gamma_m\eta\} \sin\frac{m\pi\xi}{2}$$

or

$$E_m \{\theta_{33m}\sin R\eta \sinh S\eta + \theta_{333m}\cos R\eta \cosh S\eta\} \sin\frac{m\pi\xi}{2}$$

Where

$$\theta_{11m} = \frac{1}{[\beta_m \sinh\beta_m - \gamma_m\theta_{1m}\sin\gamma_m]} \qquad \theta_{22m} = \frac{1}{[\beta_m\cosh\beta_m + \gamma_m\theta_{2m}\cosh\gamma_m]}$$

$$\theta_{33m} = \frac{1}{\{(R\cos R\sinh S + S\sin R\cosh S) + \theta_{3m}(S\cos R\sinh S - R\sin R\cosh S)\}}$$

$$\theta_{13m} = \theta_{11m} \cdot \theta_{1m} \qquad \theta_{23m} = \theta_{22m} \cdot \theta_{2m} \qquad \theta_{333m} = \theta_{33m} \cdot \theta_{3m}$$

The solution of building block (b) is then extracted from that of block (a) by replacing η by1-η. The prescribed slope will also change sign.

$$\frac{\partial W_3^b}{\partial \eta}\Big|_{\eta=0} = \sum_{m=1,3,5}^{\infty} - E_m \sin\frac{m\pi\xi}{2}$$

Building block (b) has solutions as:

$$\sum_{m=1,3,5}^{k^*} E_m \{\theta_{11m}\cosh\beta_m(1-\eta) + \theta_{13m}\cos\gamma_m(1-\eta)\} \sin\frac{m\pi\xi}{2}$$

$$+$$

$$W_3^b(\xi,\eta) = \sum_{k^*+2}^{\infty} E_m \{\theta_{22m}\cosh\beta_m(1-\eta) + \theta_{23m}\cosh\gamma_m(1-\eta)\} \sin\frac{m\pi\xi}{2}$$

$$or$$

$$E_m \{\theta_{33m}\sin R(1-\eta)\sinh S(1-\eta) + \theta_{333m}\cos R(1-\eta)\cosh S(1-\eta)\} \sin\frac{m\pi\xi}{2}$$

To arrive at the solution of block (c) or original third building block, variables ξ and η have to be interchanged. Following the same logic in variable transformation as before, the aspect ratio is now the its inverse and λ^2 is multiplied by ϕ^2. The final solution for the third building block is:

$$\sum_{p=1,3,5}^{k^*} E_p \{\theta_{11p}\cosh\beta_p(1-\xi) + \theta_{13p}\cos\gamma_p(1-\xi)\} \sin\frac{p\pi\eta}{2}$$

$$+$$

$$W_3(\xi,\eta) = \sum_{k^*+2}^{\infty} E_p \{\theta_{22p}\cosh\beta_p(1-\xi) + \theta_{23p}\cosh\gamma_p(1-\xi)\} \sin\frac{p\pi\eta}{2}$$

$$or$$

$$E_p \{\theta_{33p}\sin R(1-\xi)\sinh S(1-\xi) + \theta_{333p}\cos R(1-\xi)\cosh S(1-\xi)\} \sin\frac{p\pi\eta}{2}$$

Where

$\phi_1 = 1/\phi$

$\alpha_1 = -2DHx\ \phi_1^2\ (p\pi)^2$

$\alpha_2 = 1/Dxy\ \phi_1^4\ \{(p\pi)^4 - \lambda^4\phi^4\}$

$z = \alpha_1^2 - 4\alpha_2$

$$\beta_m^2 = \frac{1}{2}(\sqrt{z} - \alpha_1)$$

$$\gamma_m^2 = \frac{1}{2}(\sqrt{z} + \alpha_1) \quad or \quad \gamma_m^2 = -\frac{1}{2}(\sqrt{z} + \alpha_1)$$

whichever is positive

And

$z_1 = -1/2\ \alpha_1$ $\qquad$ $z_2 = 1/2\ \sqrt{-z}$,

$z_3 = \tan^{-1}(z_2/z_1)$ $\qquad$ $z_4 = (z_1^2 + z_2^2)^{1/4}$

$R = z_4 \sin(z_3/2)$ $\qquad$ $S = z_4 \cos(z_3/2)$

$$R_1 = R(3S^2 - R^2)$$
$$R_2 = S(S^2 - 3R^2)$$

$$R_3 = [R_1 - \upsilon_y^* \phi_1^2 (\frac{n\pi}{2})^2 R] \qquad R_4 = [R_2 - \upsilon_y^* \phi_1^2 (\frac{n\pi}{2})^2 S]$$

$$R_5 = [R_2 - \upsilon_y^* \phi_1^2 (\frac{n\pi}{2})^2 S] \qquad R_6 = -[R_1 - \upsilon_y^* \phi_1^2 (n\pi)^2 R]$$

$$\Theta_{1p} = -\frac{\cosh\beta_p}{\cos\gamma_p} \qquad \Theta_{2p} = -\frac{\cosh\beta_p}{\cosh\gamma_p} \qquad \Theta_{3p} = -\frac{\sin R \sinh S}{\cos R \cosh s}$$

$$\theta_{11p} = \frac{1}{[\beta_p \sinh\beta_p - \gamma_p \theta_{1p} \sin\gamma_p]} \qquad \theta_{22p} = \frac{1}{[\beta_p \cosh\beta_p + \gamma_p \theta_{2p} \cosh\gamma_p]}$$

$$\theta_{33p} = \frac{1}{\{(R\cos R\sinh S + S\sin R\cosh S) + \theta_{3p}\,(S\cos R\sinh S - R\sin R\cosh S)\}}$$

$$\theta_{13p} = \theta_{11p}\cdot\theta_{1p} \qquad \theta_{23p} = \theta_{22p}\cdot\theta_{2p} \qquad \theta_{333p} = \theta_{33p}\cdot\theta_{3p}$$

The prescribed slope will be:

$$\frac{\partial W_3}{\partial \xi}\Big|_{\xi=0} = \sum_{p=1,3,5}^{\infty} -E_p \sin\frac{m\pi\eta}{2}$$

Appendix B

Associated Mode Shapes & Contour Plots, And Computed Eigenvalues

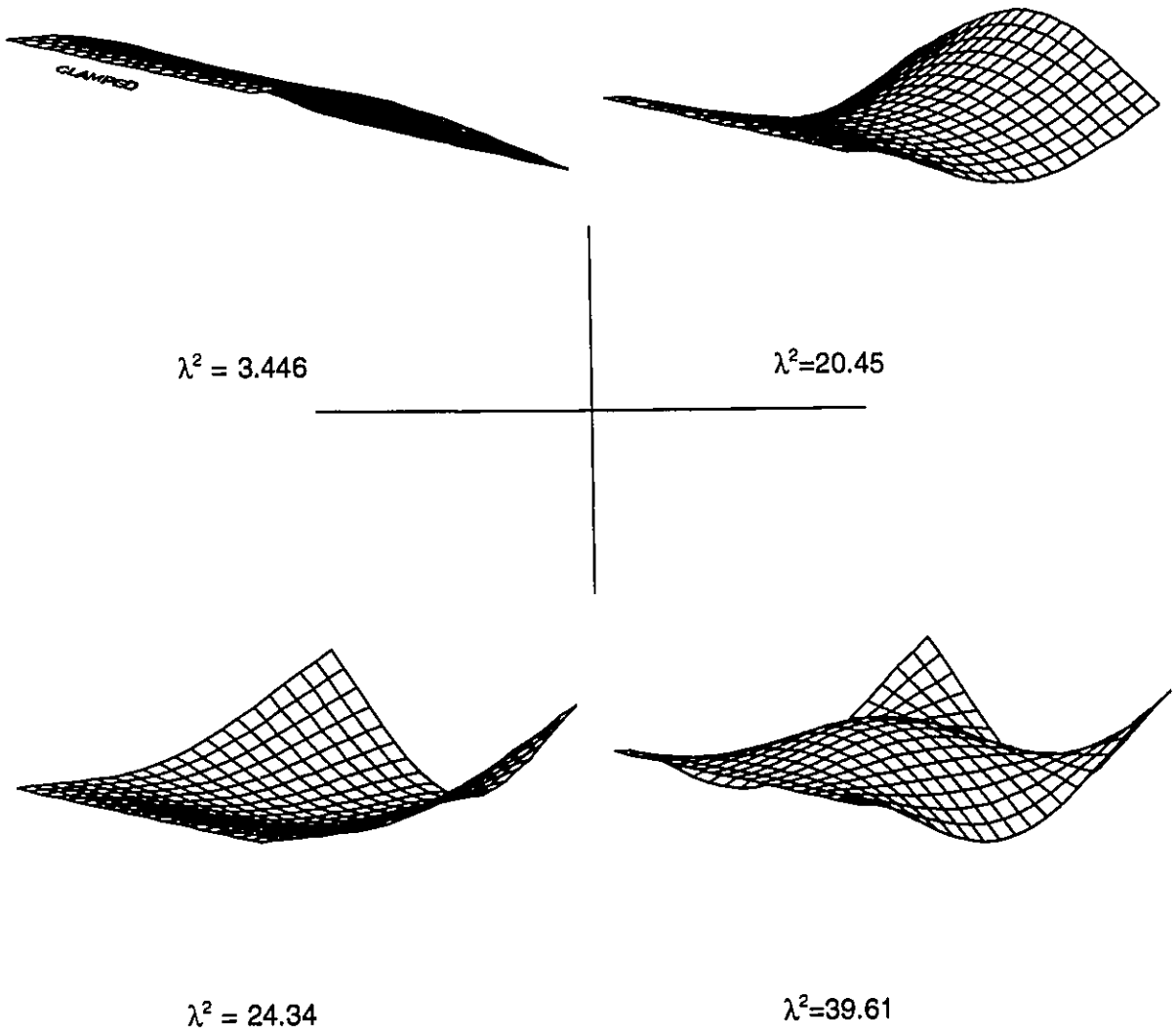

FIGURE B.1.1 First Four Associated Mode Shapes - Symmetric (DHY=0.5, DHX=0.5, ø=0.5)

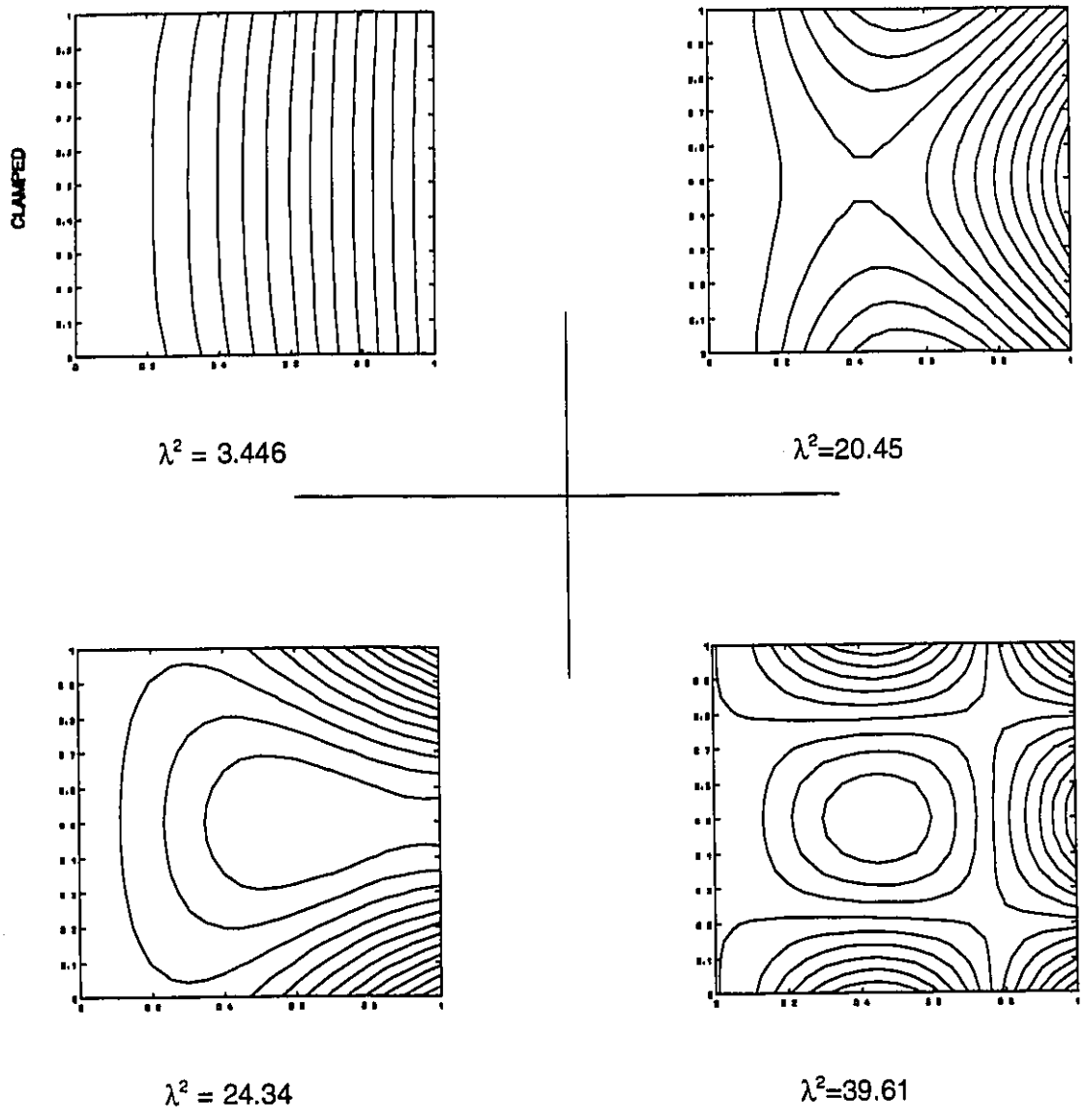

FIGURE B.1.2 First Four Associated Contour Plots - Symmetric (DHY=0.5, DHX=0.5, ø=0.5)

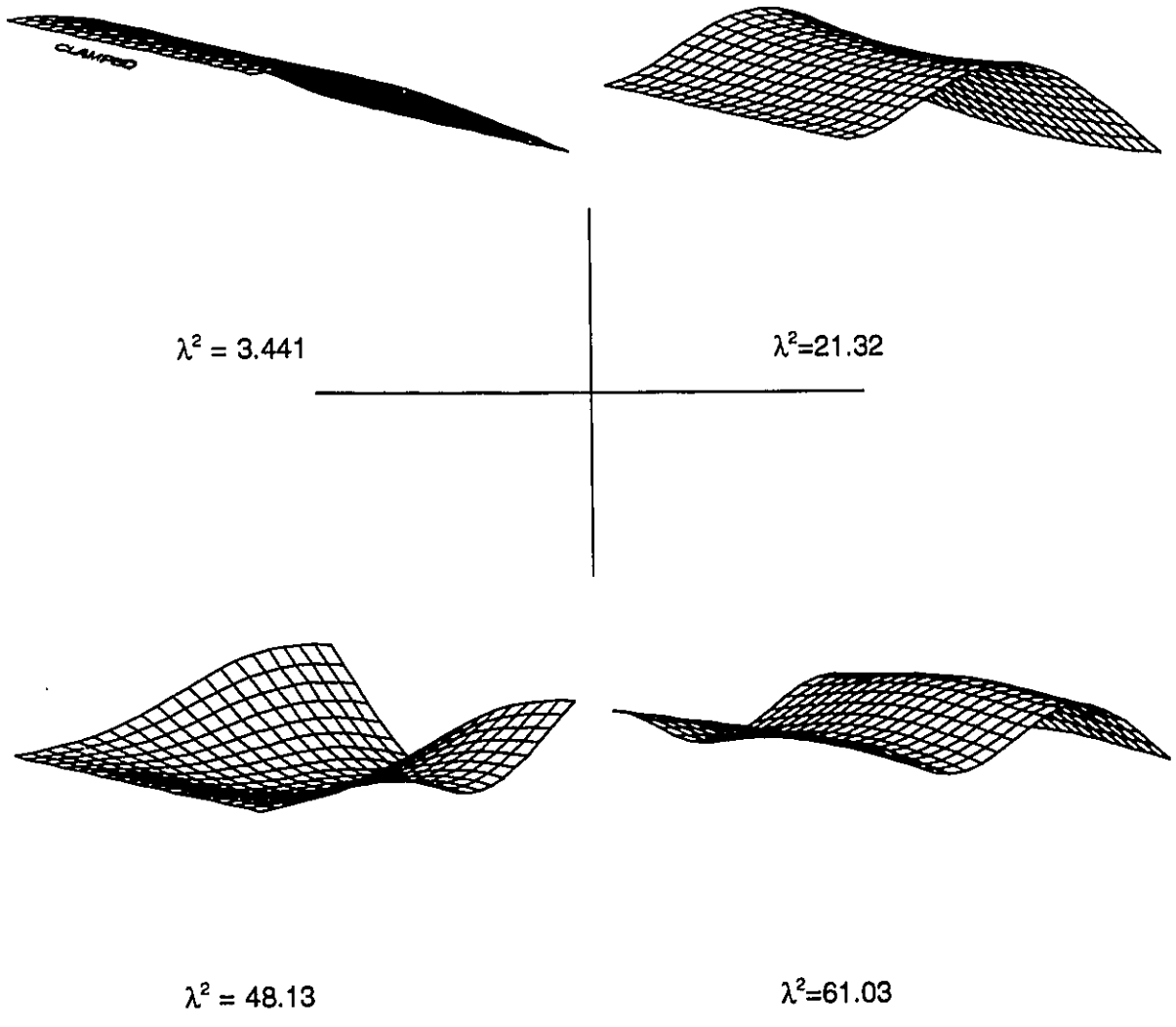

FIGURE B.1.3 First Four Associated Mode Shapes - Symmetric (DHY=0.5, DHX=2.0, ø=0.5)

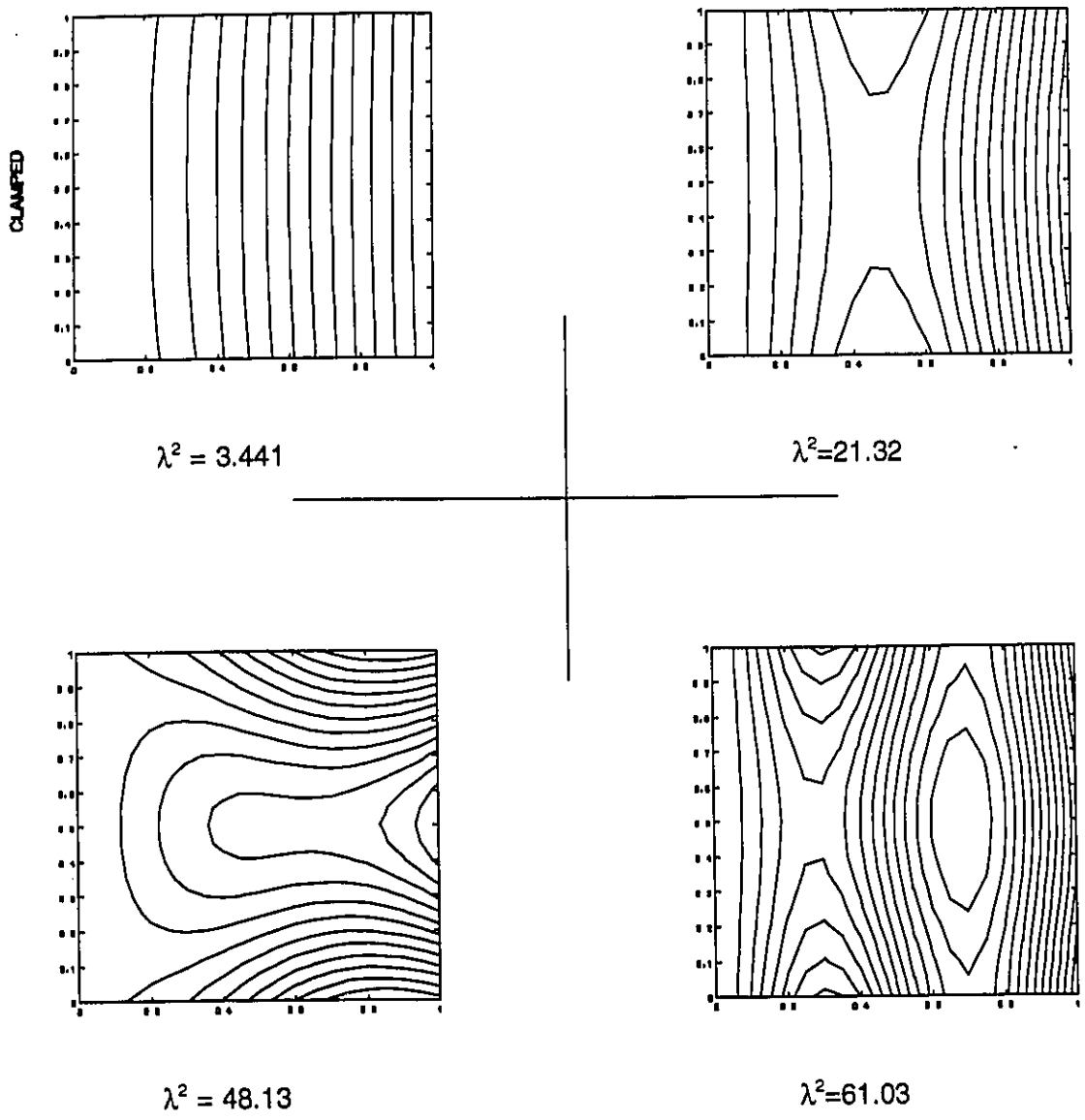

FIGURE B.1.4 First Four Associated Contour Plots - Symmetric (DHY=0.5, DHX=2.0, ø=0.5)

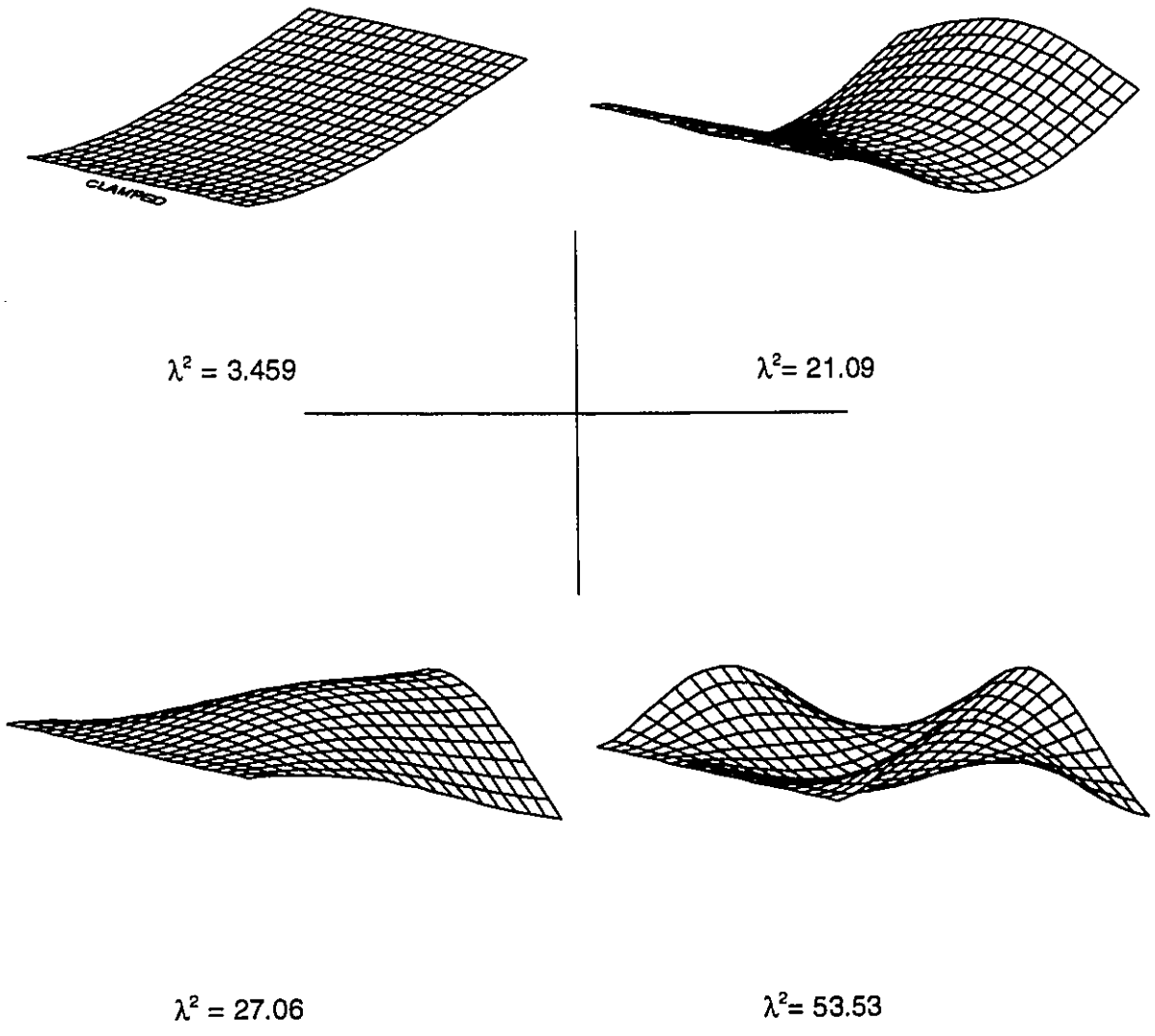

FIGURE B.1.5 First Four Associated Mode Shapes - Symmetric (DHY=1.0, DHX=1.0, ø=0.5, Special Case of Orthotropic: Isotropic)

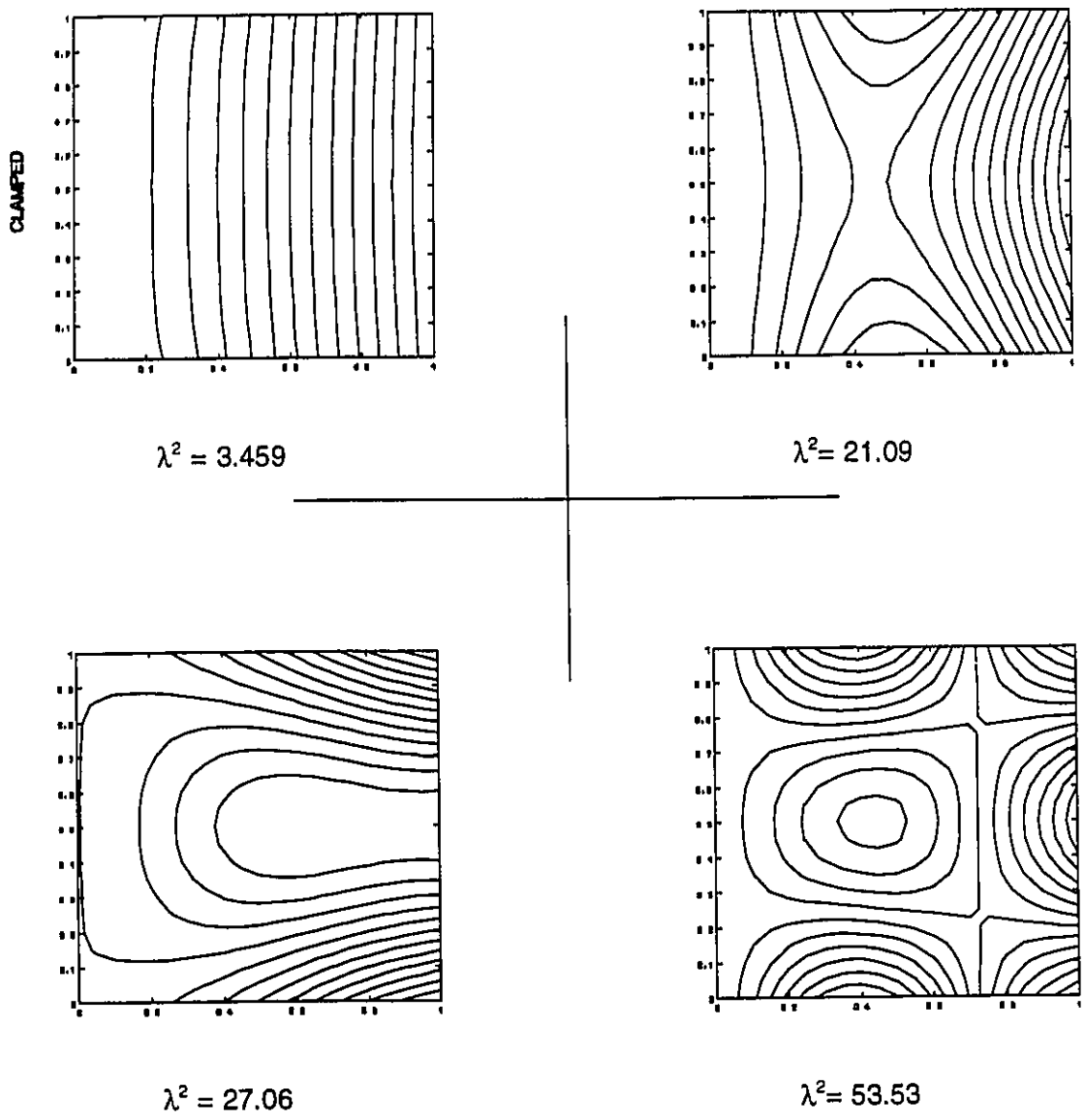

FIGURE B.1.6 First Four Associated Contour Plots - Symmetric (DHY=1.0, DHX=1.0, ø=0.5, Case of Isotropic)

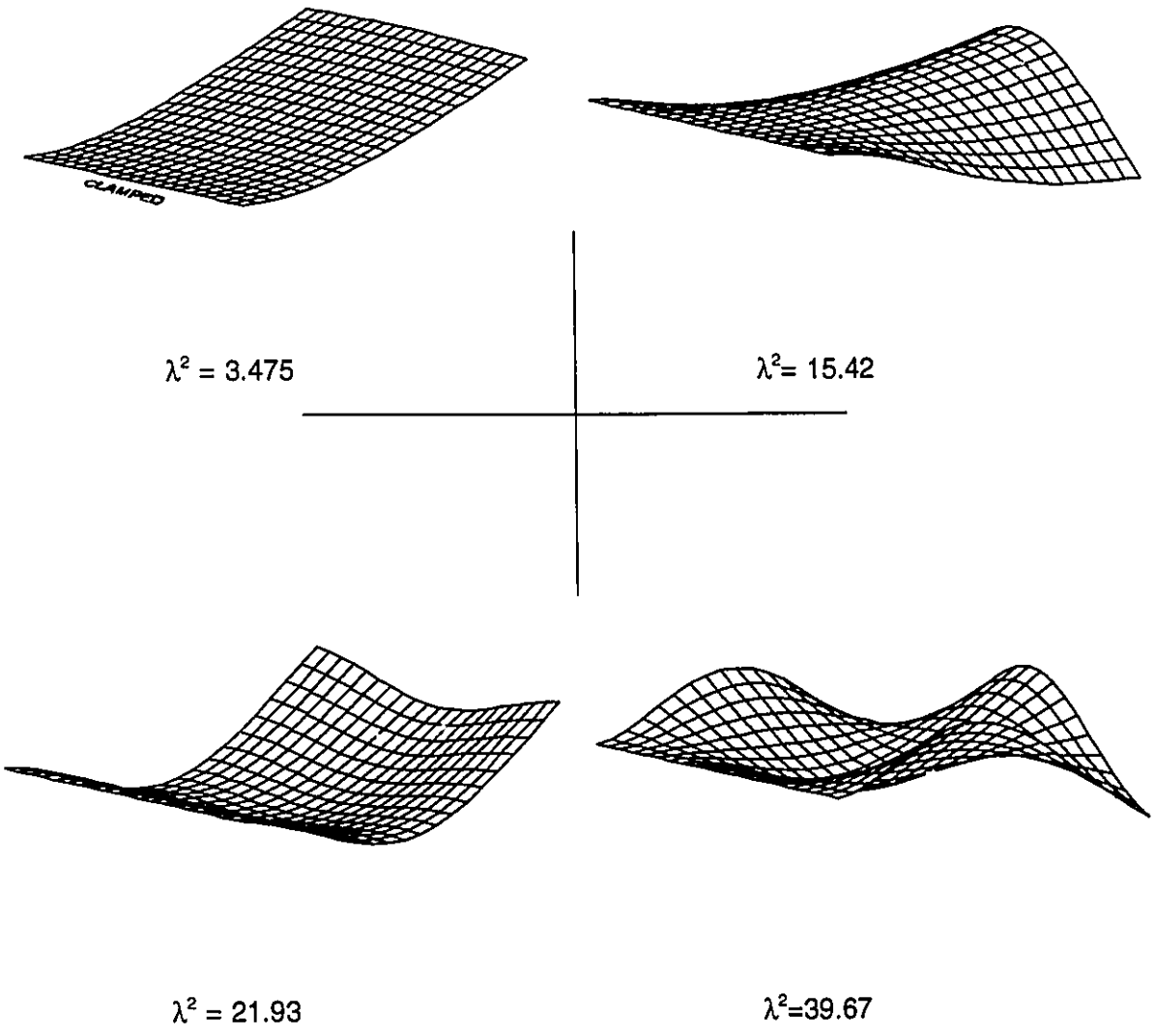

FIGURE B.1.7 First Four Associated Mode Shapes - Symmetric (DHY=2.0, DHX=0.5, ø=0.5)

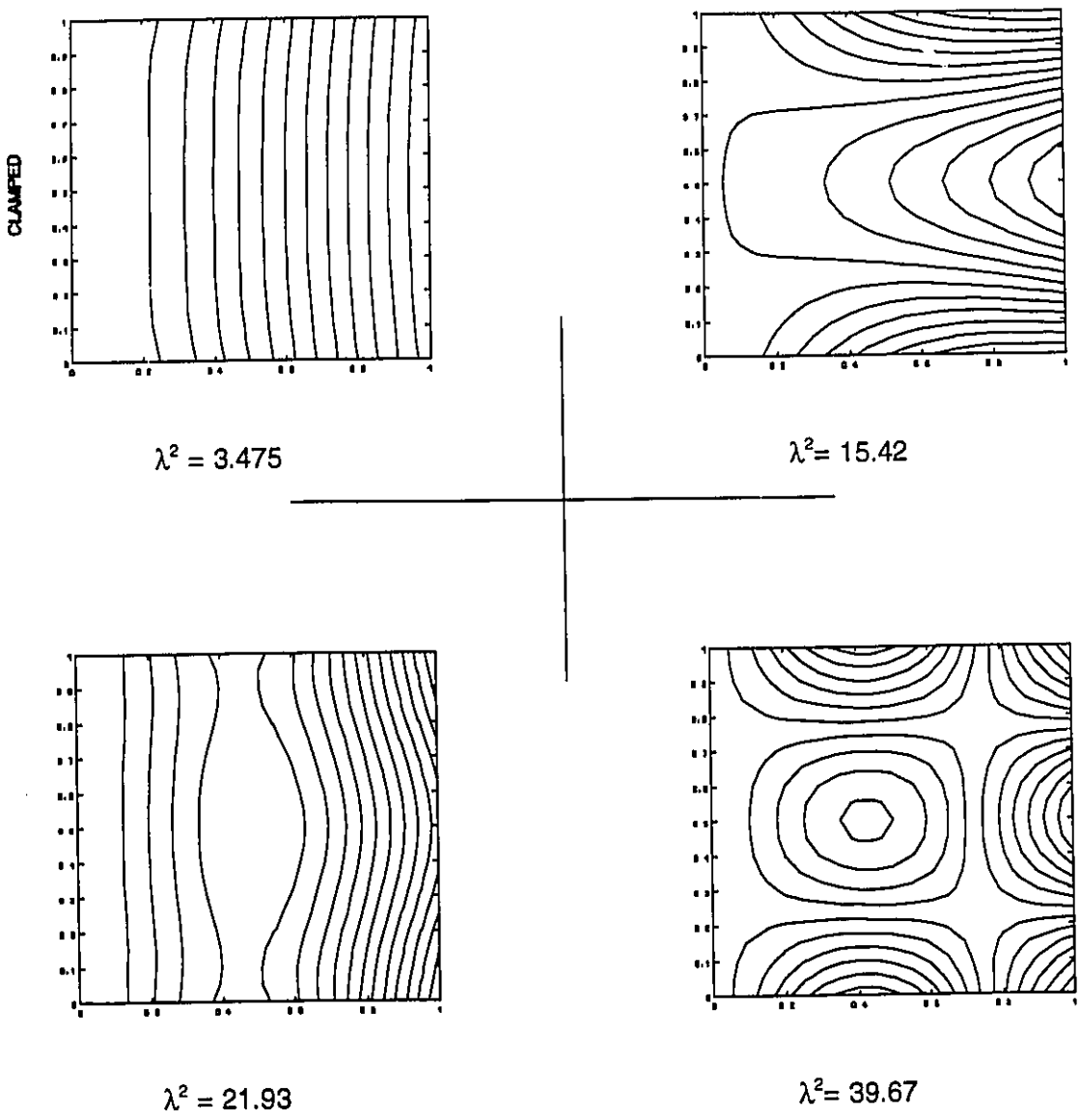

FIGURE B.1.8 First Four Associated Contour Plots - Symmetric (DHY=2.0, DHX=0.5, ø=0.5)

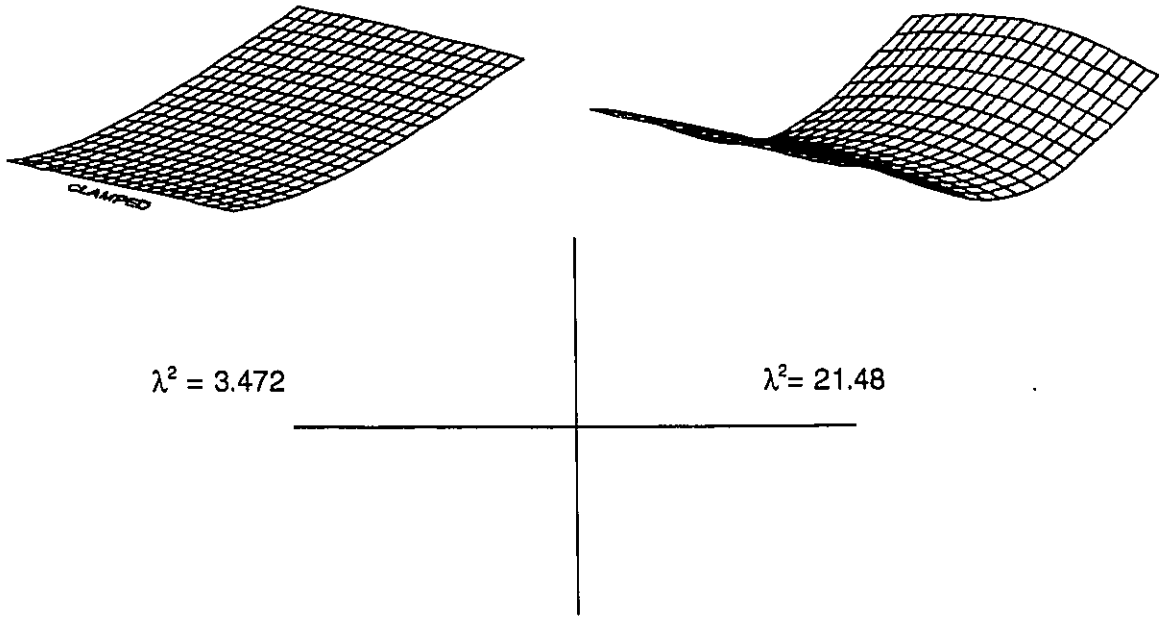

$\lambda^2 = 3.472$ $\lambda^2 = 21.48$

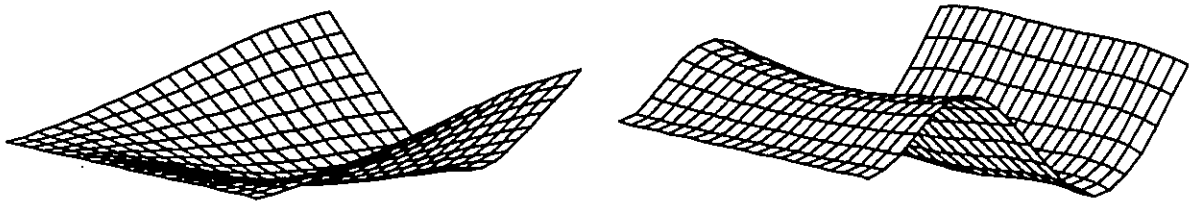

$\lambda^2 = 31.42$ $\lambda^2 = 61.13$

FIGURE B.1.9 First Four Associated Mode Shapes - Symmetric (DHY=2.0, DHX=2.0, ø=0.5)

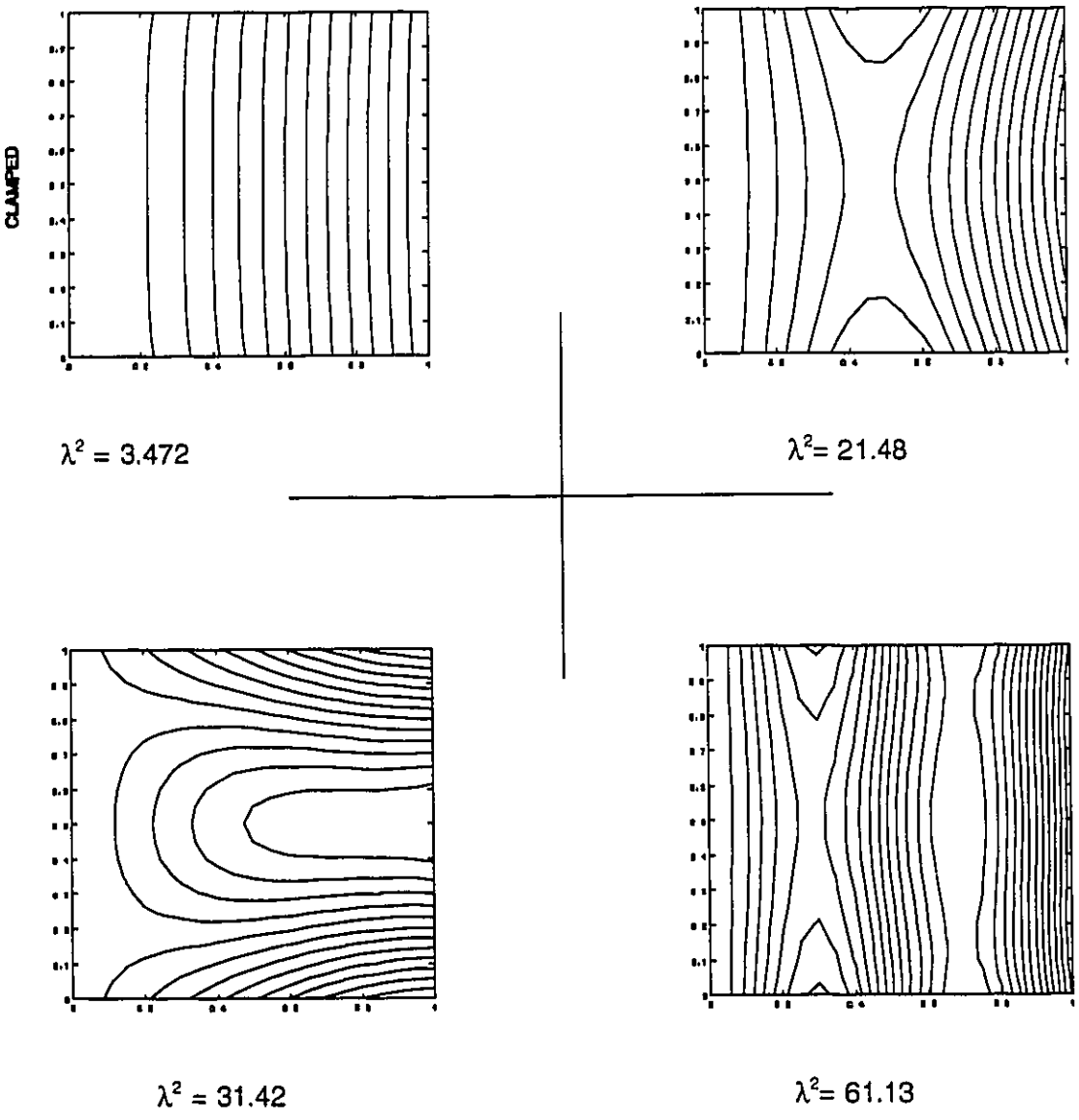

FIGURE B.1.10 First Four Associated Contour Plots - Symmetric (DHY=2.0, DHX=2.0, ø=0.5)

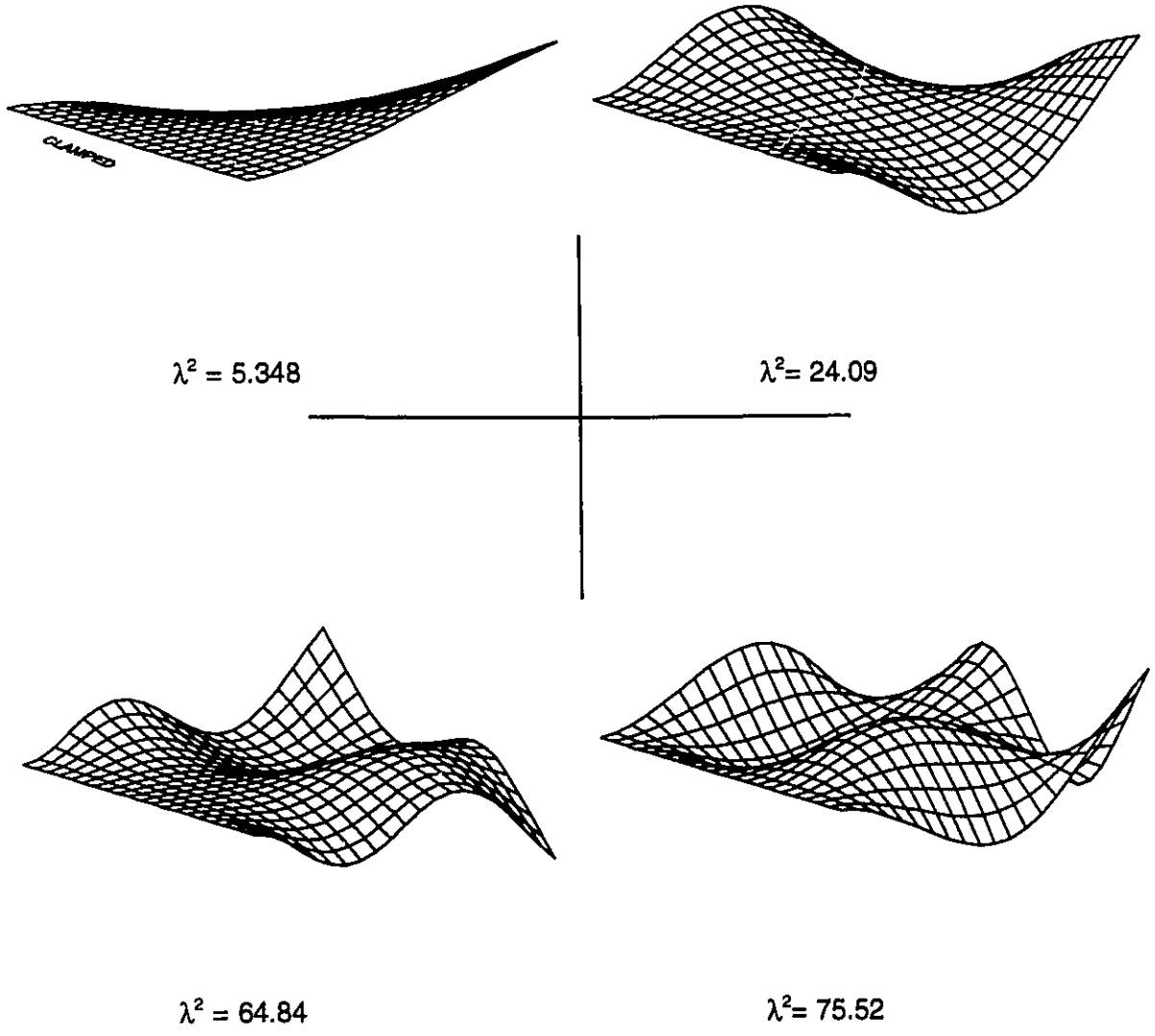

FIGURE B.2.1 First Four Associated Mode Shapes - Antisymmetric (DHY=0.5, DHX=0.5, ø=0.5)

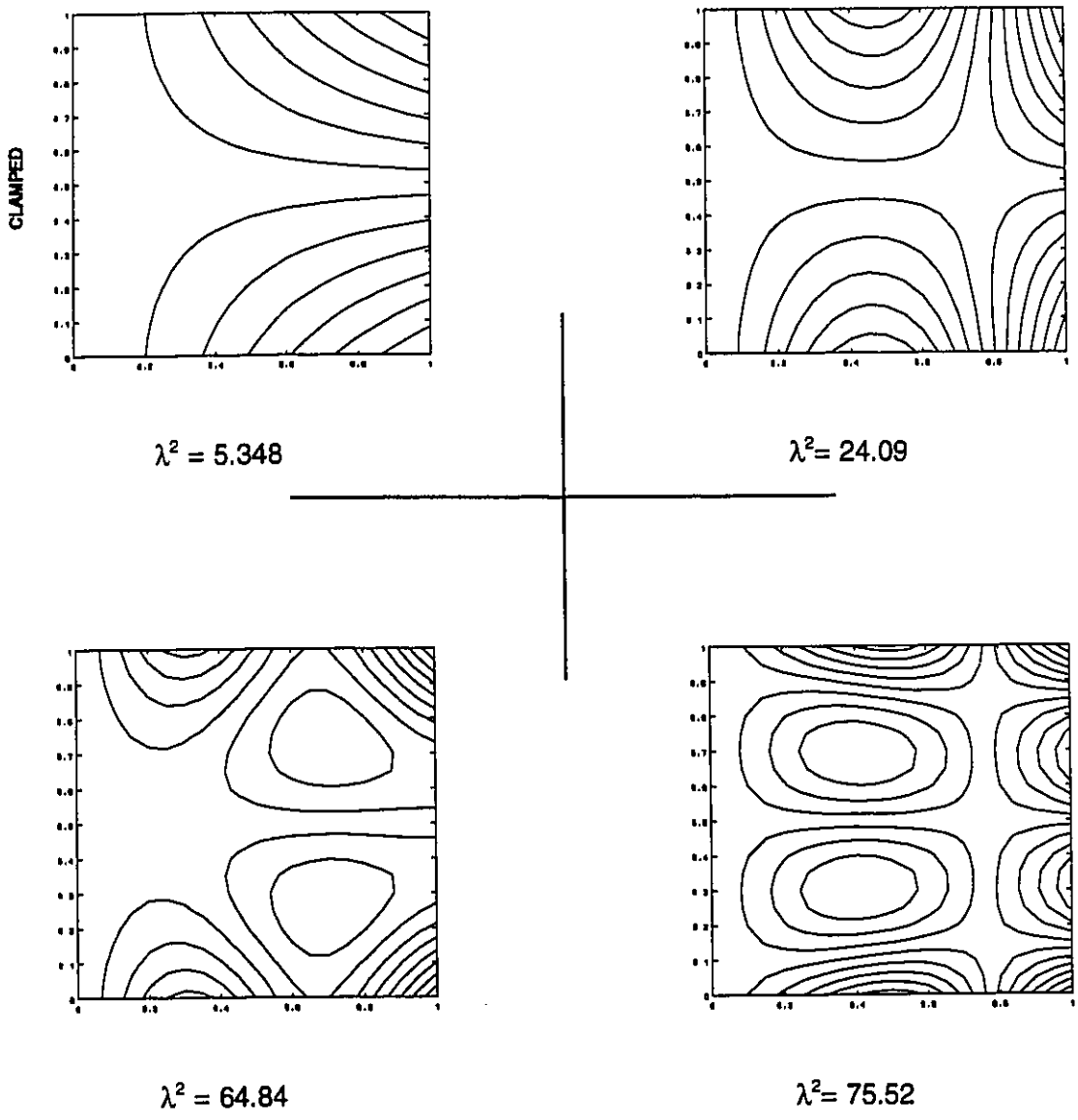

FIGURE B.2.2 First Four Associated Contour Plots - Antisymmetric (DHY=0.5, DHX=0.5, ø=0.5)

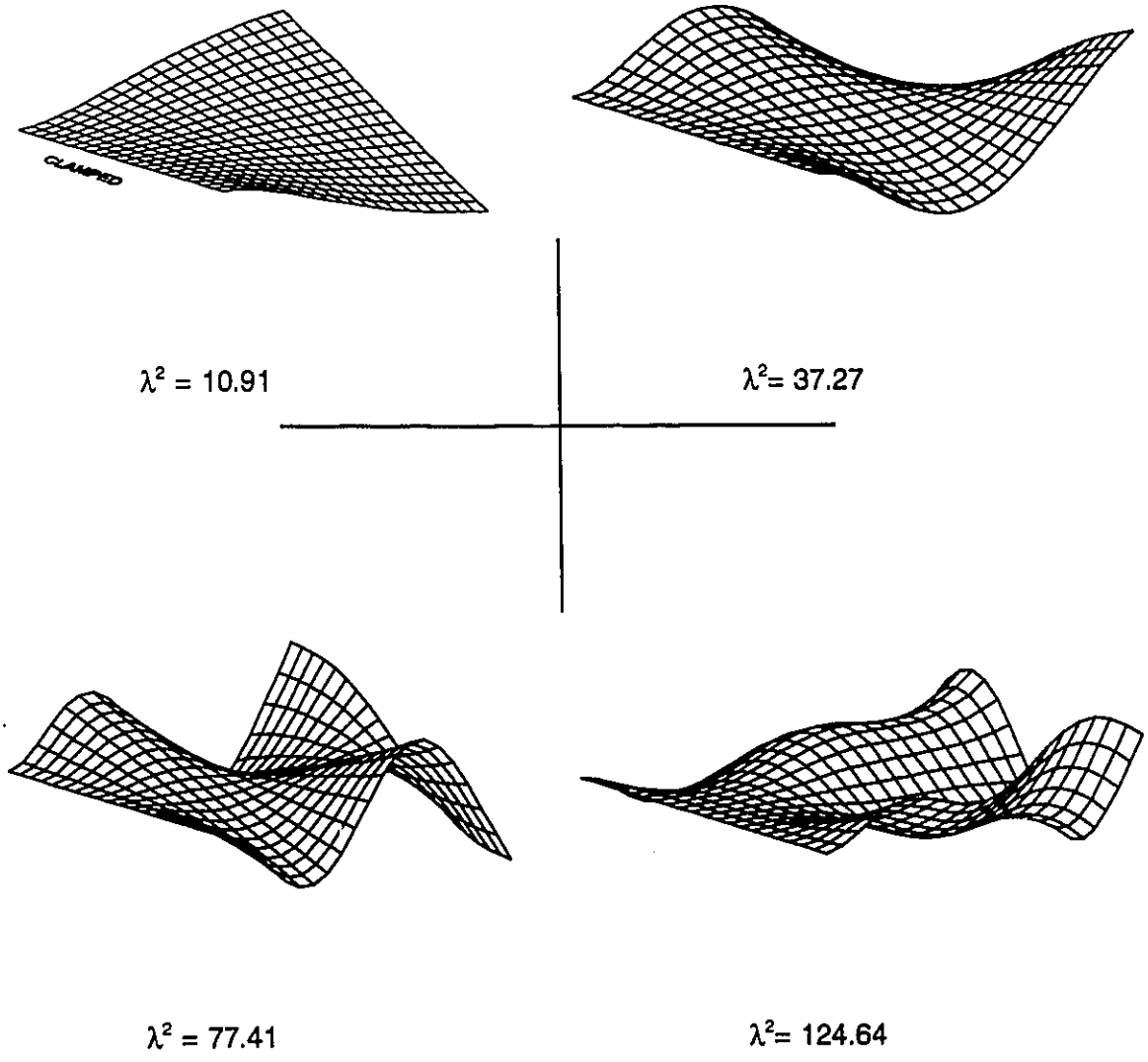

FIGURE B.2.3 First Four Associated Mode Shapes - Antisymmetric (DHY=0.5, DHX=2.0, ø=0.5)

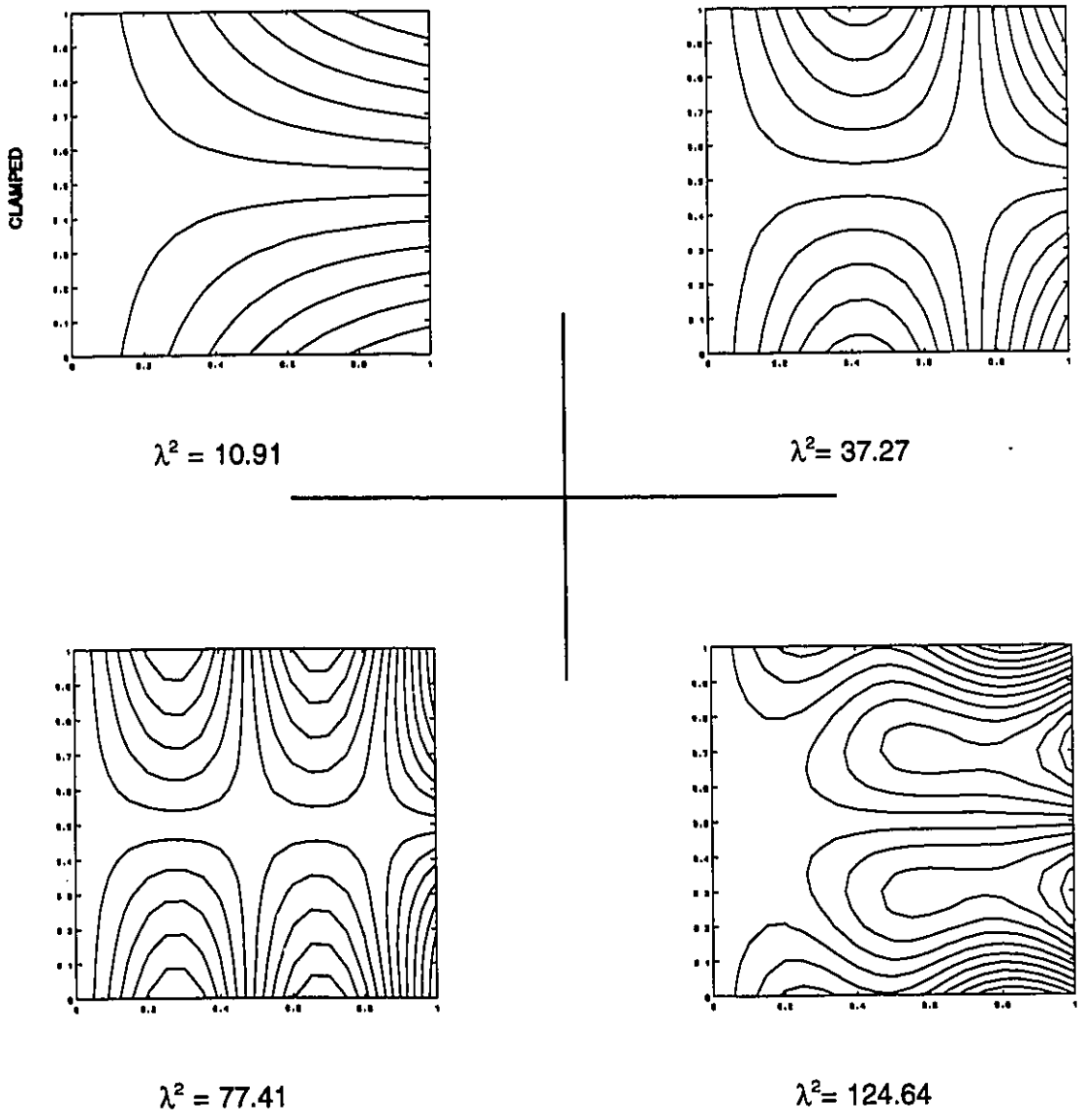

FIGURE B.2.4 First Four Associated Contour Plots - Antisymmetric (DHY=0.5, DHX=2.0, ø=0.5)

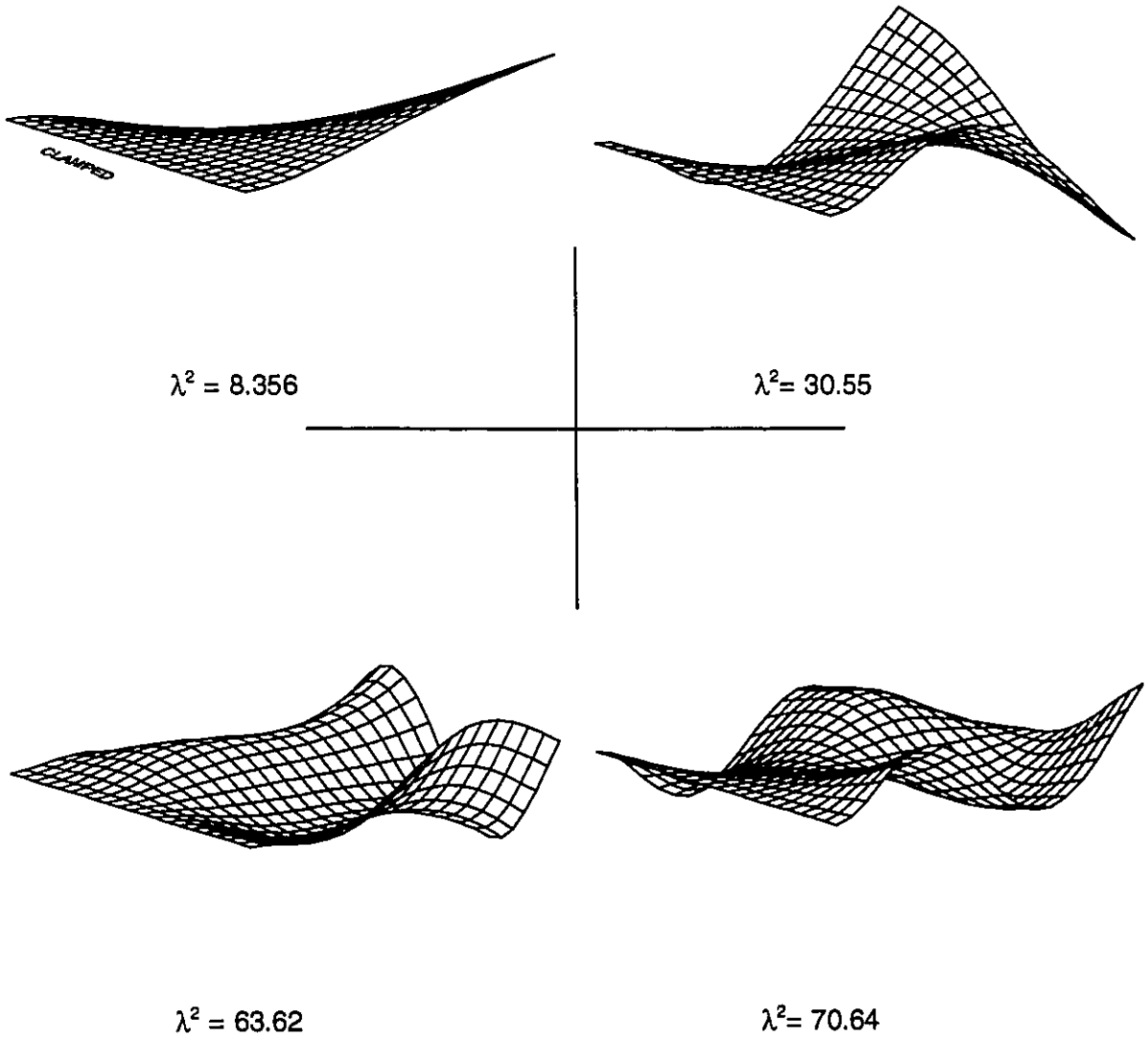

FIGURE B.2.5 First Four Associated Mode Shapes - Antisymmetric (DHY=1.0, DHX=1.0, ø=0.5, Special case of Orthotropy: Isotropic)

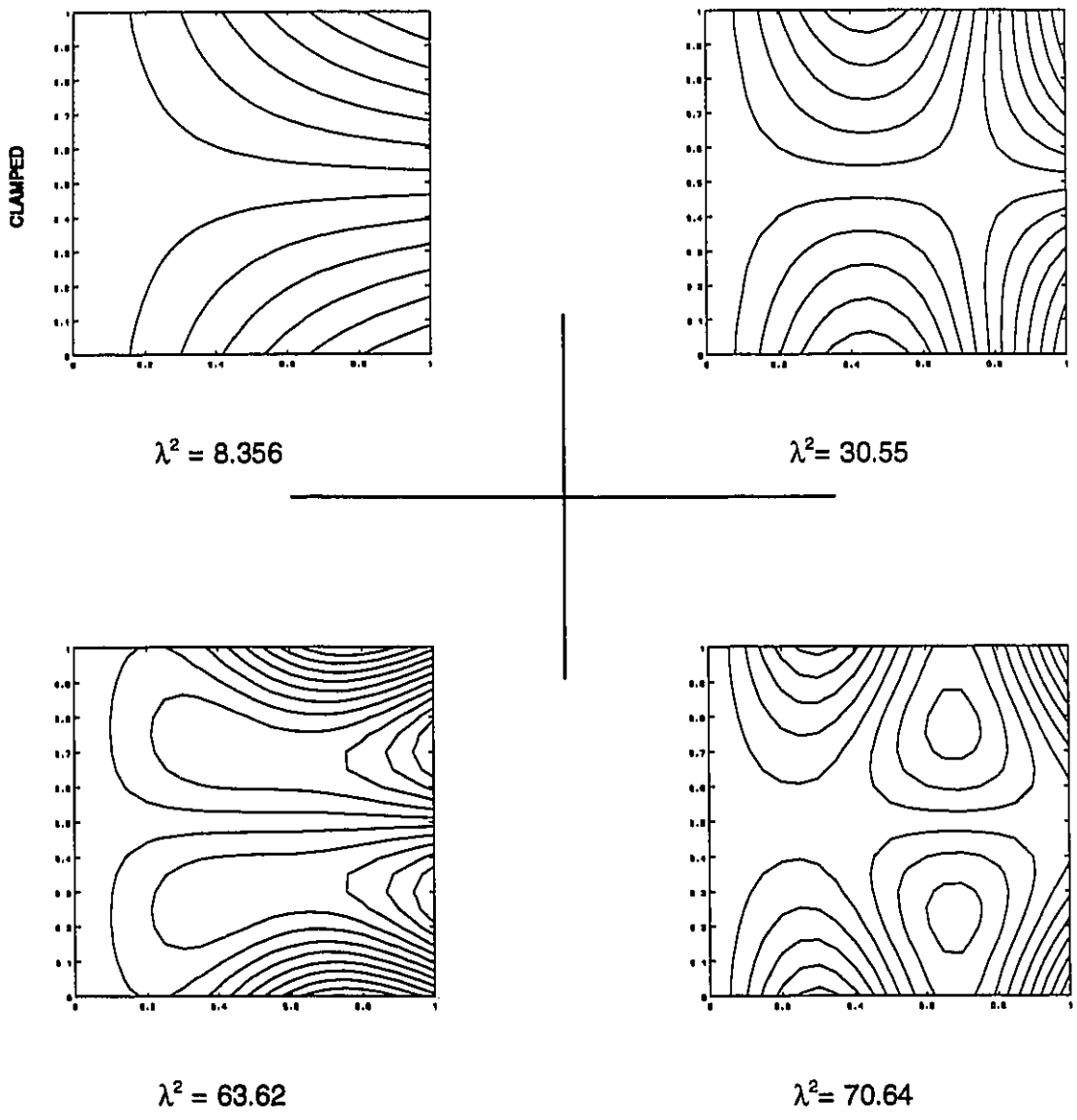

FIGURE B.2.6 First Four Associated Contour Plots - Antisymmetric (DHY=1.0, DHX=1.0, ø=0.5, Isotropic Case)

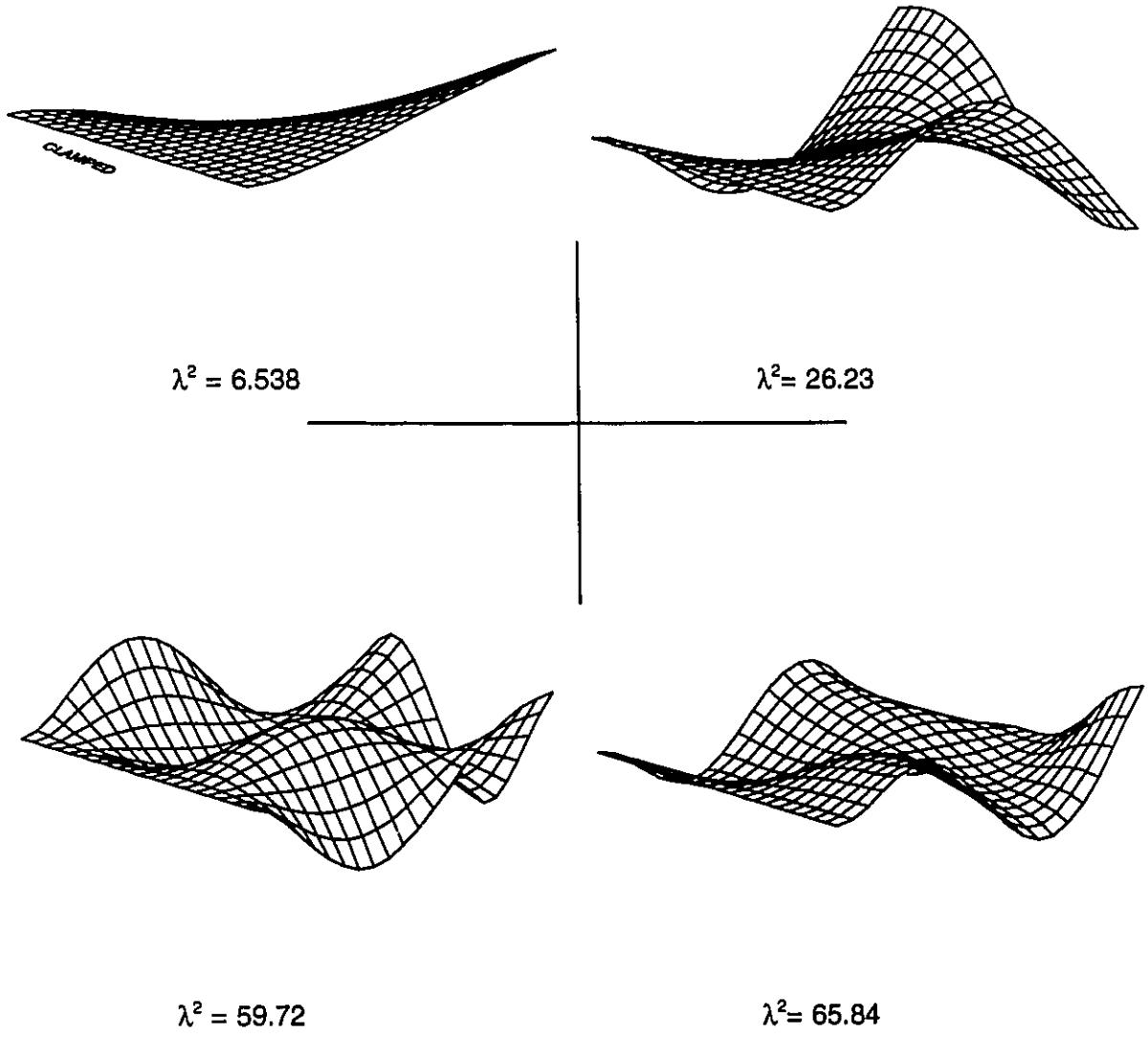

FIGURE B.2.7 First Four Associated Mode Shapes - Antisymmetric (DHY=2.0, DHX=0.5, ø=0.5)

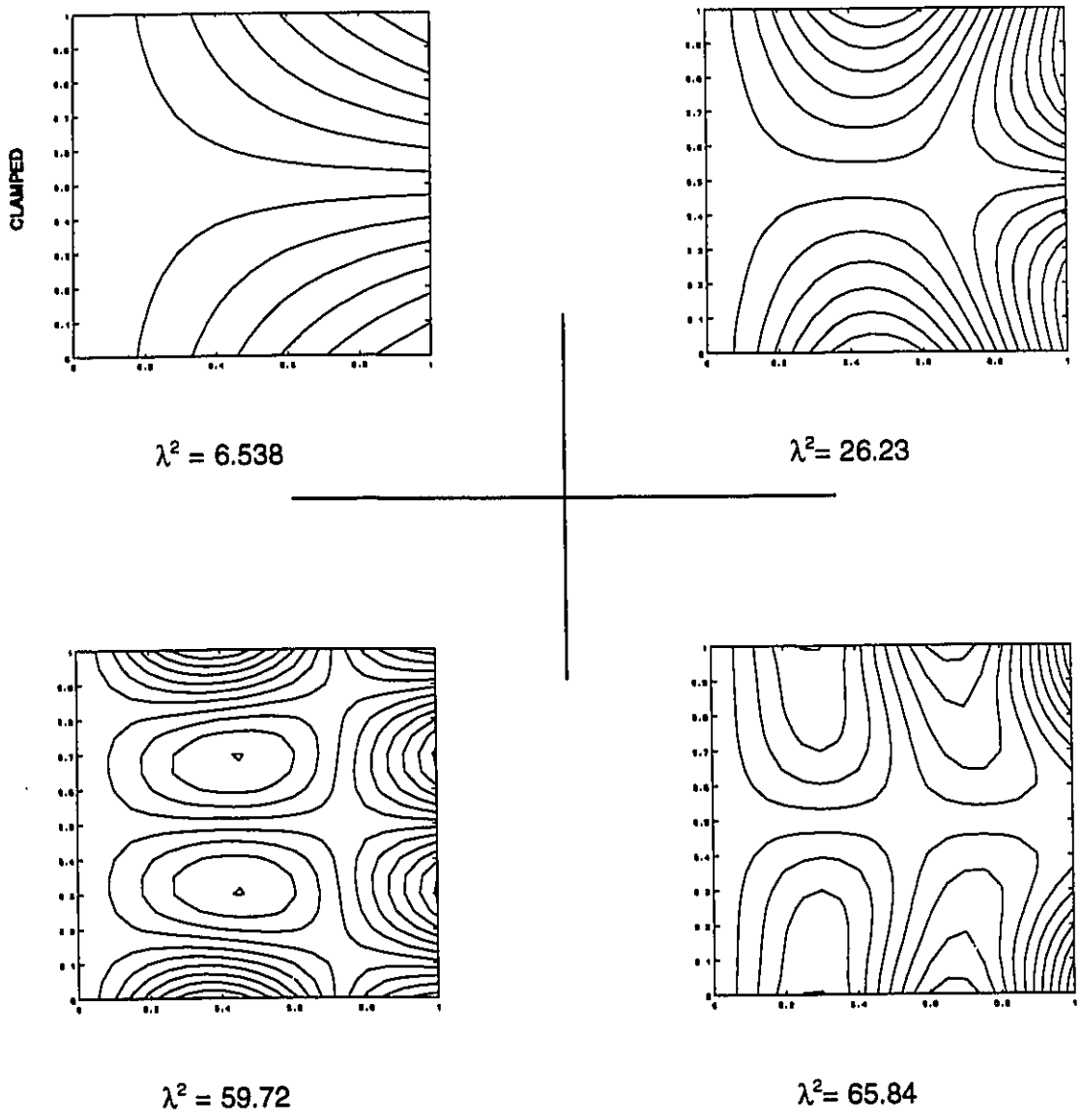

FIGURE B.2.8 First Four Associated Contour Plots - Antisymmetric (DHY=2.0, DHX=0.5, ø=0.5)

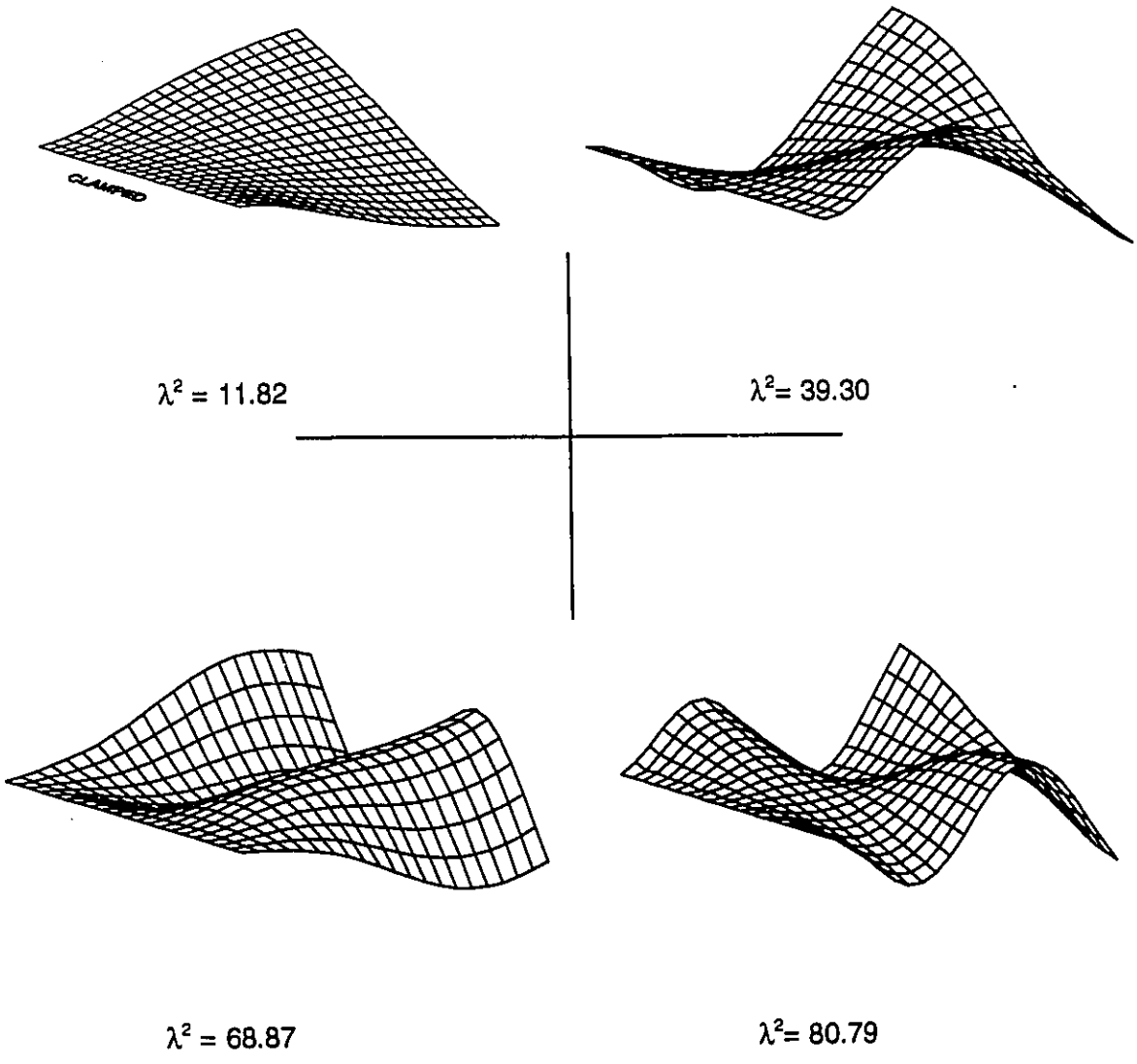

FIGURE B.2.9 First Four Associated Mode Shapes - Antisymmetric (DHY=2.0, DHX=2.0, ø=0.5)

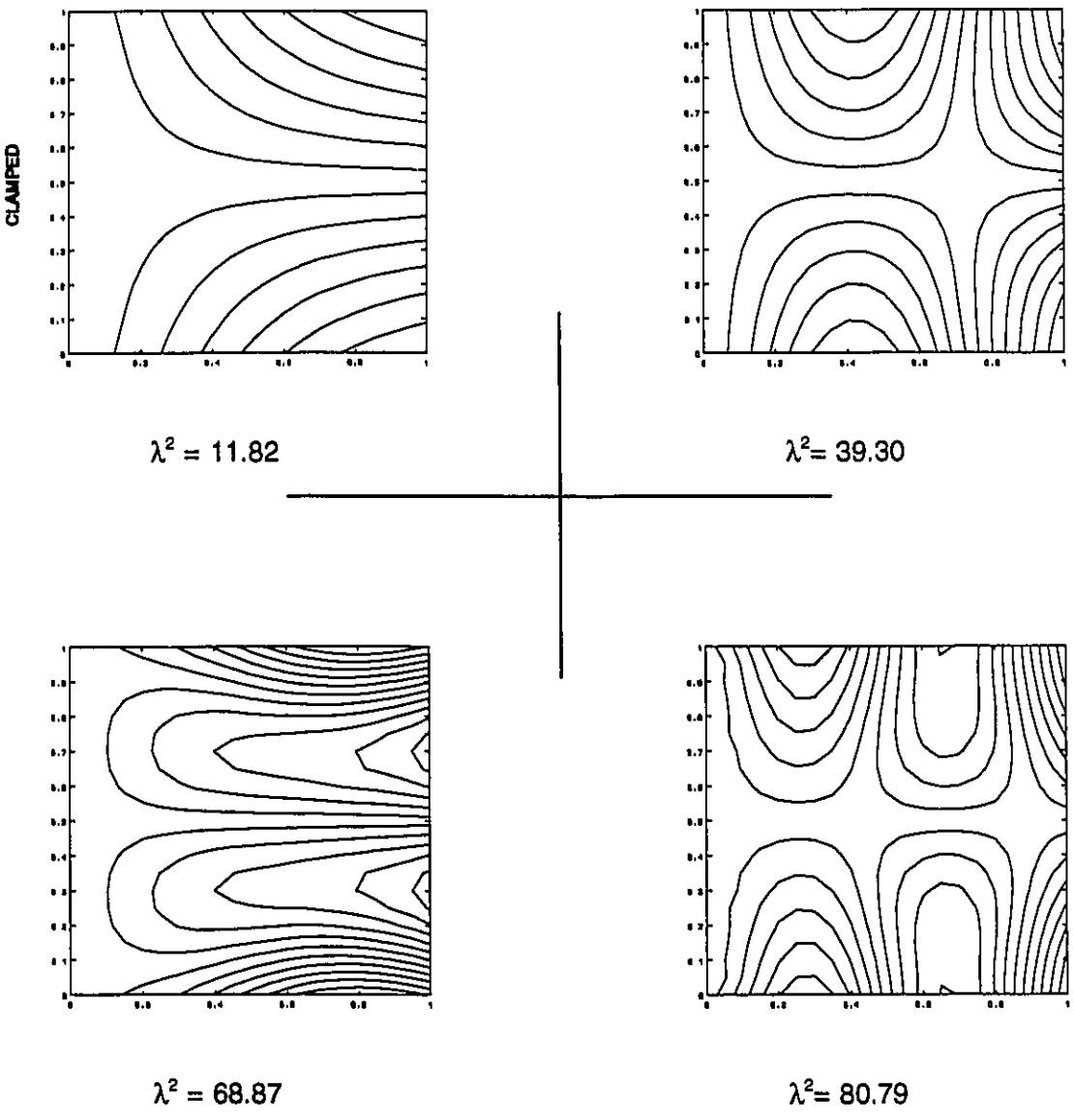

FIGURE B.2.10 First Four Associated Contour Plots - Antisymmetric (DHY=2.0, DHX=2.0, ø=0.5)

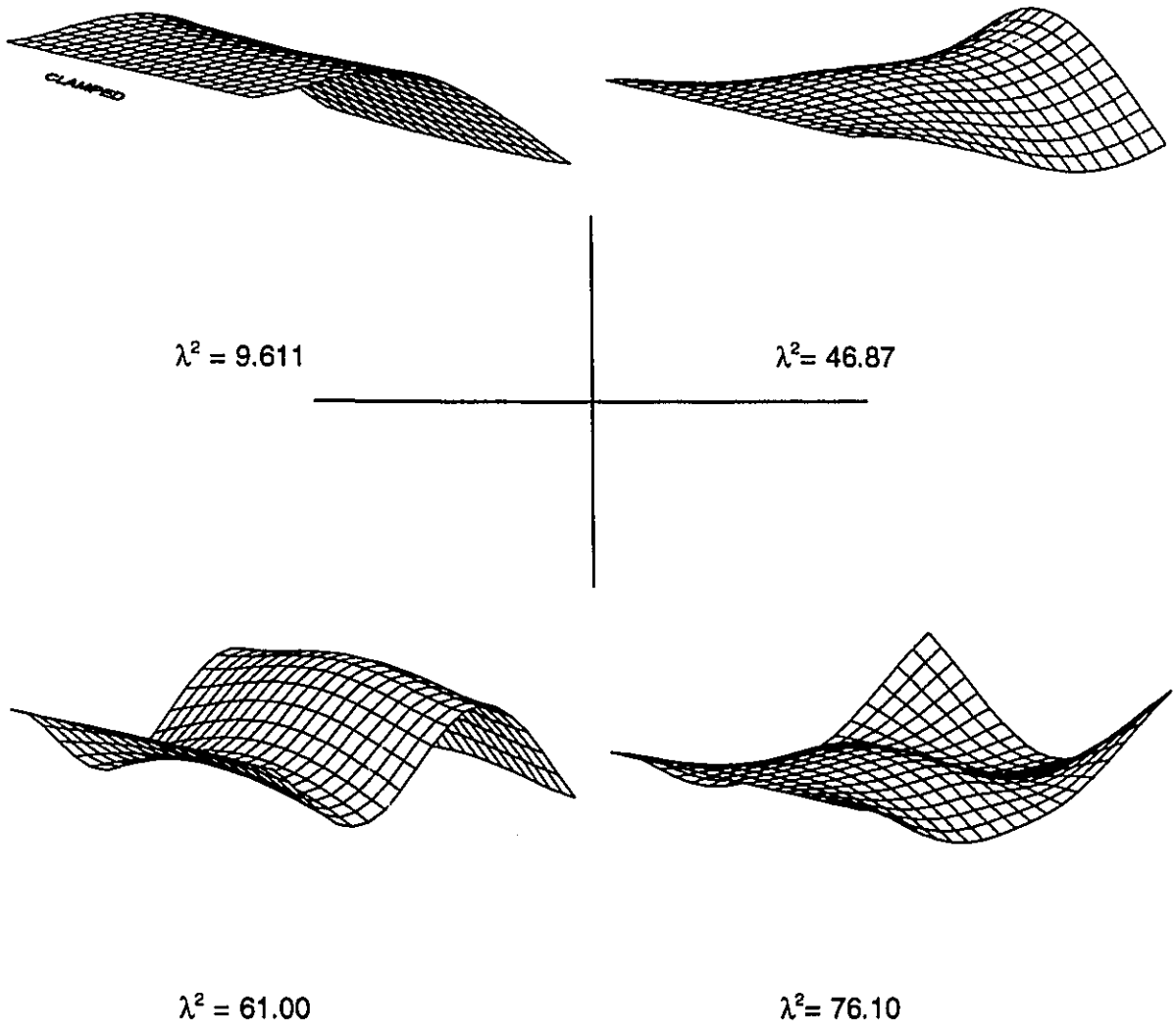

FIGURE B.3.1 First Four Associated Mode Shapes - Symmetric with Point Supports at coordinates (0.5,0.25) & (0.5,0.75), (DHY=0.5, DHX=2.0, ø=0.5, u=v=0.5)

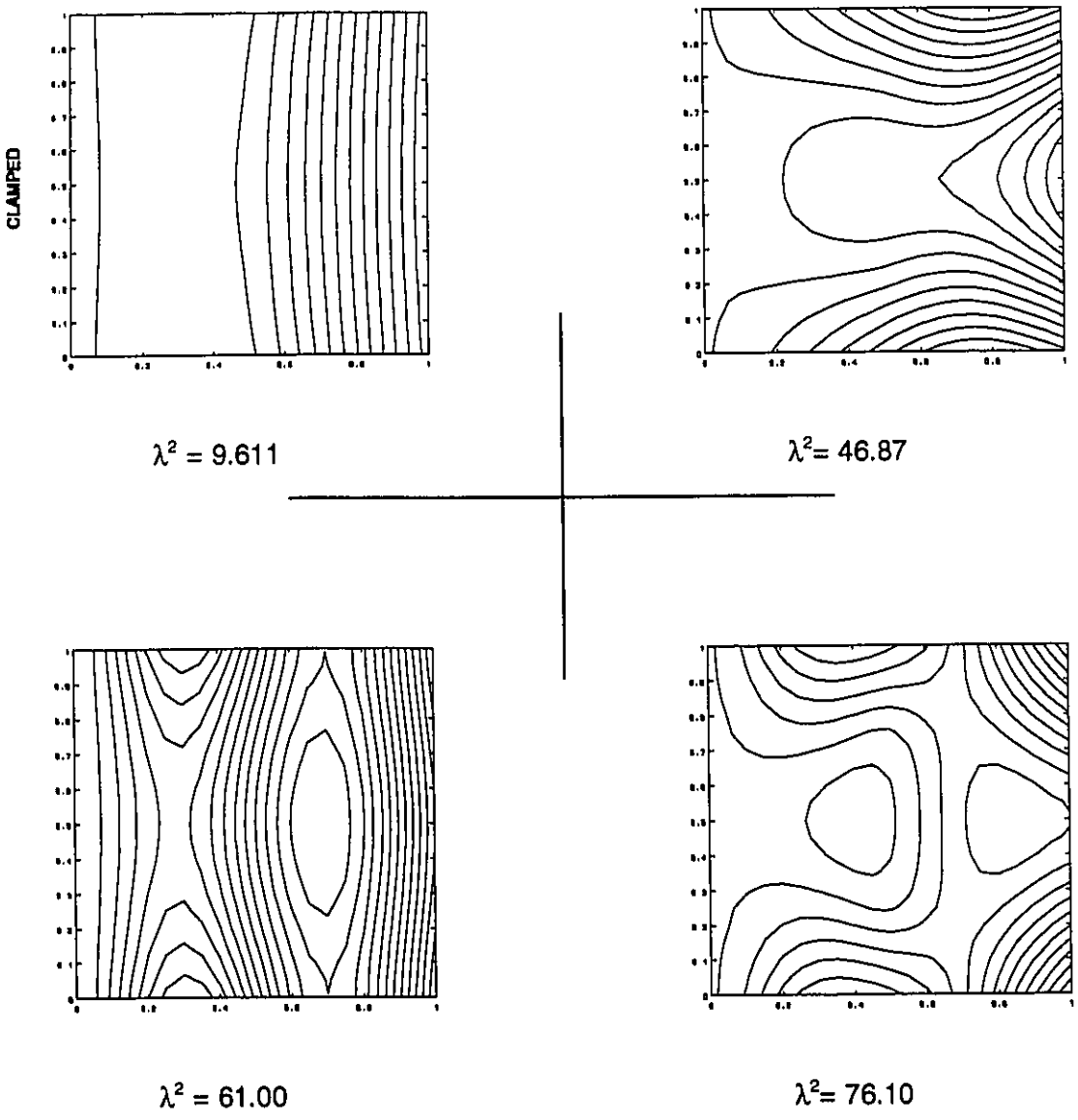

FIGURE B.3.2 First Four Associated Contour Plots - Symmetric with Point Supports at coordinates (0.5,0.25) & (0.5,0.75), (DHY=0.5, DHX=2.0, ø=0.5, u=v=0.5)

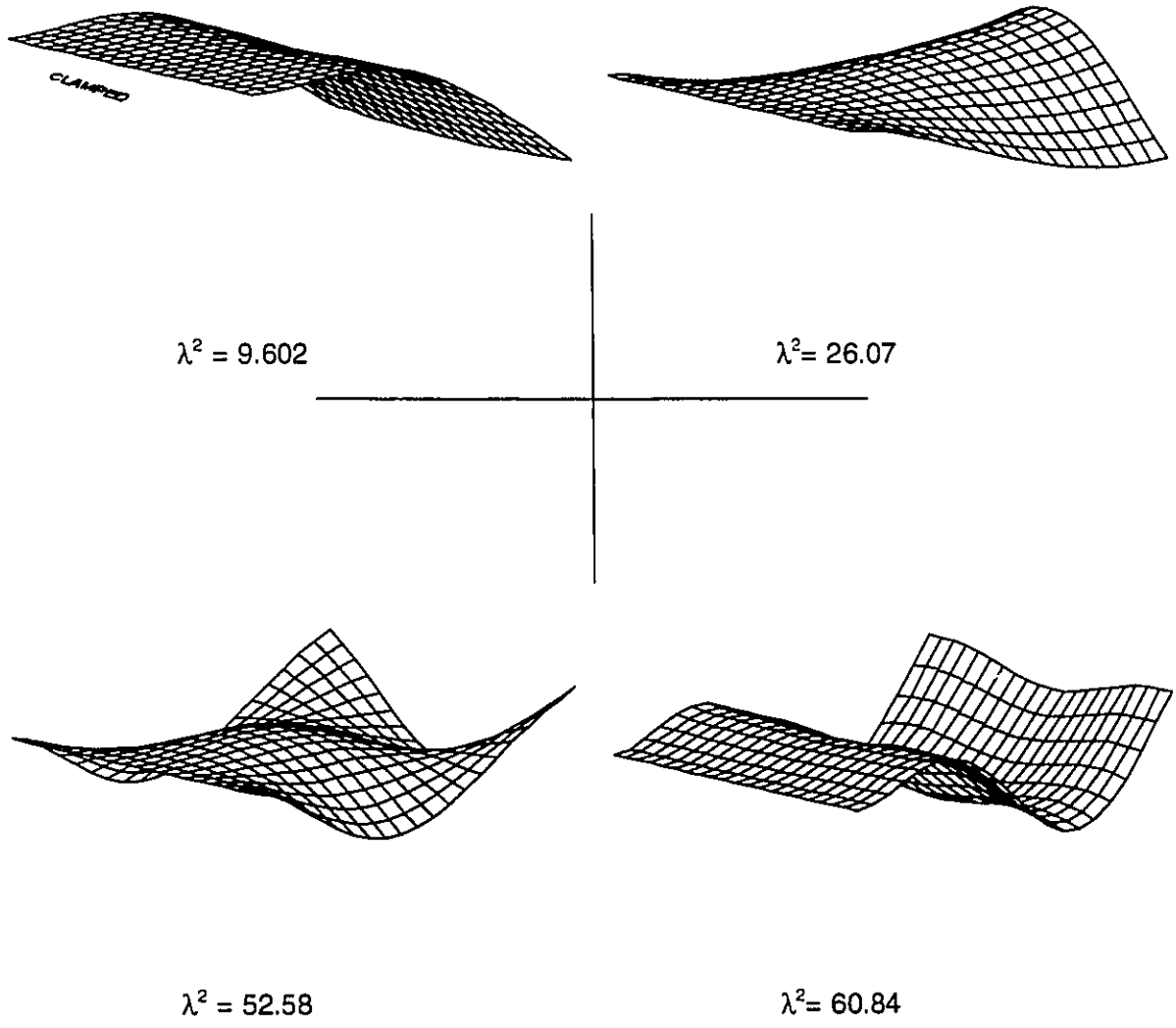

FIGURE B.3.3 First Four Associated Mode Shapes - Symmetric with Point Supports at coordinates (0.5,0.25) & (0.5,0.75), (DHY=1.0, DHX=1.0, ø=0.5, u=v=0.5, Special case of Orthotropy: Isotropic)

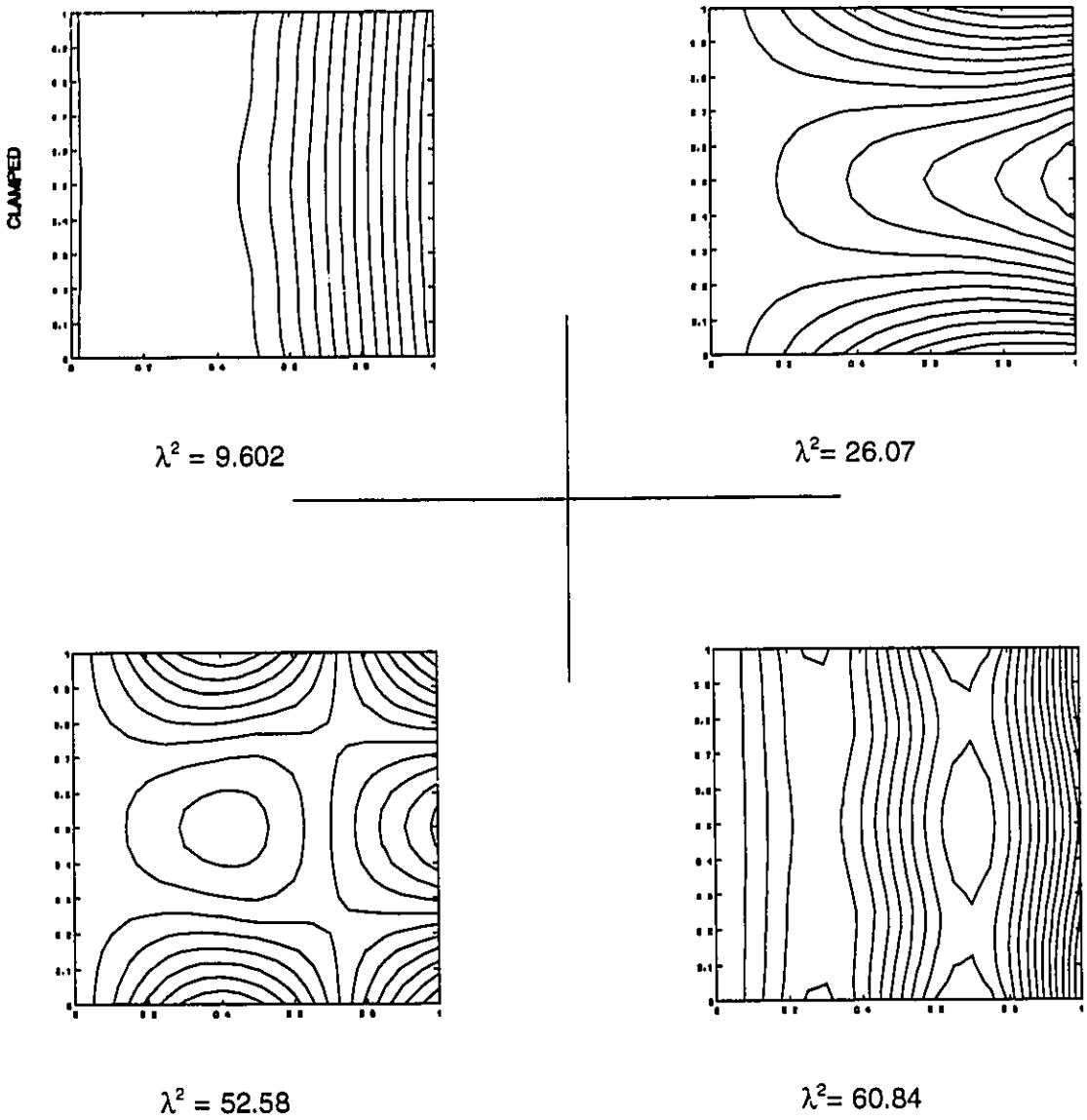

FIGURE B.3.4 First Four Associated Contour Plots - Symmetric with Point Supports at coordinates (0.5,0.25) & (0.5,0.75), (DHY=1.0, DHX=1.0, ø=0.5, u=v=0.5, Special case of Orthotropy: Isotropic)

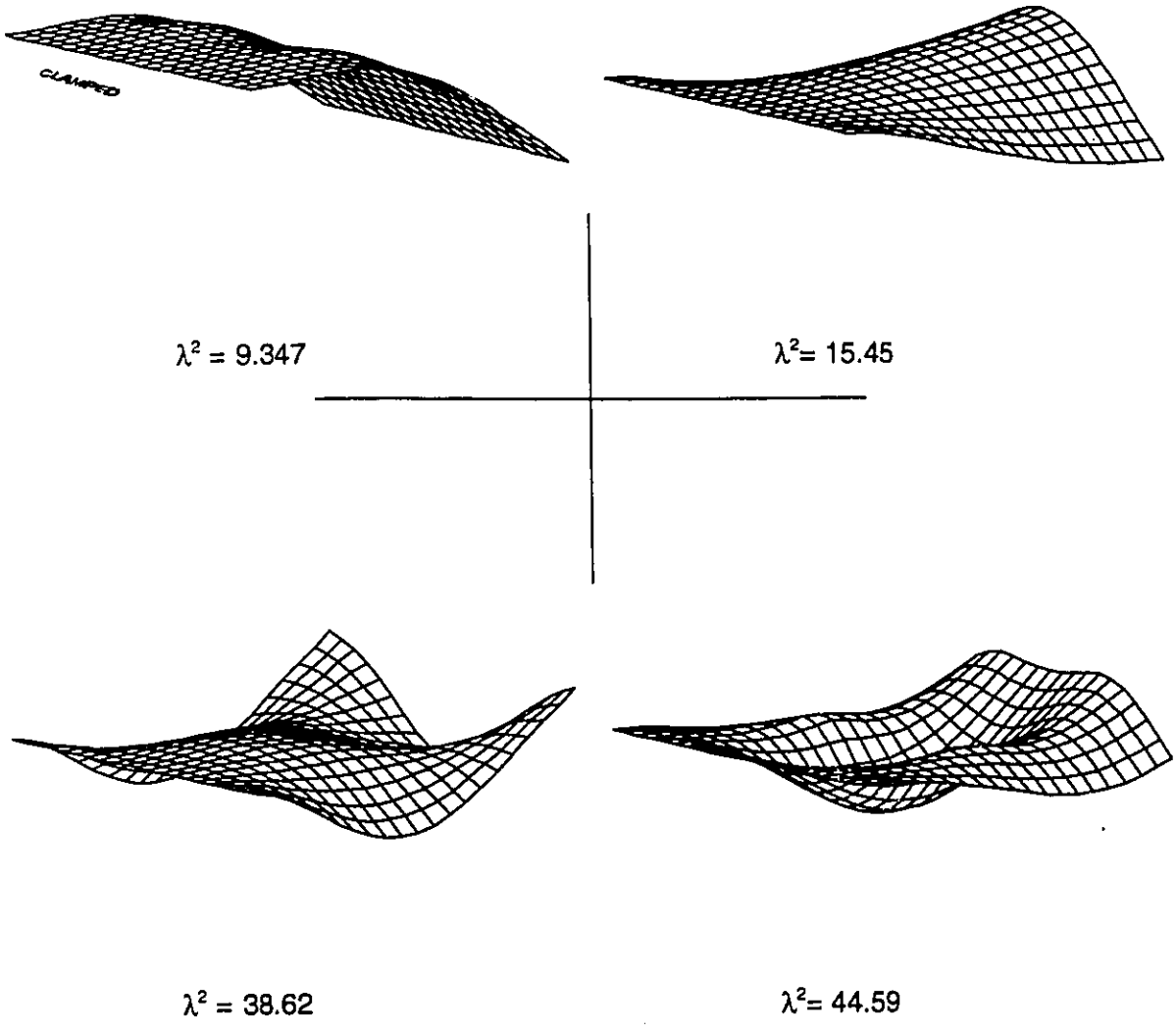

FIGURE B.3.5 First Four Associated Mode Shapes - Symmetric with Point Supports at coordinates (0.5,0.25) & (0.5,0.75), (DHY=2.0, DHX=0.5, ø=0.5, u=v=0.5)

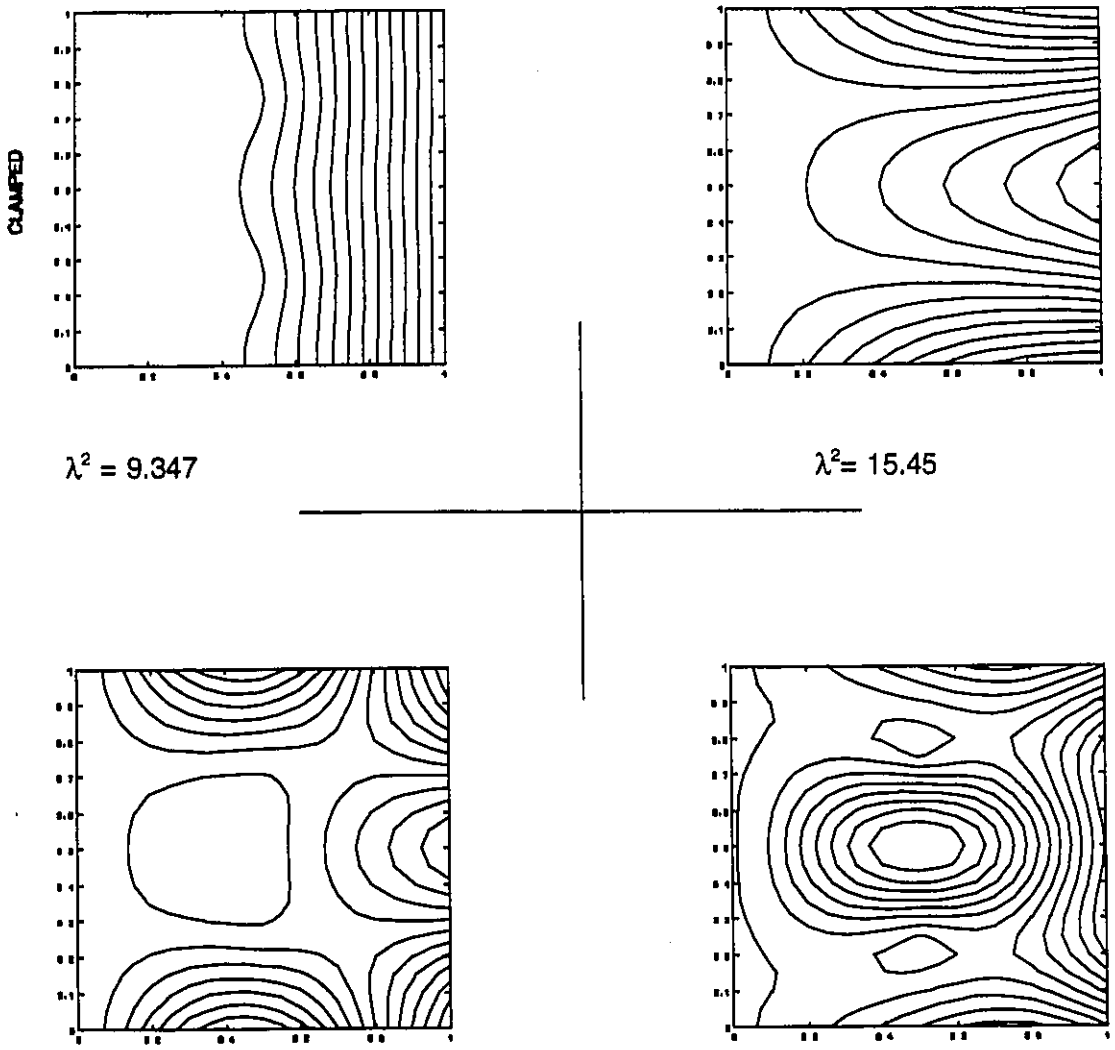

FIGURE B.3.6 First Four Associated Contour Plots - Symmetric with Point Supports at coordinates (0.5,0.25) & (0.5,0.75), (DHY=2.0, DHX=0.5, ø=0.5, u=v=0.5)

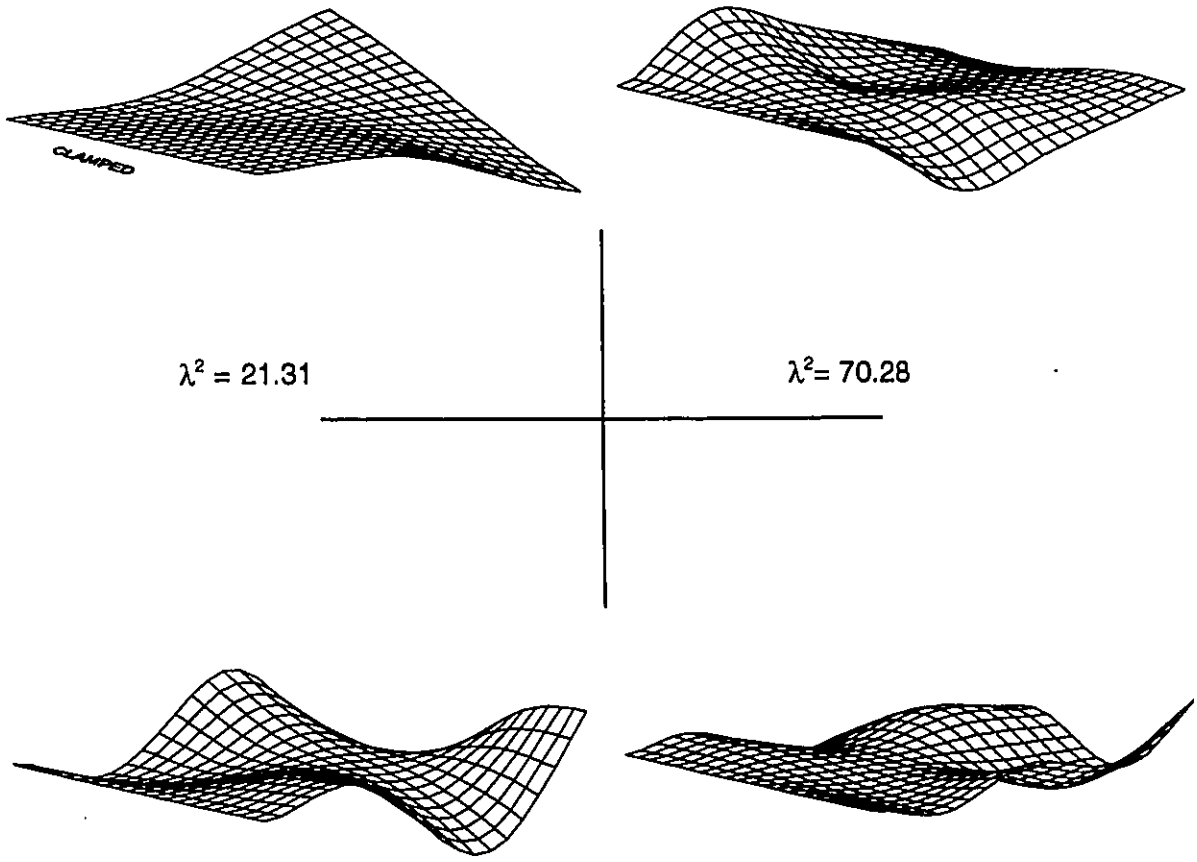

FIGURE B.3.7 First Four Associated Mode Shapes - Antisymmetric with Point Supports at coordinates (0.5,0.25) & (0.5,0.75), (DHY=0.5, DHX=2.0, ø=0.5, u=v=0.5)

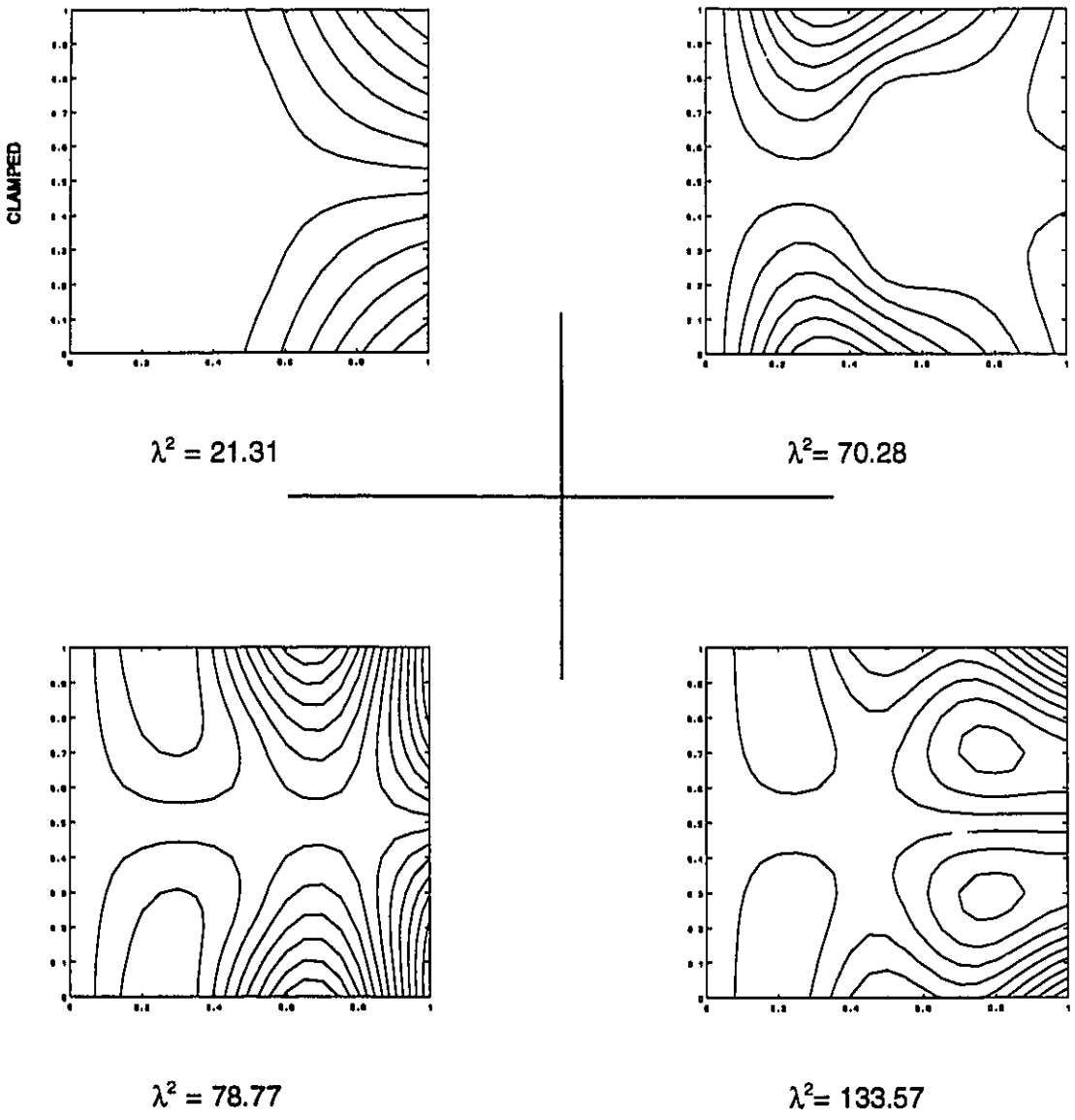

FIGURE B.3.8 First Four Associated Contour Plots - Antisymmetric with Point Supports at coordinates (0.5,0.25) & (0.5,0.75), (DHY=0.5, DHX=2.0, ø=0.5, u=v=0.5)

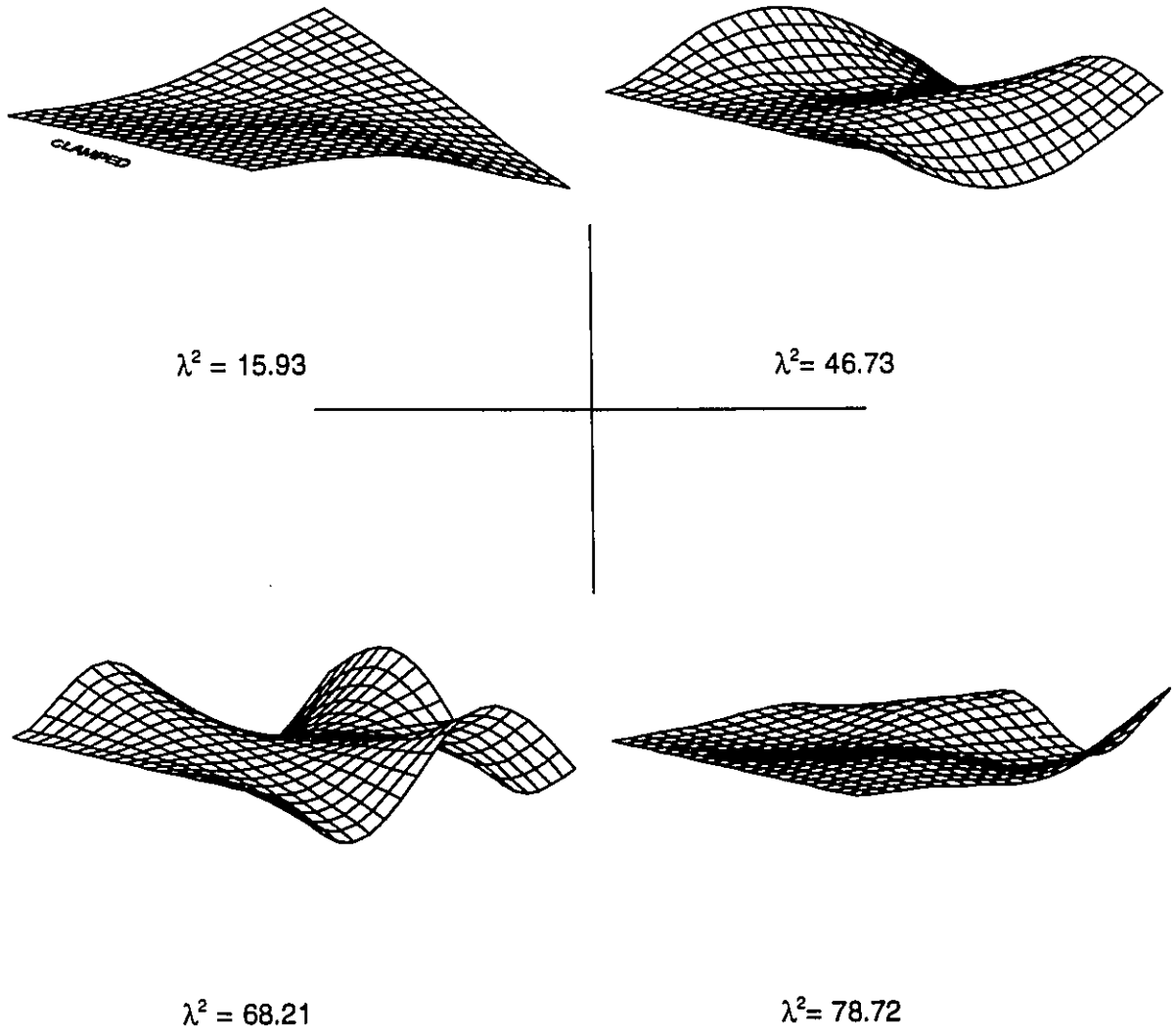

FIGURE B.3.9 First Four Associated Mode Shapes - Antisymmetric with Point Supports at (0.5,0.25) & (0.5,0.75), (DHY=1.0, DHX=1.0, ø=0.5, u=v=0.5, Special case of Orthotropy: Isotropic)

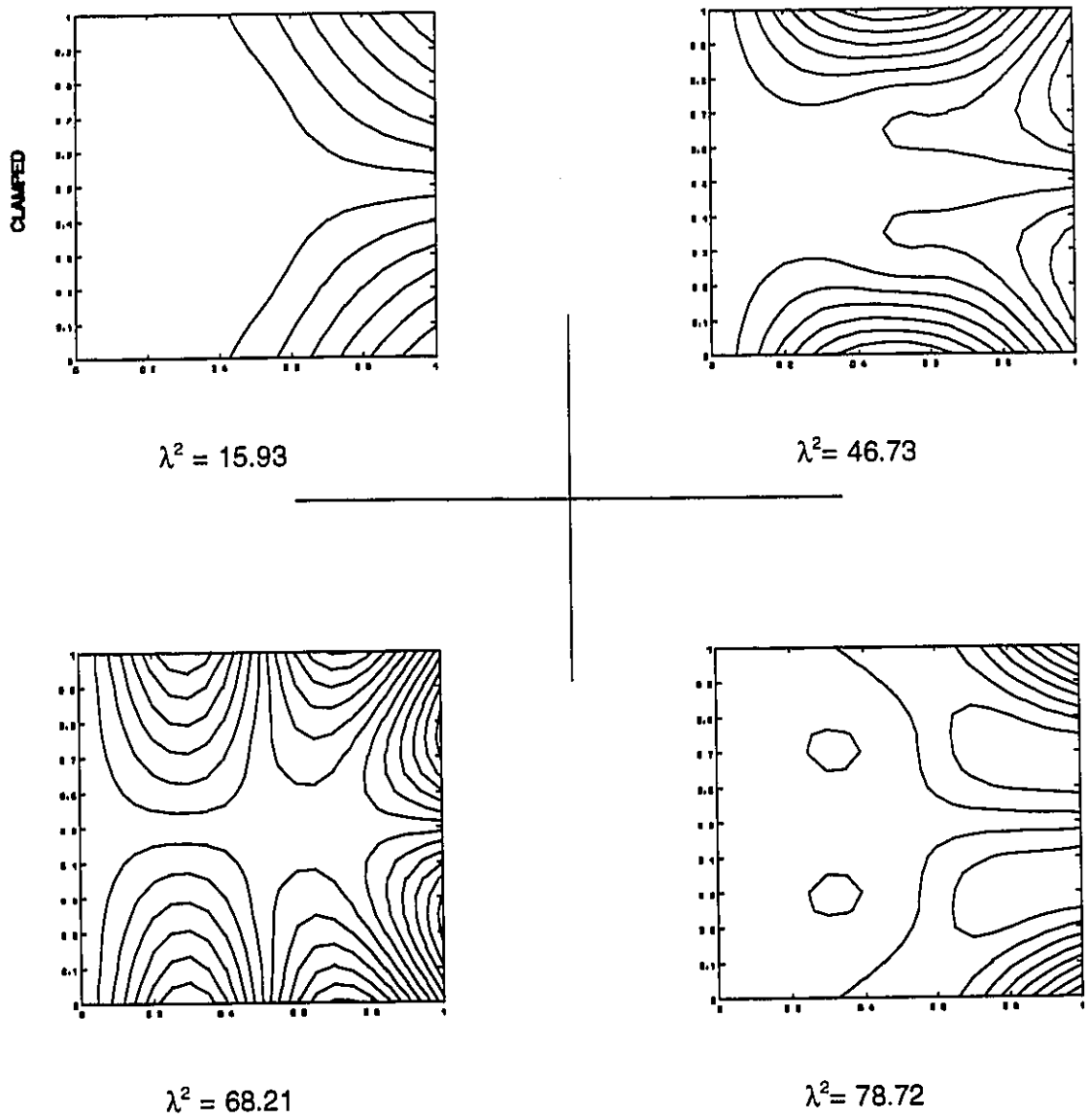

FIGURE B.3.10 First Four Associated Contour Plots - Antisymmetric with Point Supports at coordinates (0.5,0.25) & (0.5,0.75), (DHY=1.0, DHX=1.0, ø=0.5, u=v=0.5, Special case of Orthotropy: Isotropic)

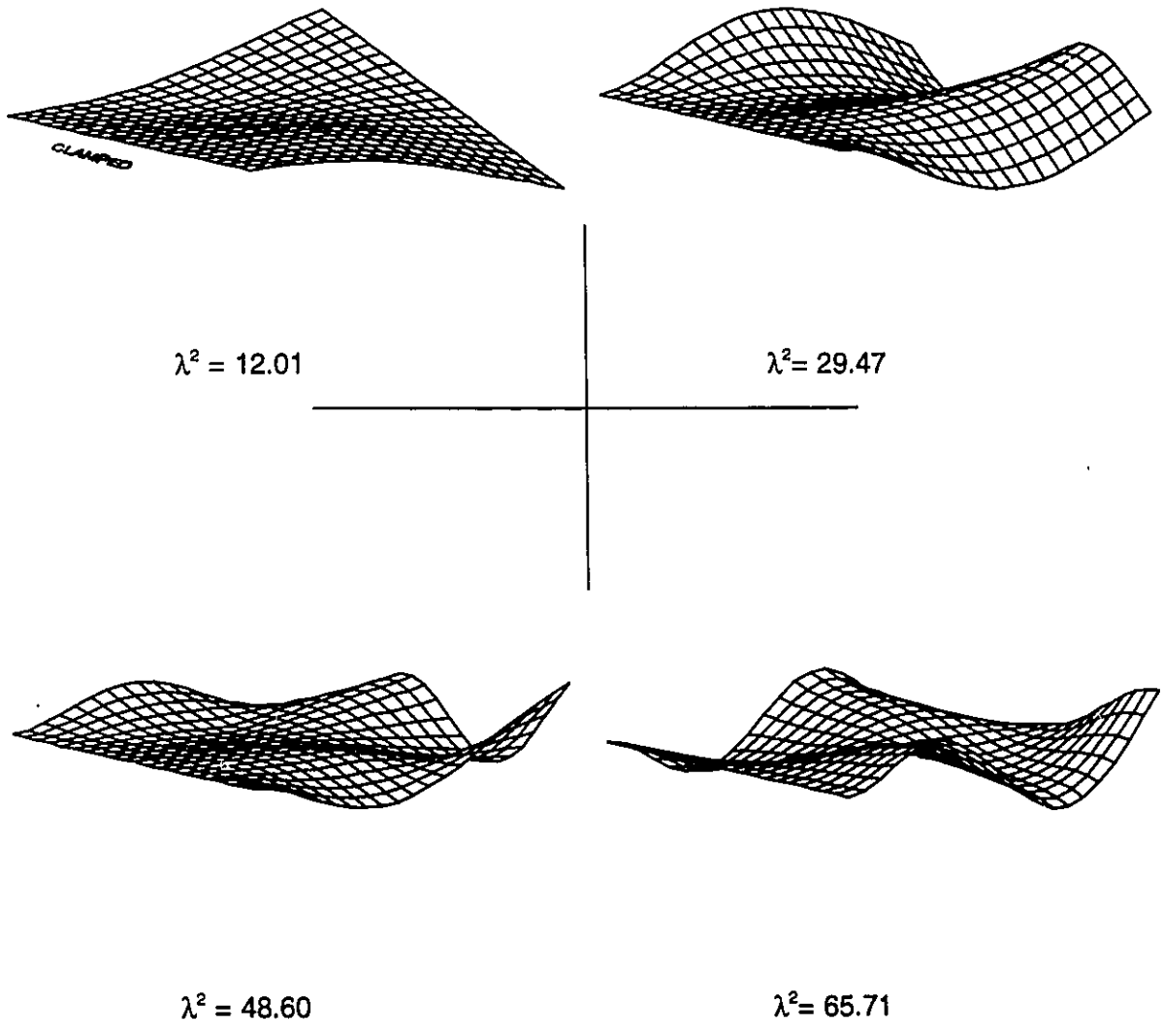

FIGURE B.3.11 First Four Associated Mode Shapes - Antisymmetric with Point Supports at coordinates (0.5,0.25) & (0.5,0.75), (DHY=2.0,DHX=0.5,ø=0.5, u=v=0.5)

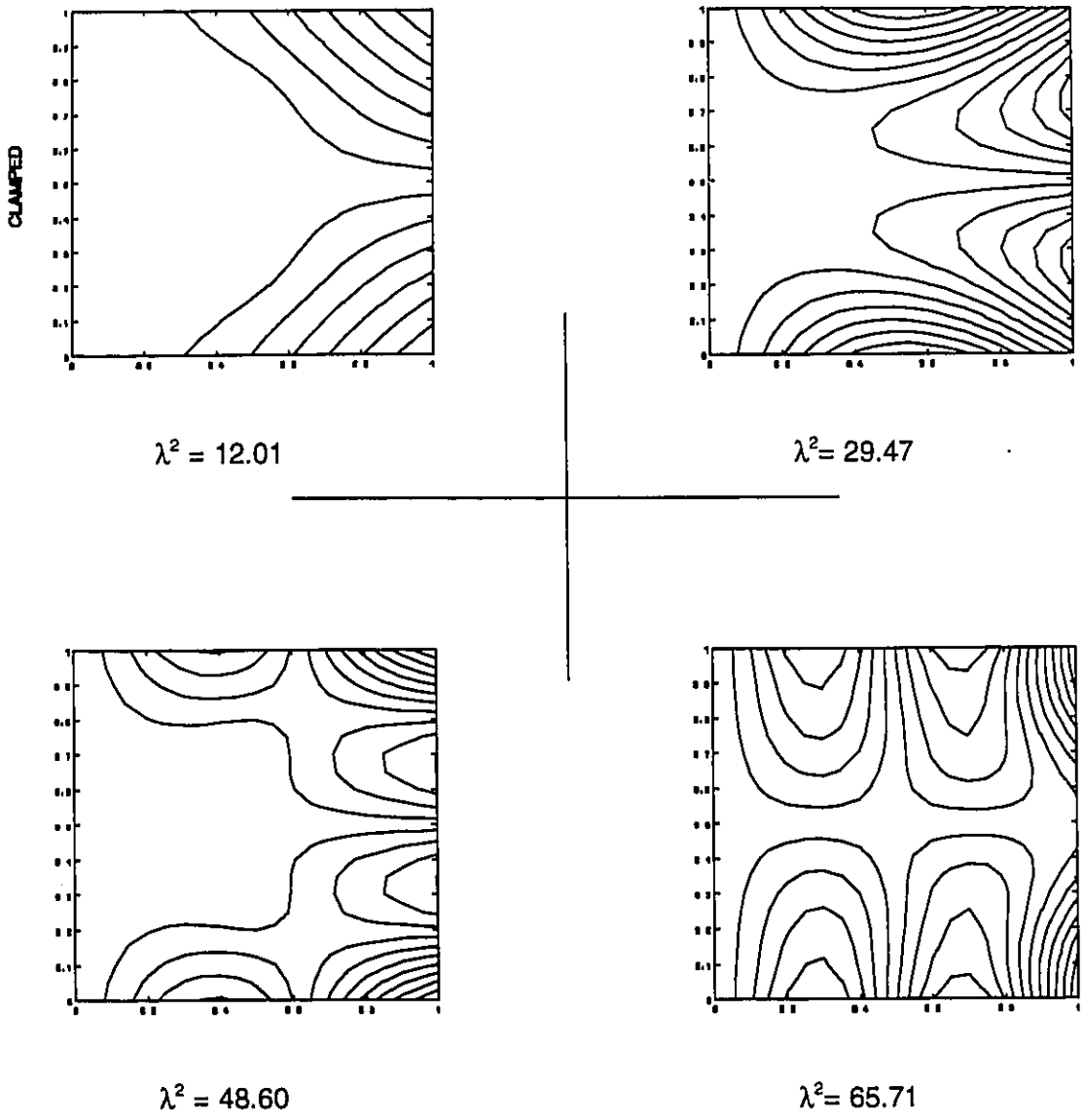

FIGURE B.3.12 First Four Associated Contour Plots - Antisymmetric with Point Supports at coordinates (0.5,0.25) & (0.5,0.75), (DHY=2.0,DHX=0.5,ø=0.5, u=v=0.5)

Computed Eigenvalues

Symmetric Modes

$$\lambda^2 = \omega a^2 \sqrt{\frac{\rho}{D_x}}$$

Computed Eigenvalues for the First Four Symmetric Free Vibration Modes of the Orthotropic Cantilever Plate ($\sqrt{\upsilon_x \upsilon_y}$ = 0.333)

ø=2b/a	1/2	1/1.5	1	1.5	2	2.5	3
ø'=b/a	1/4	1/3	1/2	3/4	1	1.25	1.5
Mode 1	3.401	3.420	3.446	3.468	3.479	3.486	3.491
2	21.15	21.16	20.45	11.42	7.543	5.849	4.993
3	59.01	49.78	24.34	21.69	21.59	19.49	14.25
4	89.16	60.38	39.61	29.02	25.47	22.04	21.77

Table B1.1 DHY= 0.5 DHX=0.5

ø=2b/a	1/2	1/1.5	1	1.5	2	2.5	3
ø'=b/a	1/4	1/3	1/2	3/4	1	1.25	1.5
Mode 1	3.400	3.419	3.444	3.466	3.478	3.485	3.490
2	21.17	21.21	21.05	14.22	9.374	7.146	5.958
3	59.30	57.61	29.47	21.84	21.71	21.52	17.68
4	108.02	65.01	48.16	33.57	28.29	24.48	21.93

Table B1.2 DHY= 0.5 DHX=0.75

ø=2b/a	1/2	1/1.5	1	1.5	2	2.5	3
ø'=b/a	1/4	1/3	1/2	3/4	1	1.25	1.5
Mode 1	3.399	3.418	3.443	3.465	3.477	3.484	3.490
2	21.19	21.23	21.18	16.47	10.89	8.244	6.796
3	59.44	59.05	34.06	22.00	21.77	21.69	20.31
4	115.41	73.63	55.22	37.63	30.90	27.14	22.23

Table B1.3 DHY= 0.5 DHX=1.0

$$\lambda^2 = \omega a^2 \sqrt{\frac{\rho}{D_x}}$$

Computed Eigenvalues for the First Four Symmetric Free Vibration Modes of the Orthotropic Cantilever Plate ($\sqrt{\upsilon_x \upsilon_y} = 0.333$)

ø=2b/a	1/2	1/1.5	1	1.5	2	2.5	3
ø'=b/a	1/4	1/3	1/2	3/4	1	1.25	1.5
Mode 1	3.399	3.417	3.442	3.463	3.476	3.483	3.489
2	21.20	21.26	21.28	19.64	13.38	10.07	8.213
3	59.58	59.60	41.76	22.80	21.85	21.77	21.66
4	116.97	89.71	60.53	44.66	35.57	30.79	25.61

Table B1.4 DHY= 0.5 DHX=1.5

ø=2b/a	1/2	1/1.5	1	1.5	2	2.5	3
ø'=b/a	1/4	1/3	1/2	3/4	1	1.25	1.5
Mode 1	3.398	3.416	3.441	3.462	3.475	3.483	3.488
2	21.21	21.27	21.32	20.85	15.42	11.59	9.402
3	59.65	59.77	48.13	24.91	21.93	21.81	21.76
4	117.34	103.11	61.03	50.65	39.67	33.85	29.21

Table B1.5 DHY= 0.5 DHX=2.0

$$\lambda^2 = \omega a^2 \sqrt{\frac{\rho}{D_x}}$$

Computed Eigenvalues for the First Four Symmetric Free Vibration Modes of the Orthotropic Cantilever Plate ($\sqrt{\upsilon_x \upsilon_y}$ = 0.333)

ø=2b/a	1/2	1/1.5	1	1.5	2	2.5	3
ø'=b/a	1/4	1/3	1/2	3/4	1	1.25	1.5
Mode 1	3.413	3.432	3.456	3.474	3.485	3.491	3.495
2	21.20	21.21	19.19	10.53	7.310	5.851	5.077
3	58.92	42.32	22.63	21.73	21.57	17.09	12.64
4	74.73	59.29	39.45	29.58	25.08	21.90	21.79

Table B1.6 DHY= 0.75 DHX=0.5

ø=2b/a	1/2	1/1.5	1	1.5	2	2.5	3
ø'=b/a	1/4	1/3	1/2	3/4	1	1.25	1.5
Mode 1	3.412	3.430	3.454	3.473	3.484	3.490	3.494
2	21.23	21.26	20.86	13.01	8.951	7.035	5.973
3	59.46	51.61	25.81	21.82	21.73	20.71	15.63
4	91.15	61.16	47.40	33.95	28.53	22.38	21.89

Table B1.7 DHY= 0.75 DHX=0.75

ø=2b/a	1/2	1/1.5	1	1.5	2	2.5	3
ø'=b/a	1/4	1/3	1/2	3/4	1	1.25	1.5
Mode 1	3.411	3.429	3.453	3.472	3.483	3.489	3.494
2	21.24	21.29	21.15	15.04	10.32	8.041	6.752
3	59.64	57.42	29.55	21.91	21.78	21.62	18.09
4	104.66	63.81	54.07	37.83	31.18	24.82	21.97

Table B1.8 DHY= 0.75 DHX=1.0

$$\lambda^2 = \omega a^2 \sqrt{\frac{\rho}{D_x}}$$

Computed Eigenvalues for the First Four Symmetric Free Vibration Modes of the Orthotropic Cantilever Plate ($\sqrt{\upsilon_x \upsilon_y} = 0.333$)

ø=2b/a	1/2	1/1.5	1	1.5	2	2.5	3
ø'=b/a	1/4	1/3	1/2	3/4	1	1.25	1.5
Mode 1	3.411	3.428	3.452	3.471	3.482	3.489	3.493
2	21.26	21.31	21.30	18.24	12.58	9.720	8.073
3	59.79	59.58	36.10	22.20	21.84	21.78	21.35
4	116.57	75.66	60.57	44.54	35.76	29.95	22.90

Table B1.9 DHY= 0.75 DHX=1.5

ø=2b/a	1/2	1/1.5	1	1.5	2	2.5	3
ø'=b/a	1/4	1/3	1/2	3/4	1	1.25	1.5
Mode 1	3.410	3.428	3.451	3.470	3.481	3.488	3.493
2	21.27	21.33	21.37	20.28	14.45	11.12	9.183
3	59.87	59.90	41.64	23.09	21.88	21.82	21.74
4	116.60	87.03	60.94	50.28	39.75	33.67	26.01

Table B1.10 DHY= 0.75 DHX=2.0

$$\lambda^2 = \omega a^2 \sqrt{\frac{\rho}{D_x}}$$

Computed Eigenvalues for the First Four Symmetric Free Vibration Modes of the Orthotropic Cantilever Plate ($\sqrt{\upsilon_x \upsilon_y} = 0.333$)

ø=2b/a	1/2	1/1.5	1	1.5	2	2.5	3
ø'=b/a	1/4	1/3	1/2	3/4	1	1.25	1.5
Mode 1	3.421	3.440	3.462	3.479	3.488	3.494	3.497
2	21.24	21.22	17.93	10.08	7.209	5.867	5.131
3	58.30	37.79	39.48	21.75	21.37	15.64	11.75
4	66.71	58.40	60.74	29.88	23.33	21.89	21.76

Table B1.11 DHY= 1.0 DHX=0.5

ø=2b/a	1/2	1/1.5	1	1.5	2	2.5	3
ø'=b/a	1/4	1/3	1/2	3/4	1	1.25	1.5
Mode 1	3.420	3.438	3.460	3.478	3.487	3.493	3.496
2	21.27	21.29	20.52	12.37	8.747	6.992	5.991
3	59.50	46.29	23.99	21.82	21.73	19.20	14.47
4	80.51	60.81	47.10	34.20	27.85	22.03	21.88

Table B1.12 DHY= 1.0 DHX=0.75

ø=2b/a	1/2	1/1.5	1	1.5	2	2.5	3
ø'=b/a	1/4	1/3	1/2	3/4	1	1.25	1.5
Mode 1	3.402	3.437	3.459	3.477	3.487	3.492	3.496
2	21.28	21.32	21.09	14.26	10.03	7.497	6.738
3	59.75	53.06	27.06	21.88	21.78	21.36	16.73
4	92.70	61.55	53.53	37.95	31.07	22.96	21.93

Table B1.13 This is a special case of orthotropic: isotropic when DHY=DHX=1.0

$$\lambda^2 = \omega a^2 \sqrt{\frac{\rho}{D_x}}$$

Computed Eigenvalues for the First Four Symmetric Free Vibration Modes of the Orthotropic Cantilever Plate ($\sqrt{\upsilon_x \upsilon_y} = 0.333$)

ø=2b/a	1/2	1/1.5	1	1.5	2	2.5	3
ø'=b/a	1/4	1/3	1/2	3/4	1	1.25	1.5
Mode 1	3.419	3.436	3.458	3.476	3.486	3.492	3.496
2	21.30	21.35	21.33	17.33	12.16	9.547	8.006
3	59.94	59.17	32.89	22.05	21.83	21.77	20.32
4	111.69	67.85	60.65	44.48	41.13	27.64	28.94

Table B1.14 DHY= 1.0 DHX=1.5

ø=2b/a	1/2	1/1.5	1	1.5	2	2.5	3
ø'=b/a	1/4	1/3	1/2	3/4	1	1.25	1.5
Mode 1	3.419	3.436	3.458	3.476	3.486	3.492	3.496
2	21.31	21.37	21.40	19.61	13.94	10.88	9.074
3	60.01	59.90	37.90	22.47	21.87	21.81	21.67
4	117.26	77.53	60.98	50.07	47.40	31.82	24.00

Table B1.15 DHY= 1.0 DHX=2.0

$$\lambda^2 = \omega a^2 \sqrt{\frac{\rho}{D_x}}$$

Computed Eigenvalues for the First Four Symmetric Free Vibration Modes of the Orthotropic Cantilever Plate ($\sqrt{\upsilon_x \upsilon_y}$ = 0.333)

ø=2b/a	1/2	1/1.5	1	1.5	2	2.5	3
ø'=b/a	1/4	1/3	1/2	3/4	1	1.25	1.5
Mode 1	3.433	3.450	3.470	3.485	3.493	3.497	3.501
2	21.29	21.22	16.33	9.624	7.124	5.897	5.194
3	53.40	32.58	21.99	21.76	19.79	14.03	10.81
4	61.56	57.23	39.59	30.03	22.10	21.87	21.07

Table B1.16 DHY= 1.5 DHX=0.5

ø=2b/a	1/2	1/1.5	1	1.5	2	2.5	3
ø'=b/a	1/4	1/3	1/2	3/4	1	1.25	1.5
Mode 1	3.432	3.449	3.468	3.484	3.492	3.497	3.500
2	21.32	21.33	19.53	11.71	8.551	6.956	6.016
3	59.10	39.87	22.62	21.82	21.66	17.20	13.21
4	68.47	60.75	46.84	34.35	24.84	21.95	21.86

Table B1.17 DHY= 1.5 DHX=0.75

ø=2b/a	1/2	1/1.5	1	1.5	2	2.5	3
ø'=b/a	1/4	1/3	1/2	3/4	1	1.25	1.5
Mode 1	3.431	3.448	3.468	3.483	3.492	3.496	3.500
2	21.34	21.37	20.88	13.45	9.748	7.859	6.729
3	59.79	45.97	24.47	21.85	21.78	19.77	15.22
4	78.32	61.06	52.99	38.05	28.55	28.67	26.64

Table B1.18 DHY= 1.5 DHX=1.0

$$\lambda^2 = \omega a^2 \sqrt{\frac{\rho}{D_x}}$$

Computed Eigenvalues for the First Four Symmetric Free Vibration Modes of the Orthotropic Cantilever Plate ($\sqrt{\upsilon_x \upsilon_y}$ = 0.333)

ø=2b/a	1/2	1/1.5	1	1.5	2	2.5	3
ø'=b/a	1/4	1/3	1/2	3/4	1	1.25	1.5
Mode 1	3.431	3.447	3.467	3.483	3.491	3.496	3.499
2	21.36	21.41	21.35	16.30	11.74	9.370	7.939
3	60.09	55.47	29.34	21.95	21.83	21.72	18.53
4	95.46	62.14	60.78	58.07	34.70	24.61	21.98

Table B1.19 DHY= 1.5 DHX=1.5

ø=2b/a	1/2	1/1.5	1	1.5	2	2.5	3
ø'=b/a	1/4	1/3	1/2	3/4	1	1.25	1.5
Mode 1	3.431	3.447	3.467	3.482	3.491	3.496	3.499
2	21.37	21.43	21.45	18.60	13.39	10.64	8.959
3	60.20	59.41	33.73	22.11	21.86	21.82	21.05
4	109.29	67.08	61.07	49.83	39.37	28.27	22.28

Table B1.20 DHY= 1.5 DHX=2.0

$$\lambda^2 = \omega a^2 \sqrt{\frac{\rho}{D_x}}$$

Computed Eigenvalues for the First Four Symmetric Free Vibration Modes of the Orthotropic Cantilever Plate ($\sqrt{\upsilon_x \upsilon_y} = 0.333$)

ø=2b/a	1/2	1/1.5	1	1.5	2	2.5	3
ø'=b/a	1/4	1/3	1/2	3/4	1	1.25	1.5
Mode 1	3.441	3.456	3.475	3.488	3.495	3.499	3.502
2	21.32	21.21	15.42	9.402	7.090	5.918	5.233
3	48.13	29.64	21.93	21.76	18.29	13.15	10.31
4	61.03	56.60	39.67	29.21	21.98	21.86	19.43

Table B1.21 DHY= 2.0 DHX=0.5

ø=2b/a	1/2	1/1.5	1	1.5	2	2.5	3
ø'=b/a	1/4	1/3	1/2	3/4	1	1.25	1.5
Mode 1	3.440	3.455	3.474	3.488	3.495	3.499	3.502
2	21.36	21.35	18.64	11.38	8.457	6.943	6.033
3	57.21	36.18	22.24	21.82	21.45	16.07	12.54
4	63.15	60.81	46.72	34.26	23.01	21.92	21.82

Table B1.22 DHY=2.0 DHX=0.75

ø=2b/a	1/2	1/1.5	1	1.5	2	2.5	3
ø'=b/a	1/4	1/3	1/2	3/4	1	1.25	1.5
Mode 1	3.439	3.455	3.474	3.491	3.494	3.499	3.502
2	21.38	21.40	20.55	13.02	9.604	7.816	6.727
3	59.57	41.71	23.27	21.85	21.76	18.47	14.40
4	70.16	61.03	52.71	38.04	26.21	21.98	21.90

Table B1.23 DHY=2.0 DHX=1.0

$$\lambda^2 = \omega a^2 \sqrt{\frac{\rho}{D_x}}$$

Computed Eigenvalues for the First Four Symmetric Free Vibration Modes of the Orthotropic Cantilever Plate ($\sqrt{\upsilon_x \upsilon_y}$ = 0.333)

ø=2b/a	1/2	1/1.5	1	1.5	2	2.5	3
ø'=b/a	1/4	1/3	1/2	3/4	1	1.25	1.5
Mode 1	3.439	3.454	3.473	3.487	3.494	3.495	3.501
2	21.40	21.45	21.36	15.75	11.51	9.278	7.905
3	60.16	50.82	27.41	21.91	21.94	21.57	17.48
4	85.20	61.44	60.88	44.32	32.00	23.00	21.95

Table B1.24 DHY=2.0 DHX=1.5

ø=2b/a	1/2	1/1.5	1	1.5	2	2.5	3
ø'=b/a	1/4	1/3	1/2	3/4	1	1.25	1.5
Mode 1	3.438	3.454	3.472	3.486	3.494	3.498	3.501
2	21.41	21.47	21.48	17.98	13.11	10.51	8.896
3	60.30	57.41	31.42	22.01	21.86	21.81	20.02
4	98.05	62.85	61.13	49.67	36.90	26.21	22.04

Table B1.25 DHY=2.0 DHX=2.0

Computed Eigenvalues

Antisymmetric Modes

$$\lambda^2 = \omega a^2 \sqrt{\frac{\rho}{D_x}}$$

Computed Eigenvalues for the First Four Antisymmetric Free Vibration Modes of the Orthotropic Cantilever Plate ($\sqrt{\upsilon_x \upsilon_y}$ = 0.333)

ø=2b/a	1/2	1/1.5	1	1.5	2	2.5	3
ø'=b/a	1/4	1/3	1/2	3/4	1	1.25	1.5
Mode 1	8.382	6.855	5.348	4.424	4.032	3.834	3.724
2	30.76	27.13	24.09	22.29	16.14	11.10	8.394
3	69.13	65.12	64.84	28.36	22.50	22.03	21.28
4	126.1	121.0	75.52	43.29	32.93	28.38	23.22

Table B2.1 DHY= 0.5 DHX=0.5

ø=2b/a	1/2	1/1.5	1	1.5	2	2.5	3
ø'=b/a	1/4	1/3	1/2	3/4	1	1.25	1.5
Mode 1	11.02	8.840	6.645	5.206	4.540	4.183	3.974
2	37.74	31.92	26.68	23.75	19.82	13.83	10.44
3	77.95	70.67	64.29	34.95	23.67	22.66	22.22
4	135.87	127.8	76.75	52.44	38.73	32.38	27.83

Table B2.2 DHY= 0.5 DHX=0.75

ø=2b/a	1/2	1/1.5	1	1.5	2	2.5	3
ø'=b/a	1/4	1/3	1/2	3/4	1	1.25	1.5
Mode 1	13.16	10.44	7.710	5.887	5.006	4.516	4.220
2	43.66	36.13	29.09	25.05	22.26	16.07	12.13
3	86.07	75.92	67.30	40.50	25.35	23.24	22.67
4	145.1	133.7	88.48	59.93	43.80	35.98	31.27

Table B2.3 DHY= 0.5 DHX=1.0

$$\lambda^2 = \omega a^2 \sqrt{\frac{\rho}{D_x}}$$

Computed Eigenvalues for the First Four Antisymmetric Free Vibration Modes of the Orthotropic Cantilever Plate ($\sqrt{\upsilon_x \upsilon_y} = 0.333$)

ø=2b/a	1/2	1/1.5	1	1.5	2	2.5	3
ø'=b/a	1/4	1/3	1/2	3/4	1	1.25	1.5
Mode 1	16.68	13.06	9.456	7.038	5.829	5.127	4.685
2	53.62	43.33	33.44	27.47	24.65	19.70	14.94
3	100.56	85.61	72.56	49.74	30.02	24.42	23.45
4	162.23	144.63	108.30	66.35	52.46	42.27	36.32

Table B2.4 DHY= 0.5 DHX=1.5

ø=2b/a	1/2	1/1.5	1	1.5	2	2.5	3
ø'=b/a	1/4	1/3	1/2	3/4	1	1.25	1.5
Mode 1	19.62	15.25	10.91	8.002	6.539	5.670	5.111
2	62.02	49.46	37.27	29.68	26.23	22.51	17.26
3	113.26	94.35	77.41	57.44	34.50	25.76	24.20
4	177.81	154.79	124.64	69.12	59.73	47.69	40.58

Table B2.5 DHY= 0.5 DHX=2.0

$$\lambda^2 = \omega a^2 \sqrt{\frac{\rho}{D_x}}$$

Computed Eigenvalues for the First Four Antisymmetric Free Vibration Modes of the Orthotropic Cantilever Plate ($\sqrt{\upsilon_x \upsilon_y}$ = 0.333)

ø=2b/a	1/2	1/1.5	1	1.5	2	2.5	3
ø'=b/a	1/4	1/3	1/2	3/4	1	1.25	1.5
Mode 1	9.419	7.632	5.844	4.710	4.210	3.955	3.810
2	33.43	28.93	25.02	21.97	14.29	10.13	7.905
3	72.48	67.21	50.84	25.14	22.72	22.16	19.13
4	129.92	112.24	63.64	41.99	32.86	26.98	22.40

Table B2.6 DHY= 0.75 DHX=0.5

ø=2b/a	1/2	1/1.5	1	1.5	2	2.5	3
ø'=b/a	1/4	1/3	1/2	3/4	1	1.25	1.5
Mode 1	11.94	9.502	7.091	5.479	4.719	4.308	4.066
2	40.24	33.66	27.63	24.04	17.63	12.51	9.705
3	81.35	72.84	61.69	30.04	23.63	22.81	22.11
4	139.78	129.12	67.86	50.39	38.29	32.07	24.42

Table B2.7 DHY= 0.75 DHX=0.75

ø=2b/a	1/2	1/1.5	1	1.5	2	2.5	3
ø'=b/a	1/4	1/3	1/2	3/4	1	1.25	1.5
Mode 1	14.02	11.08	8.128	6.148	5.183	4.643	4.315
2	46.04	37.80	30.05	25.46	20.31	14.49	11.21
3	89.44	78.12	67.60	34.61	24.59	23.37	22.75
4	149.04	135.90	74.67	57.46	43.05	35.72	27.98

Table B2.8 DHY= 0.75 DHX=1.0
Computed Eigenvalues for the First Four Antisymmetric Free Vibration Modes of the Orthotropic Cantilever Plate ($\sqrt{\upsilon_x \upsilon_y}$ = 0.333)

$$\lambda^2 = \omega a^2 \sqrt{\frac{\rho}{D_x}}$$

ø=2b/a	1/2	1/1.5	1	1.5	2	2.5	3
ø'=b/a	1/4	1/3	1/2	3/4	1	1.25	1.5
Mode 1	17.49	13.66	9.843	7.281	5.998	5.250	4.780
2	55.85	44.91	34.36	27.94	24.13	17.76	13.70
3	103.81	87.77	73.56	42.38	27.03	24.44	23.55
4	166.14	147.07	90.53	66.57	51.17	41.79	34.22

Table B2.9 DHY= 0.75 DHX=1.5

ø=2b/a	1/2	1/1.5	1	1.5	2	2.5	3
ø'=b/a	1/4	1/3	1/2	3/4	1	1.25	1.5
Mode 1	20.41	15.83	11.28	8.233	6.699	5.789	5.204
2	64.17	50.97	38.14	30.16	26.28	20.45	15.79
3	116.41	96.45	78.49	48.95	30.29	25.49	24.28
4	181.68	157.26	104.43	69.46	58.05	46.96	39.35

Table B2.10 DHY= 0.75 DHX=2.0

$$\lambda^2 = \omega a^2 \sqrt{\frac{\rho}{D_x}}$$

Computed Eigenvalues for the First Four Antisymmetric Free Vibration Modes of the Orthotropic Cantilever Plate ($\sqrt{\upsilon_x \upsilon_y}$ = 0.333)

ø=2b/a	1/2	1/1.5	1	1.5	2	2.5	3
ø'=b/a	1/4	1/3	1/2	3/4	1	1.25	1.5
Mode 1	9.970	8.042	6.106	4.862	4.307	4.020	3.858
2	34.87	29.90	25.51	20.74	13.26	9.622	7.663
3	74.33	68.30	45.12	24.31	22.84	22.07	17.42
4	131.89	98.92	63.20	41.41	32.78	24.55	22.36

Table B2.11 DHY= 1.0 DHX=0.5

ø=2b/a	1/2	1/1.5	1	1.5	2	2.5	3
ø'=b/a	1/4	1/3	1/2	3/4	1	1.25	1.5
Mode 1	12.44	9.894	7.332	5.625	4.816	4.377	4.118
2	41.59	34.60	28.14	23.91	16.32	11.81	9.329
3	83.20	74.01	55.35	27.50	23.70	22.88	21.19
4	141.89	120.73	67.36	49.38	38.08	29.85	23.12

Table B2.12 DHY= 1.0 DHX=0.75

ø=2b/a	1/2	1/1.5	1	1.5	2	2.5	3
ø'=b/a	1/4	1/3	1/2	3/4	1	1.25	1.5
Mode 1	14.50	11.43	8.356	6.288	5.278	4.711	4.368
2	47.33	38.71	30.55	25.59	18.84	13.63	10.73
3	91.25	79.29	63.62	31.30	24.55	23.45	22.69
4	151.1	135.3	70.64	56.14	42.66	34.37	25.43

Table B2.13 This is a special case of orthotropic: isotropic when DHY=DHX=1.0

$$\lambda^2 = \omega a^2 \sqrt{\frac{\rho}{D_x}}$$

Computed Eigenvalues for the First Four Antisymmetric Free Vibration Modes of the Orthotropic Cantilever Plate ($\sqrt{\upsilon_x \upsilon_y} = 0.333$)

ø=2b/a	1/2	1/1.5	1	1.5	2	2.5	3
ø'=b/a	1/4	1/3	1/2	3/4	1	1.25	1.5
Mode 1	17.95	13.99	10.06	7.412	6.087	5.317	4.832
2	57.07	45.75	34.84	28.17	22.88	16.65	13.04
3	105.54	88.92	73.58	38.14	26.32	24.50	23.61
4	168.21	148.16	80.51	66.41	50.49	41.26	30.99

Table B2.14 DHY= 1.0 DHX=1.5

ø=2b/a	1/2	1/1.5	1	1.5	2	2.5	3
ø'=b/a	1/4	1/3	1/2	3/4	1	1.25	1.5
Mode 1	20.85	16.16	11.48	8.357	6.784	5.852	5.254
2	65.33	51.77	38.60	30.41	25.80	19.16	14.98
3	118.03	97.54	78.93	43.99	28.44	25.50	24.34
4	183.62	158.46	92.30	69.74	57.13	46.48	35.78

Table B2.15 DHY= 1.0 DHX=2.0

$$\lambda^2 = \omega a^2 \sqrt{\frac{\rho}{D_x}}$$

Computed Eigenvalues for the First Four Antisymmetric Free Vibration Modes of the Orthotropic Cantilever Plate ($\sqrt{\upsilon_x \upsilon_y}$ = 0.333)

ø=2b/a	1/2	1/1.5	1	1.5	2	2.5	3
ø'=b/a	1/4	1/3	1/2	3/4	1	1.25	1.5
Mode 1	10.57	8.487	6.387	5.024	4.411	4.093	3.913
2	36.42	30.94	26.01	18.58	12.15	9.103	7.429
3	76.33	69.29	38.37	24.15	22.95	20.60	15.45
4	133.11	82.70	61.22	40.87	33.45	22.93	22.38

Table B2.16 DHY= 1.5 DHX=0.5

ø=2b/a	1/2	1/1.5	1	1.5	2	2.5	3
ø'=b/a	1/4	1/3	1/2	3/4	1	1.25	1.5
Mode 1	13.00	10.31	7.593	5.781	4.919	4.452	4.176
2	43.06	35.60	28.67	22.53	14.87	11.07	8.948
3	85.19	75.21	47.05	25.87	23.80	22.87	18.94
4	143.99	101.06	67.68	48.37	37.33	26.03	22.85

Table B2.17 DHY= 1.5 DHX=0.75

ø=2b/a	1/2	1/1.5	1	1.5	2	2.5	3
ø'=b/a	1/4	1/3	1/2	3/4	1	1.25	1.5
Mode 1	15.04	11.83	8.604	6.437	5.379	4.786	4.426
2	48.74	39.67	31.08	25.23	17.13	12.71	10.22
3	93.20	80.53	54.36	28.08	24.61	23.52	21.66
4	153.37	116.62	70.58	54.75	42.10	29.95	23.48

Table B2.18 DHY= 1.5 DHX=1.0

$$\lambda^2 = \omega a^2 \sqrt{\frac{\rho}{D_x}}$$

Computed Eigenvalues for the First Four Antisymmetric Free Vibration Modes of the Orthotropic Cantilever Plate ($\sqrt{\upsilon_x \upsilon_y}$ = 0.333)

ø=2b/a	1/2	1/1.5	1	1.5	2	2.5	3
ø'=b/a	1/4	1/3	1/2	3/4	1	1.25	1.5
Mode 1	18.47	14.37	10.29	7.548	6.181	5.388	4.890
2	58.36	46.63	35.35	28.32	20.88	15.44	12.35
3	107.33	90.11	66.50	33.43	26.17	24.58	23.63
4	170.35	142.11	75.92	65.32	49.72	36.66	27.21

Table B2.19 DHY= 1.5 DHX=1.5

ø=2b/a	1/2	1/1.5	1	1.5	2	2.5	3
ø'=b/a	1/4	1/3	1/2	3/4	1	1.25	1.5
Mode 1	21.36	16.52	11.70	8.484	6.870	5.919	5.310
2	66.54	52.57	39.07	30.64	23.98	17.73	14.12
3	119.68	98.64	76.27	38.39	27.69	25.56	24.41
4	185.61	158.60	81.31	70.08	56.11	42.34	31.30

Table B2.20 DHY= 1.5 DHX=2.0

$$\lambda^2 = \omega a^2 \sqrt{\frac{\rho}{D_x}}$$

Computed Eigenvalues for the First Four Antisymmetric Free Vibration Modes of the Orthotropic Cantilever Plate ($\sqrt{\upsilon_x \upsilon_y}$ = 0.333)

ø=2b/a	1/2	1/1.5	1	1.5	2	2.5	3
ø'=b/a	1/4	1/3	1/2	3/4	1	1.25	1.5
Mode 1	10.91	8.732	6.538	5.111	4.468	4.134	3.945
2	37.26	31.50	26.23	17.26	11.56	8.840	7.316
3	77.40	68.70	59.72	24.20	22.98	18.97	14.36
4	124.64	74.20	65.84	40.58	27.97	22.80	22.37

Table B2.21 DHY= 2.0 DHX=0.5

ø=2b/a	1/2	1/1.5	1	1.5	2	2.5	3
ø'=b/a	1/4	1/3	1/2	3/4	1	1.25	1.5
Mode 1	13.32	10.54	7.734	5.863	4.976	4.494	4.209
2	43.84	36.13	28.95	21.06	14.08	10.69	8.753
3	86.24	75.71	42.18	25.67	23.87	22.54	17.55
4	144.33	89.23	67.93	47.83	34.24	24.12	22.84

Table B2.22 DHY=2.0 DHX=0.75

ø=2b/a	1/2	1/1.5	1	1.5	2	2.5	3
ø'=b/a	1/4	1/3	1/2	3/4	1	1.25	1.5
Mode 1	15.35	12.05	8.737	6.515	5.433	4.827	4.460
2	49.47	40.16	31.36	24.10	16.19	12.22	9.961
3	94.20	81.13	48.70	27.21	24.67	23.53	20.19
4	154.32	102.85	70.86	54.01	39.54	27.30	23.29

Table B2.23 DHY=2.0 DHX=1.0

$$\lambda^2 = \omega a^2 \sqrt{\frac{\rho}{D_x}}$$

Computed Eigenvalues for the First Four Antisymmetric Free Vibration Modes of the Orthotropic Cantilever Plate ($\sqrt{\upsilon_x \upsilon_y} = 0.333$)

ø=2b/a	1/2	1/1.5	1	1.5	2	2.5	3
ø'=b/a	1/4	1/3	1/2	3/4	1	1.25	1.5
Mode 1	18.76	14.59	10.41	7.618	6.229	5.426	4.923
2	59.02	47.07	35.61	28.17	19.69	14.79	11.97
3	108.22	90.71	59.65	31.02	26.19	24.63	23.51
4	171.37	125.90	76.01	64.35	48.31	33.31	25.21

Table B2.24 DHY=2.0 DHX=1.5

ø=2b/a	1/2	1/1.5	1	1.5	2	2.5	3
ø'=b/a	1/4	1/3	1/2	3/4	1	1.25	1.5
Mode 1	21.64	16.71	11.82	8.547	6.913	5.934	5.341
2	67.14	52.96	39.30	30.71	22.63	16.94	13.66
3	120.46	99.19	68.87	35.30	27.63	25.62	24.44
4	186.57	145.29	80.79	70.27	55.26	38.42	28.77

Table B2.25 DHY=2.0 DHX=2.0

Computed Eigenvalues Symmetric Modes of Plates with Point Supports

$$\lambda^2 = \omega a^2 \sqrt{\frac{\rho}{D_x}}$$

Computed Eigenvalues for the First Four Symmetric Free Vibration Modes of the Orthotropic Cantilever Plate with Point Supports($\sqrt{\upsilon_x \upsilon_y} = 0.333$)

u = v = 0.5	ø = 0.5	ø = 1.0
Mode 1	9.564	7.444
2	22.96	8.501
3	38.51	24.19
4	60.10	28.05

Table B3.1 DHY=0.5 DHX=0.5

u = v = 0.5	ø = 0.5	ø = 1.0
Mode 1	9.650	8.761
2	30.72	13.13
3	61.06	30.04
4	67.71	40.07

Table B3.2 DHY=2.0 DHX=2.0

u = v = 0.5	ø = 0.5	ø = 1.0
Mode 1	9.611	9.348
2	46.87	15.45
3	61.00	38.63
4	76.10	44.63
u = v = 0.75		
Mode 1	20.10	11.30
2	31.51	21.92
3	57.60	39.40
4	78.36	45.43

Table B3.3 DHY=0.5 DHX=2.0

$$\lambda^2 = \omega a^2 \sqrt{\frac{\rho}{D_x}}$$

Computed Eigenvalues for the First Four Symmetric Free Vibration Modes of the Orthotropic Cantilever Plate with Point Supports($\sqrt{\upsilon_x \upsilon_y}$ = 0.333)

u = v = 0.5	ø = 0.5	ø = 1.0
Mode 1	9.602	8.494
2	26.07	10.11
3	52.58	27.42
4	60.84	32.12
u = v = 0.75		
Mode 1	17.15	7.640
2	23.24	21.70
3	49.10	29.77
4	54.84	32.17

Table B3.4 DHY=1.0 DHX=1.0

u = v = 0.5	ø = 0.5	ø = 1.0
Mode 1	9.347	6.729
2	15.45	19.02
3	38.62	31.29
4	44.59	39.72
u = v = 0.75		
Mode 1	11.30	5.658
2	21.93	17.36
3	39.39	21.60
4	45.39	26.86

Table B3.5 DHY=2.0 DHX=0.5

Computed Eigenvalues Antisymmetric Modes of Plates with Point Supports

$$\lambda^2 = \omega a^2 \sqrt{\frac{\rho}{D_x}}$$

Computed Eigenvalues for the First Four Antisymmetric Free Vibration Modes of the Orthotropic Cantilever Plate with Point Supports($\sqrt{\upsilon_x \upsilon_y} = 0.333$)

u = v = 0.5	ø = 0.5	ø = 1.0
Mode 1	11.59	7.571
2	40.60	17.11
3	60.29	26.83
4	67.47	48.88

Table B4.1 DHY=0.5 DHX=0.5

u = v = 0.5	ø = 0.5	ø = 1.0
Mode 1	21.38	11.40
2	54.33	23.67
3	78.83	43.48
4	127.10	56.56

Table B4.2 DHY=2.0 DHX=2.0

u = v = 0.5	ø = 0.5	ø = 1.0
Mode 1	21.31	12.01
2	70.28	29.47
3	78.77	48.60
4	133.57	65.71
u = v = 0.75		
Mode 1	37.11	26.04
2	57.14	45.30
3	110.53	60.23
4	126.68	83.28

Table B4.3 DHY=0.5 DHX=2.0

$$\lambda^2 = \omega a^2 \sqrt{\frac{\rho}{D_x}}$$

Computed Eigenvalues for the First Four Antisymmetric Free Vibration Modes of the Orthotropic Cantilever Plate with Point Supports($\sqrt{\upsilon_x \upsilon_y}$ = 0.333)

u = v = 0.5	ø = 0.5	ø = 1.0
Mode 1	15.93	9.065
2	46.73	19.81
3	68.21	34.57
4	78.72	46.75
u = v = 0.75		
Mode 1	30.55	18.46
2	49.17	24.48
3	65.77	34.61
4	92.21	42.92

Table B4.4 DHY=1.0 DHX=1.0

u = v = 0.5	ø = 0.5	ø = 1.0
Mode 1	12.01	6.772
2	29.47	14.34
3	48.60	25.70
4	65.71	30.34
u = v = 0.75		
Mode 1	26.04	11.29
2	33.87	20.98
3	45.30	22.98
4	60.23	33.22

Table B4.5 DHY=2.0 DHX=0.5